Scientific Committee on Consumer Safety

SCCS

OPINION ON
Hydroxyapatite (nano)
Submission IV

The SCCS adopted this document
at its plenary meeting on 26 June 2025

ACKNOWLEDGMENTS

Members of the Working Group are acknowledged for their valuable contribution to this Opinion. The members of the Working Group are:

The SCCS members:
Dr U. Bernauer (Chairperson)
Dr L. Bodin
Prof. Q. Chaudhry
Prof. P.J. Coenraads
Dr E. Gaffet (Rapporteur)
Prof. E. Panteri
Dr M. Stepnik (Rapporteur)
Dr S. Wijnhoven

The SCHEER members
Dr W.H. de Jong

External experts
Dr N. von Goetz
Dr Henriqueta Louro

All Declarations of Working Group members are available on the following webpage:
Register of Commission expert groups and other similar entities

This scientific opinion has been subject to a commenting period from 3 April to 30 May 2025. Comments received during this period were considered by the SCCS. For this final document, main changes occurred in the following sections: Table 6 (Section 3.1.9.2.: Hydroxyapatite (nano) in Cell Culture Media) and a summary Table has been added to describe the *In vitro biocompatibility and irritation of biomimetic hydroxyapatite nanoparticles on human oral epithelium* (Section 3.2.2: Other studies on toxicokinetics).

1. ABSTRACT

The SCCS concludes the following:

(1) In view of the above, and taking into account the scientific data provided, does the SCCS consider Hydroxyapatite (nano) safe when used in toothpaste up to a maximum concentration of 29.5% and in mouthwash up to a maximum concentration of 10% according to the specifications as reported in the submission, taking into account reasonably foreseeable exposure conditions?

Based on the data provided, the SCCS considers hydroxyapatite (nano) safe when used at concentrations up to 29.5% in toothpaste, and up to 10% in mouthwash.

This conclusion is based on the available evidence, which shows that hydroxyapatite (nano) does not pose a mutagenic hazard or cytotoxicity or inflammatory effects even when tested at high concentrations in a buccal mucosa cell model. Any uptake of hydroxyapatite (nano) by buccal mucosa is considered negligible, and the epithelial cells with internalised particles will be shed out over time as they are continually replaced. Also, any unintentionally ingested HAP nanoparticles during the use of oral-care products will undergo rapid dissolution in the gastric fluid and therefore do not raise any nano-specific concern over safety.

This safety evaluation only applies to the hydroxyapatite (nano) that have the following characteristics:
- composed of rod-shaped particles of which at least 87% (in particle number) have aspect ratios equal to or less than 3, and the remaining 13% have aspect ratios not exceeding 9.
- the HAP particles are not coated or surface modified.
- the Opinion is related to HAP particles with max length of the HAP nanoparticles in the present Opinion, i.e. 122 ± 43 nm.

1. Alternatively, what is according to the SCCS the maximum concentration considered safe for use of Hydroxyapatite (nano) in cosmetic products?

/

2. Does the SCCS have any further scientific concerns with regard to the use of Hydroxyapatite (nano) in oral cosmetic products?

This Opinion is not applicable to any hydroxyapatite (nano) material that is composed of or contains needle-shaped particles.

Keywords: SCCS, scientific opinion, Hydroxyapatite, submission IV, HAP, nano, CAS/EC No.: 1306-06-5/215-145-7, Regulation 1223/2009

Opinion to be cited as: SCCS (Scientific Committee on Consumer Safety), Preliminary Opinion on Hydroxyapatite (nano), submission IV version of 27 March 2025, SCCS/1677/25, final version of 26 June 2025.

About the Scientific Committees

Two independent non-food Scientific Committees provide the Commission with the scientific advice it needs when preparing policy and proposals relating to consumer safety, public health and the environment. The Committees also draw the Commission's attention to the new or emerging problems which may pose an actual or potential threat.
They are: the Scientific Committee on Consumer Safety (SCCS) and the Scientific Committee on Health, Environmental and Emerging Risks (SCHEER) and are made up of scientists appointed in their personal capacity.
In addition, the Commission relies upon the work of the European Food Safety Authority (EFSA), the European Medicines Agency (EMA), the European Centre for Disease Prevention and Control (ECDC) and the European Chemicals Agency (ECHA).

SCCS

The Committee shall provide Opinions on questions concerning all types of health and safety risks (notably chemical, biological, mechanical and other physical risks) of non-food consumer products (for example: cosmetic products and their ingredients, toys, textiles, clothing, personal care and household products such as detergents, etc.) and services (for example: tattooing, artificial sun tanning, etc.).

Scientific Committee members

Contact

European Commission
Health and Food Safety
Directorate B: Public Health, Cancer and Health security
Unit B3: Health monitoring and cooperation, Health networks
L-2920 Luxembourg
SANTE-SCCS@ec.europa.eu

ISSN ISBN
Doi ND

TABLE OF CONTENTS

2. MANDATE FROM THE EUROPEAN COMMISSION

Background

Article 2(1)(k) of Regulation (EC) No. 1223/2009 (Cosmetics Regulation) states that 'nanomaterial' means an insoluble or biopersistent and intentionally manufactured material with one or more external dimensions, or an internal structure, on the scale from 1 to 100 nm.

The nanomaterials definition covers materials in the nano-scale that are intentionally made and are insoluble/partially-soluble or biopersistent. It does not cover those that are soluble or degradable/non-persistent in biological systems. Article 16 of the Cosmetics Regulation requires cosmetic products containing nanomaterials other than colorants, preservatives and UV-filters and not otherwise restricted by the Cosmetics Regulation to be notified to the Commission six months prior to being placed on the market. Article 19 of this Regulation requires nano-scale ingredients to be labelled (name of the ingredient, followed by 'nano' in brackets). If there are concerns over the safety of a notified nanomaterial, the Commission shall refer it to the Scientific Committee on Consumer Safety (SCCS) for a full risk assessment.

The Commission services received a number of notifications under Article 16 of the Cosmetics Regulation via the Cosmetic Product Notification Portal (CPNP) for cosmetic products containing Hydroxyapatite (CAS No 1306-06-17 and EC No. 215-145-7) in nano form. Hydroxyapatite is reported in the CosIng database as an abrasive, bulking, oral care and skin-conditioning agent. It is not regulated under the Cosmetic Regulation (EC) No 1223/2009.

In view of potential concerns to human safety, the Commission services mandated the SCCS on the safety of Hydroxyapatite (nano). In October 2015[1] and in December 2021[2], the SCCS could not conclude on the safety of the Hydroxyapatite (nano) composed of rod–shaped nanoparticles for use in oral cosmetic products at the maximum concentrations and specifications reported. Furthermore, the SCCS stressed that the available data/information is not sufficient to exclude concerns over the genotoxic potential of Hydroxyapatite (nano).

In February 2022, industry submitted additional information to support the safety of Hydroxyapatite (nano) in oral products, specifically addressing the potential genotoxicity of Hydroxyapatite (nano). In March 2023[3], the SCCS concluded on the safety of Hydroxyapatite (nano) when used at concentrations up to 10 % in toothpaste, and up to 0.465 % in mouthwash, when Hydroxyapatite (nano) is composed of rod-shaped particles of which at least 95.8 % (in particle number) have an aspect ratio less than 3, and the remaining 4.2 % have an aspect ratio not exceeding 4.9 and the particles are not coated or surface modified.

Following a regulatory proposal by the Commission services to restrict the use of Hydroxyapatite (nano) in cosmetics, industry submitted evidence to demonstrate its safety at higher concentrations in oral products. The Commission, therefore, requests the SCCS to carry out a safety assessment on Hydroxyapatite (nano) in view of the new information provided.

[1] SCCS (Scientific Committee on Consumer Safety), Opinion on hydroxyapatite (nano), 16 October 2015, SCCS/1566/15, revision of 16 March 2016.
[2] SCCS (Scientific Committee on Consumer Safety), Opinion on Hydroxyapatite (nano), preliminary version of 27-28 October 2020, final version of 30-31 March 2021, SCCS/1624/2020.
[3] SCCS (Scientific Committee on Consumer Safety), Opinion on Hydroxyapatite (nano), preliminary version 4 January 2023, final version 21-22 March 2023, SCCS/1648/22.

Terms of reference

(2) In view of the above, and taking into account the scientific data provided, does the SCCS consider Hydroxyapatite (nano) safe when used in toothpaste up to a maximum concentration of 29.5% and in mouthwash up to a maximum concentration of 10 % according to the specifications as reported in the submission, taking into account reasonably foreseeable exposure conditions?

1. Alternatively, what is according to the SCCS the maximum concentration considered safe for use of Hydroxyapatite (nano) in cosmetic products?

2. Does the SCCS have any further scientific concerns with regard to the use of Hydroxyapatite (nano) in oral cosmetic products?

3. OPINION

Preamble

3.1 CHEMICAL AND PHYSICAL SPECIFICATIONS

3.1.1 Chemical identity

3.1.1.1 Primary name and/or INCI name

From the Applicant

INCI name: Hydroxyapatite
IUPAC name: Pentacalcium hydroxide triphosphate

References: SCCS, 2023, CosIng, 2023

3.1.1.2 Chemical names

From the Applicant

Hydroxyapatite
Calcium Phosphatetribasic
Calcium Hydroxyphosphate
Pentacalcium hydroxide tris(orthophosphate)

References: SCCS, 2023

3.1.1.3 Trade names and abbreviations

From the Applicant

PhPC-2022-3 (nano)

References: SCCS, 2023, Budenheim, 2022

3.1.1.4 CAS / EC number

From the Applicant

Synthetic substance: CAS; 12167-74-7; EC: 235-330-6
Synonym: CAS: 1306-06-5; EC: 215-145-7

References: SCCS, 2023, Budenheim, 2023, Enax *et al.*, 2023 (Annex 2)

3.1.1.5 Structural formula

From the Applicant

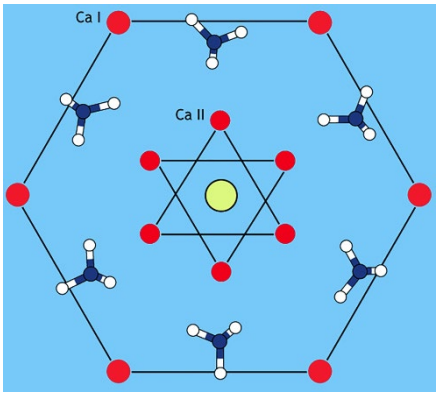

Figure 1: Schematic depiction of the hexagonal hydroxyapatite crystal structure projected down the [001] direction. Legend: Yellow=OH^-; red=Ca^{2+}, blue/white=PO_4^{3-}

Reference: Enax *et al*., 2023 (Annex 2)

3.1.1.6 Empirical formula

/

3.1.2 Physical form

From the Applicant

Liquid/paste
PhPC-2022-3 (nano) is a paste-like aqueous suspension (solid content: 29.5%)

Reference: Budenheim, 2022

3.1.3 Molecular weight

From the Applicant

502.3 g/mol ($Ca_5(PO_4)_3(OH)$)
1004.6 g/mol ($Ca_{10}(PO_4)_6(OH)_2$)

References: SCCS, 2023; Enax *et al*., 2023 (Annex 2)

3.1.4 Purity, composition and substance codes

From the Applicant

PhPC-2022-3 (nano) is a hydroxyapatite (nano) product, chemically synthesized and thus, synthetic in nature.
Purity (solid content): 29.5% (Moisture analyser (in-house method))
Water content: 70.5% (Moisture analyser (in-house method))

Composition:

Calcium:	39.6 wt%
Phosphorus (as P):	18.5 wt%
Ca:P (molar ratio):	1.67:1
P_2O_5:	12.3% (X-ray spectrometer)
CaO:	16.0% (X-ray spectrometer)
pH (1%):	9.8 (Potentiometric pH determination according DIN ISO 10523)

References: Budenheim, 2022; Enax *et al*., 2023 (Annex 2)

SCCS comments

The SCCS understands that the product PhPC-2022-3 is composed of 29.5% w/v of HAP (nano) in water, corresponding to a concentration of HAP (nano) in water equal to 295 mg/mL.

3.1.5 Impurities / accompanying contaminants

From the Applicant

Microbiology:	Total germs:	< 10 cfu/g (according to Pharm. Eu.)
	Moulds/Yeast:	< 10 cfu/g (according to Pharm. Eu.)
	Pathogenic bacteria:	absent according to Pharm. Eu.)

Reference: Microbiological CoA, 2022

Table 1: Levels of Impurities

Parameter	Unit	Value	Upper Limit	Method
Arsenic	ppm	< 1	1	Inductively coupled plasma – Mass Spectrometry (ICP-MS) based on DIN ISO 17294-2
Lead	ppm	< 1	1	
Cadmium	ppm	< 1	1	
Mercury	ppm	< 1	1	
Iron	ppm	69	100	Inductively coupled plasma optical emission spectrometry based on DIN ISO 11885
Fluoride	ppm	4	10	Photometry according to USP/NF, PhEur
Chloride	ppm	30	150	Titrimetric determination of chloride
Sulfate	ppm	160	300	Titrimetric determination
HCl-insoluble substances	%	< 0.1	0.1	According to EP and USP/NF

Reference: Budenheim, 2022

3.1.6 Solubility

From the Applicant

Hydroxyapatite (nano) is known to be insoluble or practically insoluble in water at neutral pH.
Standard water solubility: 0.0065 g/L (20 °C – EU method A.6, GLP)

Reference: SCCS, 2023a

Moreover, Hydroxyapatite (nano) is increasingly soluble in water with lower pH as is demonstrated by the Figures 2 A and B below.

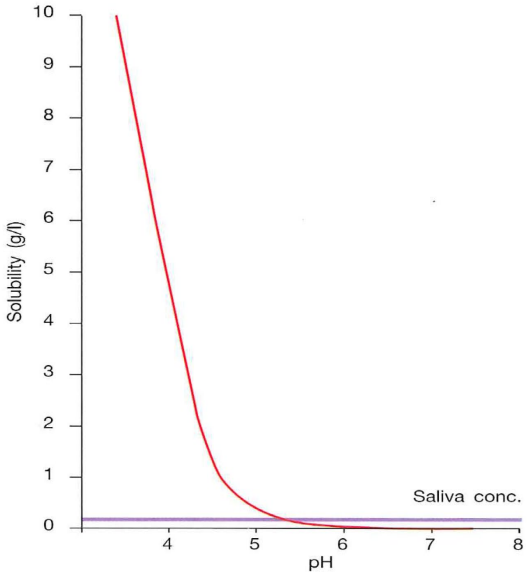

Figure 2A: Solubility of hydroxyapatite at different pH-values (Fejerskov O. and Kidd E., 2009)

Below a pH value of approximately 5.5 a dissolution of hydroxyapatite can be observed, and it is well-known that the solubility of hydroxyapatite increases strongly with decreasing pH.

As can be seen in Figure 2B, the dissolution of hydroxyapatite under acidic conditions leads to the release of physiological calcium ions, (hydrogen)phosphate ions and water. All reaction products at these physiological conditions consist of essential nutrients, necessary for the maintenance of homeostasis within normal biochemical processes in the human body at every age.

Reference: Enax *et al*., 2022

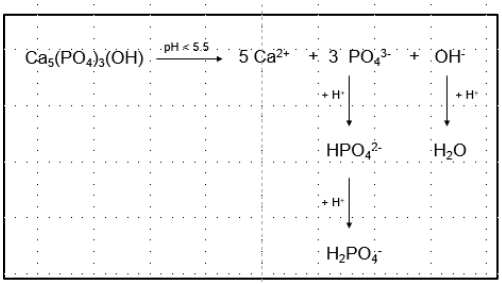

Figure 2B: Solubility reaction of hydroxyapatite in acids (Fejerskov and Kidd, 2009)

3.1.7 Partition coefficient (Log P_{ow})

From the Applicant

Not applicable.

3.1.8 Additional physical and chemical specifications

3.1.8.1 Density

From the Applicant

Density: 2.96 (± 0.02) g/cm^3, Quantachrome Penta-Pyknometer according to DIN 66137-2:2019-03

Reference: Fraunhofer, 2022 (Appendix 2 to Enax *et al*., 2023 (Annex 2))

SCCS comment
The density value provided by the Applicant, i.e. 2.96 g/cm^3, is 25% lower than the one noted by ECHA, i.e. 3.72 g/cm^3 (ref. https://echa.europa.eu/fr/registration-dossier/-/registered-dossier/15208/4/5).

3.1.8.2 X-Ray Powder Diffraction (XRD) with Subsequent Rietveld Refinement

From the Applicant

Prior to the XRD analysis, the aqueous hydroxyapatite (nano) suspension (PhPC-2022-3) was dried and gently ground before the measurement. The X-ray powder diffraction (XRD) analysis was performed with a diffractometer (Cu-K$\alpha_{1,2}$ (40 kV, 40 mA)) measured on a Si single crystalline sample holder to avoid background scattering; conditions: 2θ = 5-90°, step size: 0.01°, counting time per step: 1.5 s, total measurement time: approx. 3.5 h).

Reference: Ref 17. Annex 2 Dossier physicochemical analysis_V2.0

The X-ray powder diffractogram shows pure crystalline hydroxyapatite, without any other crystalline phase. All diffraction peaks could be assigned to hexagonal hydroxyapatite (Figure 3).

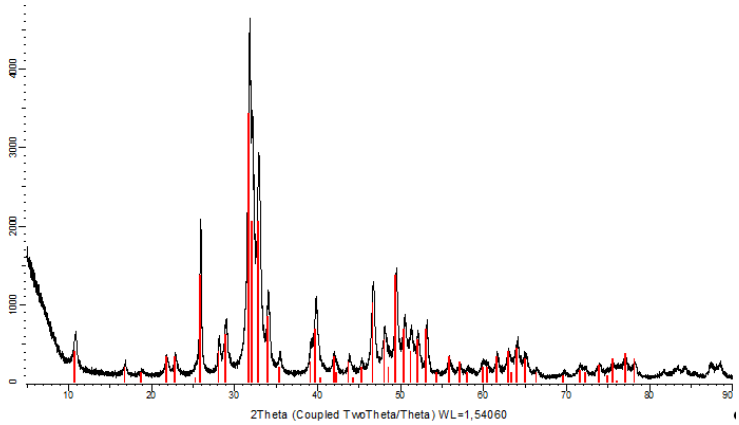

Figure 3: X-ray powder diffractogram of PhPC-2022-3 (nano) after drying and gently grinding.

The red peaks correspond to hexagonal hydroxyapatite from the ICDD database (card No.: 09-0432) [ICDD: International Centre for Diffraction Data].

The lattice parameters of hydroxyapatite (nano) were well within those of reference data (Table 2). The crystallite size was 20(1) nm, i.e., the hydroxyapatite was nanocrystalline.

To avoid confusion, it is important to consider that this number refers to the crystallite size and not to the particle size as a particle may consist of a number of crystallites.

Table 2: Lattice parameters and crystallite size of the hydroxyapatite sample PhPC-2022-3 (nano) (obtained by Rietveld-refinement) compared to reference data [ICDD: International Centre for Diffraction Data].

	PhPC-2022-3 (nano)/D20469A	**Hexagonal hydroxyapatite from database (ICDD No: 09-0432)**
a (Å)	9.425 (1)	9.418
c (Å)	6.886 (1)	6.884
V (Å)	529.8 (1)	528.8
Crystallite size (nm)	20 (1)	---

Reference: Enax *et al*., 2023 (Annex 2)

3.1.8.3 Elemental Analysis

From the Applicant

Elemental analysis of hydroxyapatite (nano) in the form of PhPC-2022-3 (nano) was performed by atomic absorption spectroscopy (AAS; calcium) and ultraviolet (UV) spectroscopy (phosphate). Calcium and phosphate analyses were performed with an atomic absorption spectrometer (AAS) [Ca^{2+}] (specific brand name omitted by the SCCS) and an ultraviolet (UV) spectrometer (specific brand name omitted by the SCCS) (PO_4^{3-} as phosphomolybdate complex) according to standard procedures. Prior to the analysis the sample was dissolved in nitric acid. The results are presented in Table 3 below.

Table 3: Calcium and phosphate contents of hydroxyapatite (nano) in the form of PhPC-2022-3 (nano) and the calculated calcium/phosphate molar ratio

	Ca^{2+}	**PO_4^{3-}**	**Calcium/phosphate molar ratio**
Sample 1: Sample 2:	141.5 g/L = 3.53 mol/L 72.6 g/L = 1.81 mol/L	203 g/L = 2.14 mol/L 98.0 g/L = 1.03 mol/L	1.65: 1 1.76: 1

The average molar calcium/phosphate ratio is 1.70:1. The different absolute concentrations in the two samples are probably due to water loss during the preparation.

The calculated calcium/phosphate molar ratio according to elemental analysis was 1.70:1 which is identical with that of stoichiometric hydroxyapatite (1.67:1) within the experimental error: The different absolute concentrations in the two samples are considered to reflect water loss during the preparation.

Reference: Enax *et al*., 2023 (Annex 2)

3.1.8.4 Energy Dispersive X-Ray Analysis (EDX)

From the Applicant

Energy-dispersive X-ray spectroscopy analyses (EDX) analysis of hydroxyapatite (nano) in the form of PhPC-2022-3 (nano) was performed with a scanning electron microscope (see images below) equipped with an EDX-detector.

The EDX analysis showed just minor ionic impurities (Na, Mg, C). However, these are considered to reflect ionic substitutions/incorporations from the synthesis including carbonate and should not be over-interpreted in quantitative terms as EDX provides only semi-quantitative analytical data.

Reference: Enax *et al*., 2023 (Annex 2)

3.1.8.5 Infrared (IR) Spectroscopy

From the Applicant

Infrared (IR) analysis (specific brand name omitted by the SCCS) of hydroxyapatite (nano) in the form of PhPC-2022-3 (nano) was performed on dried samples.

The IR spectrum shows the characteristic bands of crystalline hydroxyapatite (nano) as demonstrated in Figure 4. There were no detectable impurities, in particular no organic material that would be recognizable around 2900 cm^{-1} (C-H valence band). The sharp OH band at approximately 3600 cm^{-1} indicates well-crystalline hydroxyapatite (nano).

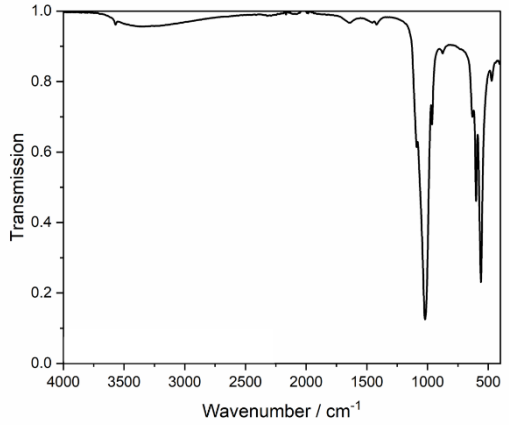

Figure 4: Infrared (IR) spectrum of dried hydroxyapatite (nano) in the form of PhPC-2022-3 (nano)

References: Enax *et al*., 2023 (Annex 2), Ref 17. Annex 2 Dossier_physicochemical analysis_V2.0

3.1.9 Particle size

3.1.9.1 Pure (Pristine) Hydroxyapatite (nano)

From the Applicant
The pure hydroxyapatite (nano) in the form of PhPC-2022-3 (nano) was analysed by transmission electron microscopy (TEM) and energy-dispersive X-ray spectroscopy (EDX) to characterize the hydroxyapatite (nano) primary particles and their aggregation/ agglomeration state. The stability of suspension was assessed by dynamic light scattering (DLS) analysis.

a) **Transmission Electron Microscopy (TEM) and Energy-Dispersive X-Ray Spectroscopy (EDX) Analysis:**

Hydroxyapatite (nano) in the form of PhPC-2022-3 (nano) was analysed by transmission electron microscopy coupled with energy dispersive X-ray spectroscopy previously diluted in

ultrapure water to a final concentration of 59 ng of hydroxyapatite (nano)/ml. Particle size analysis was performed manually by processing the images with the dedicated ImageJ software and size measurements (both length and width) of at least 500 particles were collected to assure statistical robustness of the results. In compliance with ECHA "Appendix for nanoforms applicable to the Guidance on Registration and Substance Identification" (Reference: ECHA, 2022), dimensions of individual particles were measured tracing segments corresponding to the longest dimension (i.e., length) and the smallest dimension perpendicular to it (i.e., width). Figure 5A reports an example of the segments used to determine length and width of particles. According to ECHA guidance, the aspect ratio (AR) of each individual particle was calculated as length to width ratio.

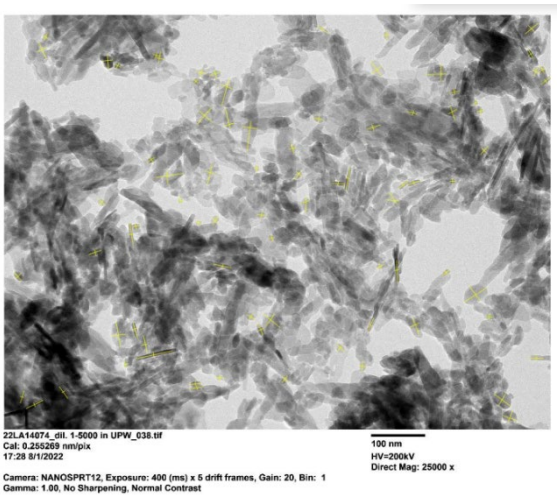

Figure 5A: Example of manual size measurements on Transmission Electron Microscopy (TEM) micrographs of hydroxyapatite (nano). Yellow lines represent segments used to obtain length and width and calculate the AR of particles. To avoid errors, only clearly visible particles were measured.

Length and width

Figures 5B (a, b, c) report representative transmission electron microscopy (TEM) micrographs of PhPC-2022-3 (nano) diluted in ultrapure water to a final concentration of nanohydroxyapatite of 59 ng hydroxyapatite (nano)/mL (dilution factor: 5000x). Primary particles are rod-shaped with rounded edges, and they form ellipsoidal/spheroidal aggregates/agglomerates made of tens to hundreds of particles. EDX analysis (Figure 3.1.9 – B (d)) confirms the presence of calcium (Ca), phosphorous (P), and oxygen (O) as constitutive elements of hydroxyapatite. Signals of carbon (C) and nickel (Ni) in the spectrum are due to the carbon-coated nickel grid used as sample support. To define number-based primary particle size distribution, both length and width were independently measured.

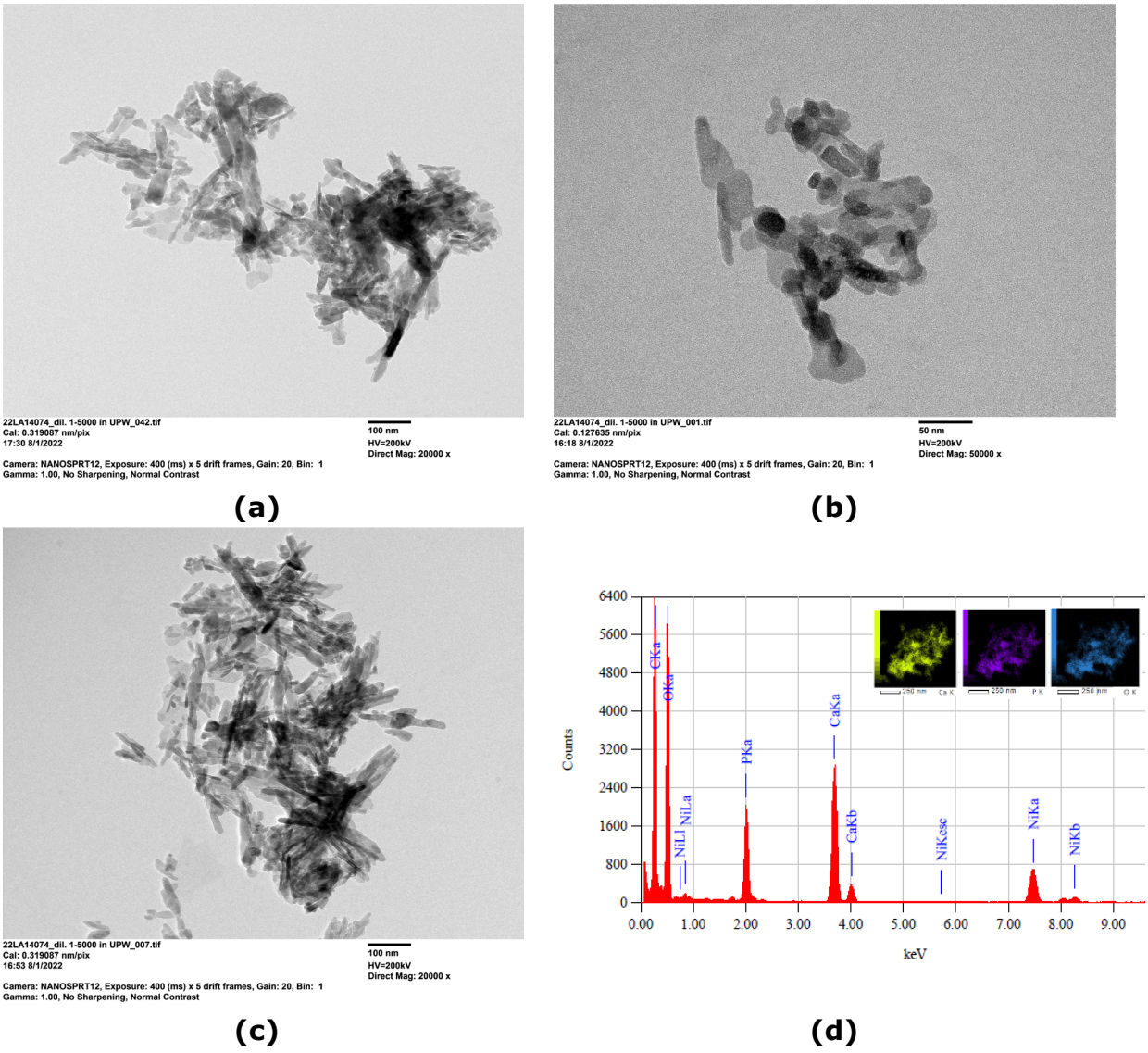

Figure 5B: Transmission electron microscopy (TEM) number-based primary particle size distribution of hydroxyapatite (nano) in the form of PhPC-2022-3 (nano) diluted 1:5000 in ultrapure water. TEM micrographs at magnitude (a) 20000x, (b) 50000x, (c) 20000x. EDX spectrum of particles (d). Signals of Carbon (C) and Nickel (Ni) in the spectrum are due to the carbon-coated nickel grid used as sample support.

The median particle length and width obtained on a significant number of measured particles (≥ 500 particles) are 21 nm and 12 nm, respectively.

Thus, the median value of both dimensions in the detected particles falls within the range 1-100 nm, the analysed hydroxyapatite (nano) in the form of PhPC-2022-3 (nano) was confirmed to represent a nano-scaled material.

The detailed elements related to the size distribution (length and width) are reported in Annex A.

Aspect ratio
The detailed elements related to the aspect ratio distribution are reported in Annex A.

The descriptive parameters of particle AR distribution were produced and reported as minimum, first quartile, median, median absolute deviation (MAD), mean, standard deviation,

third quartile, maximum and 10th, 50th and 90th percentiles. The 10th, 50th and 90th percentile values correspond to the minimum threshold below which 10 %, 50 % and 90 % of the particles in the distribution have an aspect ratio smaller than these values, respectively. Therefore the 50th percentile corresponds to the median value of the aspect ratio.

The ratio between length (measured as the longest dimension) and its associated width (measured as the smallest dimension perpendicular to length) was calculated producing the AR of each individual particle analysed by TEM-EDX.

In the analysed particles, AR ranges from 1.00 (lower limit) to 8.97 (upper limit) with median (i.e., 50th percentile) ± MAD of 1.51 ± 0.26. Average ± standard deviation is 1.96 ± 1.19. AR values corresponding to 10th and 90th percentile are 1.19 and 3.31 respectively, indicating that 10 % and 90 % of particles have AR smaller than these values. The aspect ratio analysis in this respect demonstrated that at least 87.2% (in particle number) had an aspect ratio of less than 3, while the remaining 12.8% had an aspect ratio greater that 3 but not exceeding 8.97, when calculated on a significant number of hydroxyapatite (nano) particles (522).

SCCS comments on aspect ratio
The SCCS noted that the aspect ratio of pristine HAP (nano) particles, between length (measured as the longest dimension) and its associated width (measured as the smallest dimension perpendicular to length), was calculated for each individual particle analysed by TEM-EDX.

The SCCS general comments on the pristine HAP (nano)
The descriptive parameters provided for the pristine materials (median length and width, min and max length, min and max width; AR average, AR median, AR 3rd quartile, AR 90th percentile, AR max) are as follows:
• **Length:** 21 ± 3 nm (median), 8 ± 1 nm (min.), 122 ± 43 nm (max.)
• **Width:** 12 ± 3 nm (median), 4.8 ± 0.6 nm (min.), 49 ± 17 nm (max.)
• **Aspect Ratio (AR):** 1.96 (average), 1.51 (median), 2.02 (AR 3rd quartile), 3.31 (AR 90th percentile), 8.97 (AR max), with 12.8% of particles exhibiting an AR equal to or larger than 3.0.

b) **Dynamic Light Scattering (DLS) Analysis:**

From the Applicant

Hydroxyapatite (nano) in the form of PhPC-2022-3 (nano) was analysed by dynamic light scattering (DLS) analysis according to DIN ISO 22412:2018-09.

Analysis by DLS showed a nanoparticulate particle size distribution with an average particle size (X_{DLS}) of 205 nm (± 5%) (Figure 5C), which agrees with the scanning electron microscopy (SEM) analysis (see Figure 5D below). The polydispersity index (PDI) was calculated to be 0.21 and therefore it was demonstrated that hydroxyapatite (nano) in the form of PhPC-2022-3 (nano) is a monodisperse material as the PDI was below the threshold of 0.3.

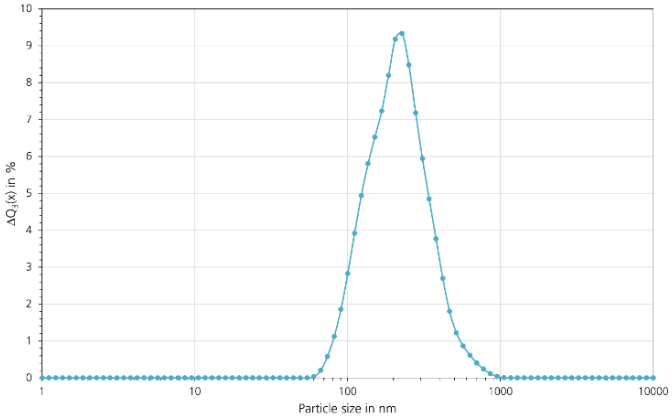

Figure 5C: Volume-weighted particle size distribution by Dynamic light scattering (DLS) analysis of hydroxyapatite (nano)

Reference: Enax *et al*., 2023 (Annex 2)

c) **Scanning Electron Microscopy (SEM):**

From the Applicant

Scanning electron microscopy (SEM) analysis of the pure hydroxyapatite (nano) in the form of PhPC-2022-3 (nano) was performed on palladium-gold sputtered samples.

The SEM-analysis showed nanosized rod-shaped (approx. 100-200 nm length) hydroxyapatite nano-crystallites with a mostly homogeneous particle size distribution as is demonstrated in Figure 5D, below.

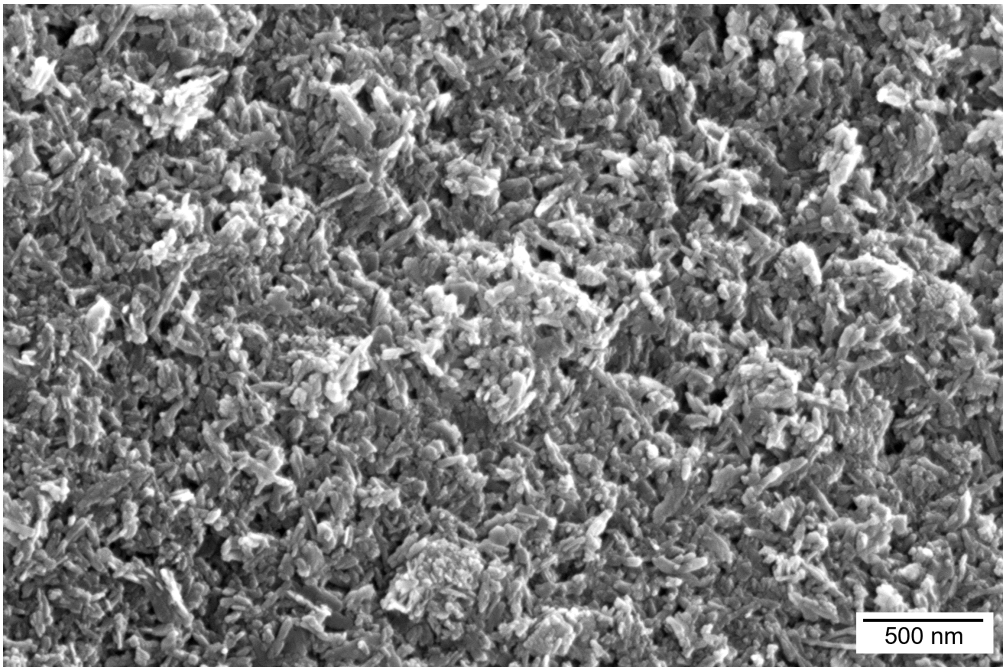

Figure 5D: Scanning electron microscopy (SEM) image of hydroxyapatite (nano)

Reference: Enax *et al*., 2023 (Annex 2)

Overall, the above presented results showed clearly that the investigated hydroxyapatite (nano) in the form of PhPC-2022-3 (nano) is a clear nanoparticular material with a median

primary particle length and width of 21 nm and 12 nm, respectively. It is a monodisperse material and consists of chemically and crystallographically pure nanoparticulate hydroxyapatite in a rod-shaped form.

3.1.9.2 Hydroxyapatite (nano) in Cell Culture Media

From the Applicant

The particle size distribution of dispersed hydroxyapatite (nano) in the form of PhPC-2022-3 (nano) in cell culture media used for genotoxicity tests was analysed by TEM and DLS.
Besides the morphological analysis, the primary aim was the selection of appropriate concentrations of the subsequently performed Micronucleus Test (MNT) and Mouse Lymphoma Assay (MLA).

For the DLS analysis, the samples were diluted in the cell culture media used for the MNT and MLA with and without metabolic activation (S9) reagent. Cell culture media as such were used as blank. In the presence of comparable average particle sizes between two consecutive dilutions, the one with higher reproducibility among replicates (i.e., lower relative standard deviation) was selected as the first visible precipitate-free dispersion to be used for genotoxicity tests, and no further dilutions were applied. TEM analyses of the most suitable concentrations were also performed, with the aim of assessing particle size and aggregation/agglomeration state of hydroxyapatite (nano) particles.

The "PhPC-2022-3 nano-hydroxyapatite (aqueous suspension) », batch n° D204669A used in this study contained 29.5 % of nano-hydroxyapatite, which is the nanomaterial to be tested. Hence for example, to prepare the concentration of 20 g/mL of nano-hydroxyapatite, 67.7960 mg of "PhPC-2022-3 nano-hydroxyapatite (aqueous suspension)", batch D20469A are weighted per mL of F10 medium. In detail, a stock solution of test substance was prepared by dilution 1102.5 mg in 16.26 mL of F10 medium in order to obtain the first working solution of 20 g/mL of nano-hydroxyapatite.

Ref.: Ref 4 22.523987.00001_FR_signed MLA,
from Dossier Submission References

Table 4: Concentration of PhPC-2022-3 (nano) and corresponding concentration of hydroxyapatite (nano)

PhPC-2022-3 (nano) concentration (mg/mL)	**Hydroxyapatite (nano) concentration (mg/mL)**
1.6949	0.5000
0.8475	0.2500
0.4237	0.1250
0.2119	0.0625
0.1059	0.0313
0.0530	0.0156
0.0265	0.0078
0.0132	0.0039
0.0066	0.0020

Finally, it can be concluded that hydroxyapatite (nano) predominantly retained its agglomeration/aggregation state in cell culture media.

MNT and MLA cell culture media
Stable conditions with no visible precipitates were identified. In the presence of MNT cell culture medium without S9, particles were stable without forming precipitates at a concentration of 0.0313 mg/ml.

In the presence of MLA cell culture medium without S9 the first concentration considered stable and without precipitates was 0.0156 mg/ml.

DLS analysis was not suitable to define hydroxyapatite (nano) stability in cell culture media with S9 as the DLS signal was highly unstable and not reproducible probably due to available aggregate/agglomerates.

Therefore, the two conditions without visible precipitates were selected for TEM analysis, i.e., 0.0625 mg/mL for MNT cell culture medium with S9; and 0.0078 mg/mL for MLA cell culture medium with S9, respectively.

Based on these findings, the respective stable concentrations without forming precipitates were selected for the MNT and MLA studies.

SCCS comment
Table 5 below, which provides a summary, has been prepared by the SCCS to help put the concentration quotations used by Applicants for the MNT and MLA test conditions into perspective. The "*" has been added by the SCCS to distinguish the tests without and with S9.

Table 5: HAP (nano) concentrations in MNT and MLA culture cell media (adapted by the SCCS)

HAP (nano) concentration (mg/mL)	MNT without S9	MNT with S9	MLA without S9	MLA with S9
0.1250	/	C1*	/	/
0.0625	C1	C2* (ii)	/	/
0.0313	C2 (i)	C3*	C1	/
0.0156	C3	/	C2 (i)	C1*
0.0078	/	/	C3	C2* (ii)
0.0039	/	/	C4	C3*
0.0020	/	/	C5	C4*
0.0010	/	/	/	C5*

(i): Conditions without visible precipitate for MNT cell culture without S9, i.e. 0.0313 mg/mL and for MLA cell culture without S9, i.e. 0.0156 mg/mL
(ii): Conditions without visible precipitates were selected for TEM analysis, i.e., 0.0625 mg/mL for MNT cell culture medium with S9; and 0.0078 mg/mL for MLA cell culture medium with S9

Particle size and aspect ratio
The fully detailed elements for HAP (nano) particle sizes and aspect ratio provided by the Applicant are reported in Annex C and in Annex D for the MLA and MNT assays, respectively. The HAP (nano) particle size and aspect ratio distributions in the MLA and MNT assays reported in Annex C and Annex D are based on measurement of each individual particle.

Table 6: Particle size of HAP (nano) as a function of the assay condition at the first concentration without visible precipitates (Median Length, median width and aspect ratio) - for full information of all the tested conditions, see Annexes B, C and D.

Assay condition	Median Length (nm)	Median Width (nm	Median Aspect Ratio
Pristine HAP (nano)	21 ± 3	12 ± 3	1.51**
Micronucleus Test (MNT) Medium without S9 (0.0313 mg/mL)*	21	13	1.62***
Micronucleus Test (MNT) Medium with S9 (0.0625 mg/mL)	22	12	1.83***
Mouse Lymphoma Assay (MLA) Medium without S9 (0.0156 mg/mL)*	20	12	1.67***
Mouse Lymphoma Assay (MLA) Medium with S9 (0.0078 mg/mL)*	24	14	1.71***

(*): First concentration without visible precipitates.
(**): Median aspect ratio calculated from aspect ratio distribution determined for each individual particle
(***): Median aspect ratio calculated from median length and median width of particle size distribution

SCCS comments

i) Aspect ratio

The SCCS noted that the aspect ratio of HAP (nano) particles in MLA culture media, reported in the above Table (Table 6) was not issued from a number-based distribution of aspect ratio calculated on each individual HAP (nano) particles. The aspect ratio was calculated as the ratio of median length to median width.

ii) Presence of fibre shape HAP (nano) particles in MNT and MLA cell culture media

The characterisation data for the test material used for MNT (Table 7) and MLA (Table 8) tests based on individual HAP (nano) particle size and aspect ratio (see Annexes C and D) indicate that for some MNT and MLA conditions, the AR 90th percentile was equal to or greater than 3, which is regarded as the threshold between rod shape and fibre shape:

Table 7: Aspect Ratio (AR) 90th percentile under the MN test conditions:

AR 90th percentile	Codifications	Concentration (mg/mL)	S9	Exposure
3.13	MNT (C1* 4h +S9)	0.1250	with S9	after 4h
3.04	MNT (C3* +S9 before exposure)	0.0313	with S9	before exposure
3.03	MNT (C2* +S9 before exposure)	0.0625	with S9	before exposure
3.01	MNT (C3 24h – S9)	0.0156	without S9	after 24h

Table 8: Aspect Ratio (AR) 90th percentile under the MLA test conditions:

AR 90th percentile	Codifications	Concentration (mg/mL)	S9	Exposure
4.47	MLA (C2*+S9 before exposure)	0.0078	with S9	before exposure
4.15	MLA (C4 24h – S9)	0.0390	without S9	after 24 h
4.09	MLA (C5–S9 before 24h exposure)	0.0020	without S9	before exposure
4.07	MLA (C3* + S9 before exposure)	0.0039	with S9	before exposure
3.80	MLA (C1 4h – S9)	0.0313	without S9	after 4h
3.76	MLA (C4 – S9 before 4h exposure)	0.0039	without S9	before 4h exposure
3.72	MLA (C1 24h – S9)	0.0313	without S9	after 24h
3.66	MLA (C3 – S9 before 24h exposure)	0.0078	without S9	before 24h exposure
3.65	MLA (C5 24h – S9)	0.0020	without S9	after 24h
3.57	MLA (C1 - S9 before 4h exposure)	0.0313	without S9	before 4h exposure
3.56	MLA (C4* 0h + S9 before exposure)	0.0020	With S9	before exposure
3.56	MLA (C1* 0h + S9 before exposure)	0.0156	With S9	before exposure
3.54	MLA (C4 4h – S9)	0.0039	without S9	after 4h
3.54	MLA (C5* 4h + S9)	0.0010	with S9	after 4h
3.34	MLA (C5* + S9 before exposure)	0.0010	with S9	before exposure
3.33	MLA (C1 - S9 before 24 h exposure)	0.0313	without S9	before 24h exposure
3.08	MLA (C2* 4h + S9)	0.0078	With S9	after 4h
3.02	MLA (C2 24 – S9)	0.0156	without S9	after 24 h

10% of particles exhibit aspect ratio > 3. Data indicate that for the above-listed MNT and MLA culture cell media test conditions, whilst most (90th percentile) of the particles are rod shaped, a fraction of the particles can be considered to be at the borderline between rod and fibre shapes.

SCCS comment
The SCCS has noted that the aspect ratio of the test materials was more or less the same (3.01 up to 3.13) in MNT conditions, but there was a significant change (3.02 up to 4.47) under MLA conditions of the cell culture media.

3.1.10 Crystal structure

/

3.1.11 UV absorption

/

3.1.12 Surface characteristics

From the Applicant:

The surface area was determined by Brunauer–Emmett–Teller (BET) measurement.

The analysis of the specific surface area according to BET requires to extract the particles from the suspension. This was realized by freeze drying. Specific surface area according to BET and powder density were measured at the dried sample. The reproducibility of BET measurements was ± 5 %, while for density measurements ± 0.02 g/cm³ were considered. The obtained results are summarized in Table 9.

Table 9: Results of the surface area characteristics including accompanied parameter for PhPC-2022-3 (nano)

Parameter	Result
pH value	10.7
Specific surface area in m²/g	90.6 (± 5%)
Specific surface area in m²/cm³	269 (± 5%)
Density in g/cm³	2.96 (± 0.02)

References: Fraunhofer, 2022 (Appendix 2 to Enax *et al*., 2023 (Annex 2), Ref 17 Annex 2 Dossier_physicochemical analysis_V2.0, Ref 23 Appendix 2_Report_Fraunhofer

SCCS comment
The SCCS notes that the "surface area" expressed as m^2/cm^3 in Table 9 *(based on information issued from Tab. 5: Density and specific surface area (BET) of PhPC-2022-3 (nano), Ref 17 Annex 2 Dossier_physicochemical analysis_V2.0)* should have been named as Volumic Specific surface area (i.e. VSSA), instead of Specific Surface area (i.e. SSA).

3.1.13 Zeta Potential

From the Applicant

Zeta potential: -29.5 ± 1.4 (pH 10.3, Electrophilic Light Scattering (ELS) according to ISO 13099-2:2012-06)

Reference: Fraunhofer, 2023

3.1.14 Homogeneity and stability

From Applicant
Shelf-life of hydroxyapatite (nano), i.e., PhPC-2022-03: at least 18 months (CoA)

Reference: Budenheim, 2022

3.1.15 Dispersibility

The SCCS notes: the assessment of dispersibility described below was provided along with the study on gene mutations at the *Hprt* locus using the Chinese hamster cell line V79.

From the Applicant

As part of the main experiment, approx. 2 ml of the solvent control and of the test item concentrations of 6.4, 16, and 100 µg/mL were collected and measured by DLS for 24 hours in order to analyse the stability of the suspension and the agglomeration/aggregation behaviour of the test item in culture medium over the time.

These samples were sent via direct transfer at ambient temperature.

This data is used to reflect the stability of the suspension and agglomeration/aggregation behaviour of the test material during the cell culture exposure in the genotoxicity experiment.

As stated in the Short Report (No. RICC005, non-GLP conditions): "For neither of the nanoparticle samples a systemic change in the particle size could be observed in the tested frame".

Reference: From ICCR Study Number: 4114412, extracted pages 15 – 16, from Annex 5 - Report 4114412 (ICCR, 2024; Fraunhofer IAP, 2024; ZentriForce, 2024)

The details (experiment protocol and results) of the study of the stability of the suspension and agglomeration/aggregation behaviour of the test material during the cell culture exposure in the genotoxicity experiment is reported in Annex G.

The following Tables indicate the averages and standard deviation of z-average and intensity-based D10, D50 and D90 at T0 and Tend (at 37°C for 24 hours).

Table 10 (corresponding to Table Annex G.4, in Annex G): Averages and standard deviation of z-average and intensity-based D10, D50 and D90 radii, T0 as a function of the different concentrations (0, 6.4 ug/mL, 16 ug/mL and 100 ug/mL)

Sample name	z-average diameter (nm)	z-average radius (nm)	D10 (nm)	D50 (nm)	D90 (nm)
4114412 - 1.1	16.3 ± 0.3	8.1 ± 0.2	3.2 ± 0.1	11.7 ± 0.6	59.7 ± 15.0
4114412 - 6.1	28.4 ± 7.5	14.2 ± 3.7	3.3 ± 0.2	21.2 ± 10.2	160.9 ± 51.0
4114412 - 7.1	48.9 ± 27.1	24.4 ± 13.5	3.6 ± 0.6	48.8 ± 55.4	139.8 ± 55.5
4114412 - 9.1	238.0 ± 27.2	119.0 ± 13.6	86.1 ± 24.7	127.6 ± 13.0	287.9 ± 149.3

Table 11 (corresponding to Table Annex G.7, in Annex G): Averages and standard deviations of z-average and intensity-based D10, D50 and D90 radii, Tend as a function of the different concentrations (0, 6.4 ug/mL, 16 ug/mL and 100 ug/mL).

Sample name	z-average diameter (nm)	z-average radius (nm)	D10 (nm)	D50 (nm)	D90 (nm)
4114412 - 1.1	15.6 ± 0.2	7.8 ± 0.1	3.1 ± 0.1	10.6 ± 0.4	58.5 ± 10.2
4114412 - 6.1	32.6 ± 0.4	16.3 ± 0.2	3.3 ± 0.1	20.2 ± 1.1	172.0 ± 19.9
4114412 - 7.1	58.3 ± 17.7	29.2 ± 8.8	3.7 ± 0.4	78.9 ± 19.5	239.0 ± 147.3
4114412 - 9.1	203.5 ± 19.0	101.8 ± 9.5	79.5 ± 14.6	117.0 ± 15.6	164.6 ± 19.3

Conclusion by the Applicant of the DLS accelerated stability experiment
The z-average diameter of the solvent control sample was 16.3 nm at T0 and 15.6 nm at Tend.
The z-average diameters ranged from 28.4 nm to 238 nm at T0, and from 32.6 to 203 nm at Tend.
For neither of the nanoparticle samples, a systematic change in the particle size could be in the tested time frame.

Reference: Annex 3 - Short Report Nano characterization of the test solution with dynamic light scattering (DLS) (non-GLP) - Final Technical Report – DLS Accelerated Stability Study, extracted from document named Annex 5 - Report 4114412 (ICCR, 2024; Fraunhofer IAP, 2024; ZentriForce, 2024)

SCCS comment

i) DLS measurement of accelerated study performed at 37°C from T0 up to Tend
The SCCS does agree that the accelerated study performed at 37°C for 24 hours did not lead to a systematic change in the particle size distribution based on DLS measurements.
The Applicant did not give a clear description in the dispersibility report of how the suspension was prepared. Information could be found in the toxicological report provided by the Applicant (attached to the mutagenicity study).
The detection of particles in the solvent control has been attributed by the Applicant to cell culture medium components such as serum proteins ((Ref 11 22.523987.00001_FR_Attachment_3 MLA uptake).

ii) Comparison of the particle size distribution (DLS measurement) between the PhPCC-2022-3 (nano) suspension and performed accelerated study performed at 37°C during 24 hours
The particle size distribution measured by DLS on the pristine PhPCC-2022-3 (nano) is different from the one measured after accelerated stability experiment, according to the following observations:
Pristine materials: Analysis by DLS showed a nanoparticulate particle size distribution with an average particle size (X_{DLS}) of 205 nm (± 5%). The polydispersity index (PDI) was calculated to be 0.21

Reference: Enax *et al*., 2023 (Annex 2)

Accelerated stability experiment: The z-average diameters ranged from 28.4 nm (6.4 ug/mL), 48.9 nm (16 ug/mL) to 238 nm (100 ug/mL) at T0, and from 32.6 (6.4 ug/mL), 58.3 nm (16 ug/mL) to 203 nm (100 ug/mL) at Tend.

Reference: Annex 3 - Short Report Nano characterization of the test solution with dynamic light scattering (DLS) (non-GLP) - Final Technical Report – DLS Accelerated Stability Study, extracted from document named Annex 5 - Report 4114412 (ICCR, 2024; Fraunhofer IAP, 2024; ZentriForce, 2024), provided in September 2024

3.1.16 Other parameters of characterisation

/

SCCS comment
According to the information provided previously, the nanoparticle form of the hydroxyapatite material considered here is fully synthetic and inorganic. It is a white, odourless paste. The manufacturing process for HAP (nano) involves continuous wet chemical precipitation carried out close to room temperature, which results in a diluted slurry. As such, the process does not involve any calcination step (Ref.: SCCS/1624/20 Final Opinion).

3.1.17 Summary on supplementary physicochemical characterisation

From the Applicant

Hydroxyapatite (nano) in the form of PhPC-2022-3 (nano) was comprehensively characterized with various analytical methods in compliance to the most recent SCCS requirements.
It is fully synthetic and inorganic in nature and consists of rod-shaped particles as demonstrated by scanning electron microscopy (SEM). Elemental analysis revealed a calcium/phosphate molar ratio of 1.70:1, and X-ray powder diffraction (XDR) and infrared (IR) analysis confirmed that it is a crystalline hydroxyapatite (nano).

Transmission electron microscopy (TEM) analysis demonstrated a median primary particle length and width of 21 nm and 12 nm, respectively. In cell culture media hydroxyapatite (nano) retained predominantly its agglomeration/aggregation state and stable conditions with no visible precipitates were evident at lower concentrations, while higher concentrations revealed precipitates. Based on these findings appropriate concentrations were selected for a subsequently performed Micronucleus Test (MNT) and Mouse Lymphoma Assay (MLA).

The analyses of TEM images on hydroxyapatite (nano) revealed Aspect Ratio (AR) values corresponding to 10^{th} and 90^{th} percentile of 1.19 and 3.31 respectively. This indicated that at least 87.2% (in particle number) have an aspect ratio of less than 3, and the remaining 12.8% have an aspect ratio greater than 3 but not exceeding 8.97.

The surface area determined by Brunauer–Emmett–Teller (BET) demonstrated a specific surface area of 269 m^2/cm^3 and a Zeta potential of -29.5 ± 1.4 was shown by Electrophilic Light Scattering (ELS) analysis.

Hydroxyapatite (nano) is known to be insoluble or practically insoluble in water at neutral pH but is increasingly soluble in water with lower pH. Below a pH value of approximately 5.5 a dissolution of hydroxyapatite can be observed which leads to the release of calcium ions, (hydrogen)phosphate ions, and water.

The stability of the tested hydroxyapatite (nano) during a longer period was guaranteed as the shelf-life is at least 18 months.

Reference: SCCS Dossier on Hydroxyapatite (nano)
KG 2023-08-09

3.2 TOXICOKINETICS

3.2.1 Dermal / percutaneous absorption

From the Applicant

No information available. However, as the submission is intended for oral care use only, a dermal absorption study is considered to be not necessary for this type of use.

SCCS comment
The SCCS agrees that a dermal absorption study is not necessary for HAP (nano), as it is intended for use in oral products.

3.2.2 Other studies on toxicokinetics

From the Applicant

The possible penetration into buccal mucosal cells was studied in two types of three-dimensional (3-D) reconstituted human oral epithelial models. The results indicated clearly that the nanoparticles of the tested analogue hydroxyapatite (nano) form did not penetrate the stratum corneum in SkinEthic HGE samples and penetrated only the outermost layer of cells without stratum corneum. It was shown that there was no permeation into the deeper layers of the epithelium in either tissue model.

Absorption by gastric compartment and stability of an analogue hydroxyapatite (nano) form confirmed that the material would solubilize in the gastric fluid, if ingested.

References: Dossier on Hydroxyapatite (nano)
KG 2023-08-09; Ramis *et al*., 2018; SCCS 2021, 2023a

SCCS comment
In response to the SCCS concerns expressed in the letter to the Applicant on potential internal uptake of HAP (nano) via buccal mucosal cells as reported by Ramis *et al*. (2018) and cytotoxicity, the Applicant provided a new study. The summary of the study with the SCCS comments on the study are presented below.

From the Applicant

***IN VITRO* BIOCOMPATIBILITY AND IRRITATION OF BIOMIMETIC HYDROXYAPATITE NANOPARTICLES ON HUMAN ORAL EPITHELIUM**

Study design summarised by the SCCS:

Reference:	Report 202400112-01 (TERCIT, 2024)
Date of report:	18.09.2024
Study period:	May – sept 2024
Guideline:	/
Test system:	SkinEthic™ Human Oral Epidermal model comprised of TR146 cells
Replicates:	6 replicates: 3 for MTT assay and 3 for histological evaluation
Test substance:	Hydroxyapatite (nano) Ph-PC-2022-3
Batch (Purity):	D20469A
Vehicle:	PBS
Concentrations#:	47.3, 0.092 and 0.046 mg/mL
Treatment:	48 hours
Positive controls:	Triton™ X-100: PBS + 1% Triton™ X-100
Negative control:	PBS
GLP:	No
Published:	No

Objective
The objective of this study was to determine the biocompatibility and possible irritation potential of hydroxyapatite nanoparticles (HAP-NP) on human oral mucosa epithelial tissue. The study was conducted in alignment with previous studies on HAP-NP published in Ramis *et al.* (2018) and in accordance with the "SCCS Notes of guidance for the testing of cosmetic ingredients and their safety evaluation" in its 12th revision (SCCS/1647/22) and "Guidance on the safety assessment of nanomaterials in cosmetics" in its 2nd revision (SCCS/1655/23). An *in vitro* model of reconstructed human oral epithelium (HOE) was employed to assess the impact of biomimetic HAP-NP. The *in vitro* endpoints selected for analysis included the 3-(4,5-Dimethylthiazol-2-yl)-2,5-Diphenyltetrazolium bromide, abbr. MTT, metabolism assay of cell viability, enzyme release (lactate dehydrogenase activity, abbr. LDH), and inflammatory cytokine release (interleukin-1 alpha, abbr. IL-1α). Additionally, histological analyses were

performed for detailed visualization of the overall tissue architecture, enabling the identification of any morphological changes or damage caused by the HAP-NP. Fluorescence staining with OsteoImage™ Mineralization Assay, Von-Kossa staining and transmission electron microscopy (TEM) of HAP-NP exposed HOE tissue cells were performed to determine the presence of calcium deposits, HAP-NP and its possible cellular uptake.

References: Ramis *et al.* (2018), SCCS/1647/22, SCCS/1655/23

Methods

Reconstructed Human Oral Epithelium

The Human Oral Epithelium (HOE) (EpiSkin™, Lyon, France https://www.episkin.com/HOE-Oral-Epithelium) is an *in vitro* reconstructed human oral epithelium (HOE) consisting of an airlifted, living, multi-layered tissue construct produced in polycarbonate inserts in a serum-free and chemically defined medium. The SkinEthic™ HOE model comprises TR146 cells (derived from a squamous cell carcinoma of the buccal mucosa) cultivated on an inert polycarbonate filter at the air-liquid interface in a chemically defined medium. This model forms an epithelial tissue devoid of stratum corneum, resembling histologically the mucosa of the oral cavity, featuring normal ultrastructure and functionality similar to human oral mucosa epithelium.

The HOE (size 0.5 cm^2, Batch Number 24-HOE-022_S) were shipped at room temperature in a multiwell plate filled with an agarose-nutrient solution in which they are embedded. HOE tissues were processed upon arrival following the manufacturer's protocol and incubated overnight in a cell incubator at 37 °C, 5% CO_2 and saturated humidity.

Samples

The Applicant provided a suspension of HAP-NP (Ref. Ph-PC-2022-3, Batch Number D20469A) with a solid content of approximately 29.5%, according to the certificate of analysis provided, dated 18/05/2022, and with an absence of microbial contamination (germs < 10 cfu/g; moulds/yeast < 10 cfu/g) and with expiry date until December 12/2024. The sample was kept at room temperature (RT) until use. A pH of 9.8 was obtained from a 1% or 10 mg/ml suspension in water.

Treatments

The protocol procedure was followed to prepare the treatments for biocompatibility and irritation assessment, as follows: after mixing for 30 seconds with a vortex mixer and immediate processing, the highest test concentration C1 (47.25 mg/mL HAP-NP) was prepared by taking 1.6 mL of Ph-PC-2022-3 sample (29.5% HAP-NP) and adding up to 10 mL of Dulbecco's Phosphate Buffered Saline (PBS) (1x) (specific brand name omitted by the SCCS) (Ref. PBS-1A). After that, a series of 1:2 dilutions were performed by mixing the suspension for 30 seconds with a vortex mixer and processing it immediately by taking 5 mL of suspension and 5 mL PBS. The pH of the obtained solutions was measured with a pH-meter (specific brand name omitted by the SCCS).

For treating the HOE tissues, C1 and two additional concentrations were selected based on the following conditions: the highest concentration that shows no visible precipitates at the bottom of the vial after 30 minutes at room temperature (C1/1024 ≙ 0.046 mg/mL), and the lowest concentration that shows visible precipitation (C1/512 ≙ 0.092 mg/mL). Finally, concentrations given in the Table below were subsequently tested in this study.

According to that, the treatments evaluated were:

(1) control: PBS (Negative control)
(2) Triton™ X-100: PBS + 1% Triton™ X-100 (Positive control)
(3) C1 (47.3 mg HAP-NP/mL)
(4) C1/512 (0.092 mg HAP-NP/mL)
(5) C1/1024 (0.046 mg HAP-NP/mL)

Treatments were prepared in sterile conditions, and pH was adjusted to physiological levels and values relevant to the sponsor's planned application in cosmetic oral care products (pH 7.3 ± 0.3) using either NaOH 0.1M or HCl 1M.

Table: Concentrations of HAP-NP for the biocompatibility study

Dilution	C1	C1/512	C1/1024
mg/mL	47.3	0.092	0.046
pH	7.33	7.32	7.35

Experimental setup
Treatments were administered on top of the tissues (40 µL) after a maintenance media change. Each condition was assessed with 6 different replicates. Tissues were incubated for 48 h in a cell incubator at 37 °C, 5% CO_2 and saturated humidity with the treatments. After that, half of the replicates (n=3 per condition) were submitted to MTT evaluation. The other half was fixed for histological examination with haematoxylin and eosin (H&E) and Von-Kossa staining (specific brand name omitted by the SCCS) and TEM (transmission electron microscopy) evaluation. Incubation media was kept for further analyses: LDH activity and IL-1α quantification.

LDH activity
Lactate dehydrogenase (LDH) activity in the culture media at the end of the 48h incubation period was used as an index of cell death. LDH activity was determined spectrophotometrically.
50 µl of culture medium and 50 µl of the reaction mixture were incubated for 30 min at 25 °C. Oxidation of NADH at 490 nm in the presence of pyruvate, was measured according to the manufacturer's kit instructions (specific brand name omitted by the SCCS). Results are presented as a percentage of the LDH activity compared to negative control for each time point (mean ± SEM).

Viability test (MTT)
After 48 h exposure, 3 tissues from each group were rinsed with 2 mL of PBS and placed on 300 µL of 0.5 mg/mL MTT (specific brand name omitted by the SCCS). After 3 hours of incubation at 37 °C, 5% CO_2, tissues were placed in 2 mL of isopropanol. Extraction was performed overnight at RT. Optical density was measured on 200 µL of extracts at 570 nm (reference filter: 690 nm), and each sample was read per duplicate. Results are expressed as viability percentage compared to negative control (mean ± SEM).

IL-1α determination
Incubation medium was intended to quantify IL-1α using IL-1 alpha Human ProQuantum Immunoassay Kit (specific brand name omitted by the SCCS). Media samples were diluted 10-fold, and a standard protein curve was prepared according to the manufacturer's instructions. Binding of the analyte was performed overnight at 4°C upon incorporation of the antibody-conjugate mixture. Following the addition of the Ligase enzyme and Master Mix, quantification of IL-1α protein was determined on a qPCR instrument. The standard curve was adjusted to a sigmoidal 4PL model and protein concentration per sample was interpolated by Ct values. Results are expressed as IL-1α concentration (pg/mL) compared to negative control (mean ± SEM).

Histology
At the end of the incubation period, half the area of each test and control tissue was fixed in a balanced 4 % formalin solution at 4 °C overnight and later embedded in paraffin. Six-micron vertical sections were stained with Mayer’s haematoxylin and eosin (H&E) and photographed under a microscope.

Observation with TEM
Half the area of each tissue was fixed in a balanced 2.5% glutaraldehyde solution, dehydrated and later embedded in resin. Six-micron vertical sections were photographed under a TEM microscope. HAP-NP visualization and confirmation will be done using EDX analysis using a TEM-STEM (specific brand name omitted by the SCCS).

Results
LDH activity
The LDH assay was used as an indicator of cytotoxicity, as this enzyme leaks out through the plasma membrane of damaged cells. As shown in Figure 6 below, after 48h treatment, all groups showed significant differences compared to the positive control (treated with the detergent Triton™ X-100 at 1%). In addition, no significant differences were found between the negative control (PBS control group) and the different concentrations of HAP-NP analysed.

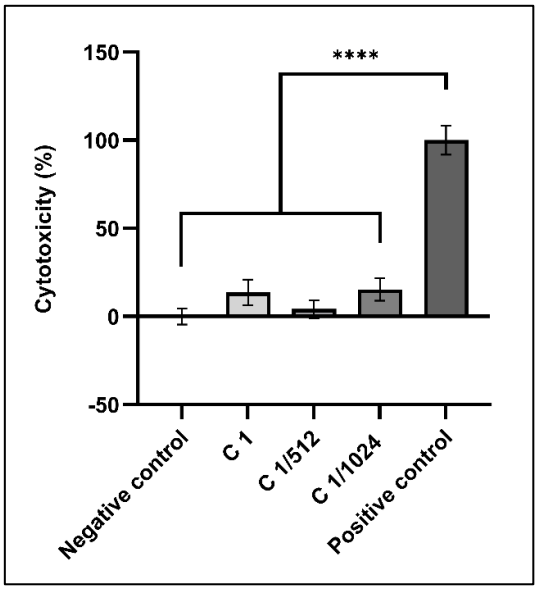

Figure 6: LDH activity of SkinEthic™ tissues culture media after treatment with HAP-NP at different concentrations. Lactate dehydrogenase (LDH) activity, an indicator of cytotoxicity, was measured in culture media at the end of the different exposure times of HAP-NP with the samples and controls. Positive control (that was set to 100%) was obtained from culture media of SkinEthic™ tissues treated with 1% of the detergent Triton™ X-100. Negative control (0% cytotoxicity) was obtained from tissues treated with PBS w/o HAP-NP. Values represent the mean ± SEM. Data was identified as parametric using the Shapiro-Wilk test. A parametric ANOVA with uncorrected Tukey's multiple-comparisons test was performed to compare and detect significant differences. ****$p < 0.0001$.

Viability test (MTT)
The MTT assay was used as a marker of cell viability, as it measures the MTT reduction by mitochondrial reductase enzymes. As shown in Figure 7 below, all treatments were biocompatible, showing significantly higher viability than the Triton™ X-100 positive control group. In addition, no significant differences were found between treatments or compared to the PBS negative control group.

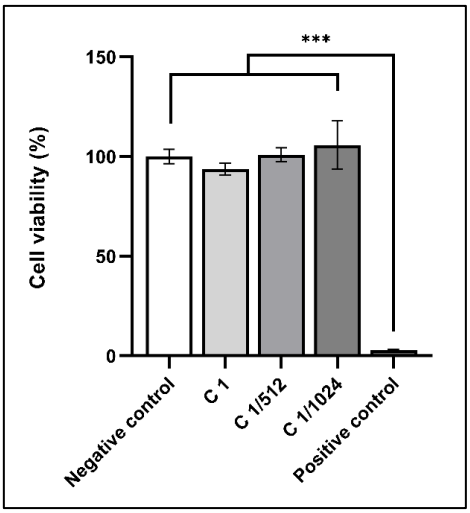

Figure 7: MTT viability of SkinEthic™ tissues after treatment with HAP-NP in PBS at different concentrations. MTT, an indicator of the number of viable cells, is measured in the tissues after 48h of treatment. 100% viability control was obtained from tissues treated with PBS alone (negative control). 0% viability control was obtained from tissues treated with 1% Triton™ X-100 (positive control). Values represent the mean ± SEM. Data was identified as parametric using the Shapiro-Wilk test. A parametric ANOVA with uncorrected Fisher's multiple-comparisons test was performed to compare and detect significant differences. ***p < 0.001.

IL-1α determination

IL-1α is a pro-inflammatory cytokine involved in inflammatory cell response. As indicated in Figure 8, the negative and positive controls showed significant differences in their IL-1α release. A tendence of a dose-response for the tested HAP-NP groups was observed, with significant differences compared to the positive control for the C1/512 and C1/1024 groups. Finally, no significant difference was obtained between the different HAP-NP concentrations and the negative control.

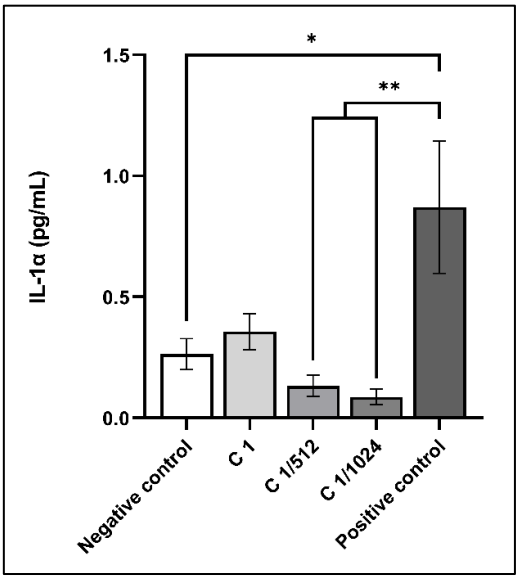

Figure 8: IL-1α quantification of SkinEthic™ tissues culture media after 48 h of treatment with HAP-NP at different concentrations. Values represent the mean ± SEM. Data was identified as parametric using the Shapiro-Wilk test. A parametric ANOVA with uncorrected Tukey's multiple-comparisons test was performed to compare and detect significant differences. *p < 0.05, **p < 0.01.

Histology

Figure 9 shows representative images of the tissues after 48h of treatment with HAP-NP at different concentrations stained with H&E and the associated score. The general morphological structure of the tissues is presented in comparison to the negative control and positive controls, with a score of 0 (absence of epithelium changes) and 4 (total tissue necrosis and/or tissue disintegration), respectively. Both control groups (PBS and Triton™ X-100) showed the expected histological appearance. Of all the groups tested, only tissues from the C1/512 group showed some moderate epithelial changes. In the C1 group, minor changes could be due to histological processing artefacts, as they were observed exclusively in the lower part of the tissue (in contact with the much stiffer polycarbonate filter). All three replicates of C1/1024 conditions showed histological conditions similar to the negative control (PBS, score 0).

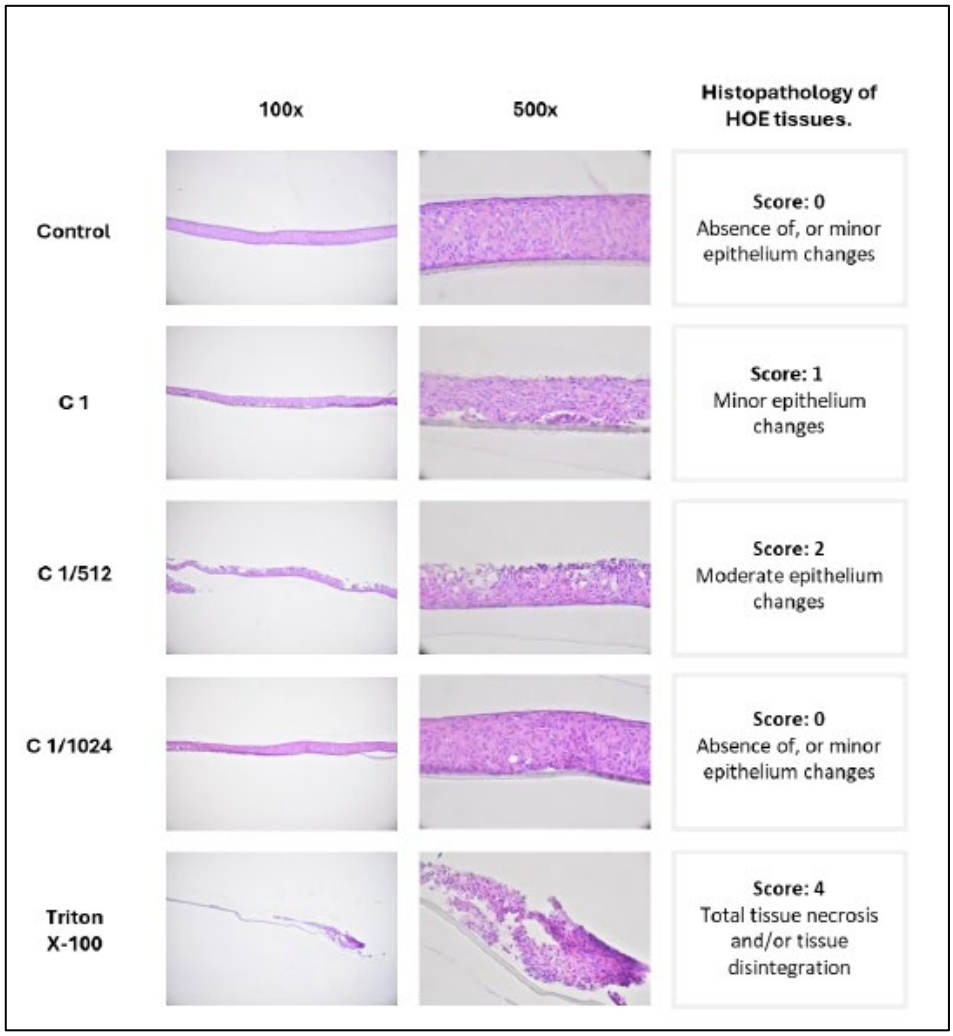

Figure 9: Representative images of HOE tissues after 48h of treatment with different concentrations of HAP-NP and the detergent Triton™ X-100 (1%), stained with Haematoxylin-Eosin. The histopathological scoring scale of the tissues is shown (0, no epithelial changes or minor epithelial changes; 1, minor epithelial changes; 2, moderate epithelial changes; 3, marked to severe epithelial changes; 4, total tissue necrosis and/or tissue disintegration).

Figure 10 shows representative images of the Von-Kossa staining for the histological visualization of calcium deposits. A positive staining control of HAP-NP, fixed on a slide by heat, confirmed specificity and validity of the staining method for the material PhPC-2022-3.

As seen in the images, HAP-NP, a calcium hydroxyphosphate, was visible through silver nitrate staining only in highest test concentration group C1, remaining at the apical side of the tissue without apparent and visible tissue uptake. In contrast, no visible HAP-NP were detected in the C1/512 and C1/1024 groups. Some few stain dots found were not noticed in all replicates and therefore judged as irrelevant processing artefacts.

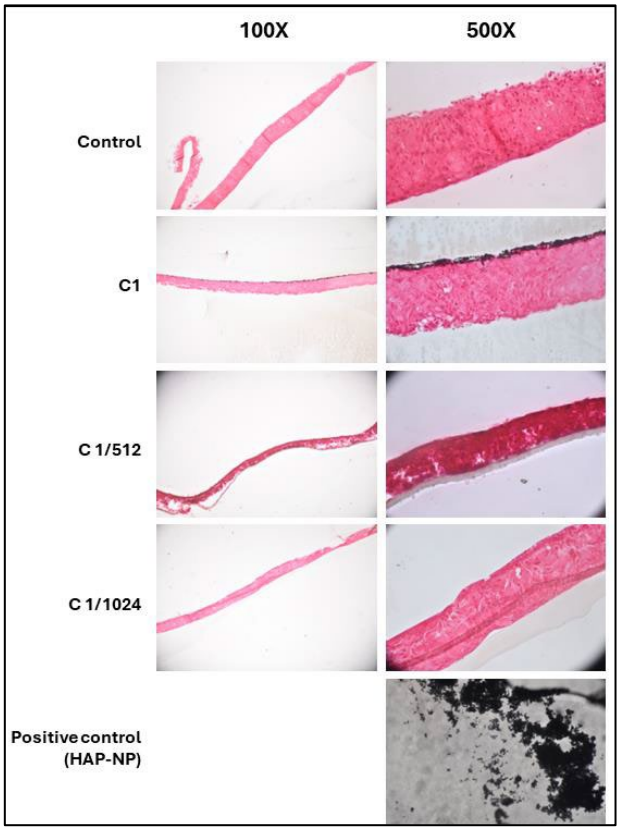

Figure 10: Representative images of the HOE tissues, after 48 h of treatment with different concentrations of HAP-NP, were stained in parallel to pristine HAP-NP using the Von-Kossa method.

OsteoImage™

The OsteoImage™ Mineralization Assay was applied to histological tissue sections to potentially determine hydroxyapatite accumulations by fluorescence microscopy. However, tissue autofluorescence was observed, even after subtraction of the negative control in all test samples. No specific staining of HAP-NP could be achieved. The staining kit was originally developed for imaging of mineralization processes and is not explicitly intended by the manufacturer for use in paraffin sections of epithelial cell models. Based on these results, the staining was found to be not appropriate for the detection of HAP-NP in HOE tissue sections under used conditions.

Transmission Electron Microscopy (TEM)

The HAP-NPs of the material PhPC-2022-3 were visualised by TEM and their composition was confirmed by energy-dispersive X-ray spectroscopy (EDX) analysis. Figure 11 shows representative micrographs of HAP-NPs, as well as the EDX analysis of the material, which allowed the identification of their morphology and confirmation of composition (Ca/P ratio). Representative images were obtained for each of the tissues treated with different concentrations of HAP-NP (C1, C1/512 and C1/1024) and for the negative control (Figure 12). In some epithelial cells, agglomerates/aggregates of particles could be detected in the micrographs (indicated by framed boxes). EDX confirmed the identity of HAP-NP as indicated by the example of concentration C1 on a treated tissue sample (Figure 13). For each experimental group, a mapping of the elements calcium and phosphorus was performed

(Figure 14), showing a clustering of these elements consistent with the position of the observed HAP-NP.

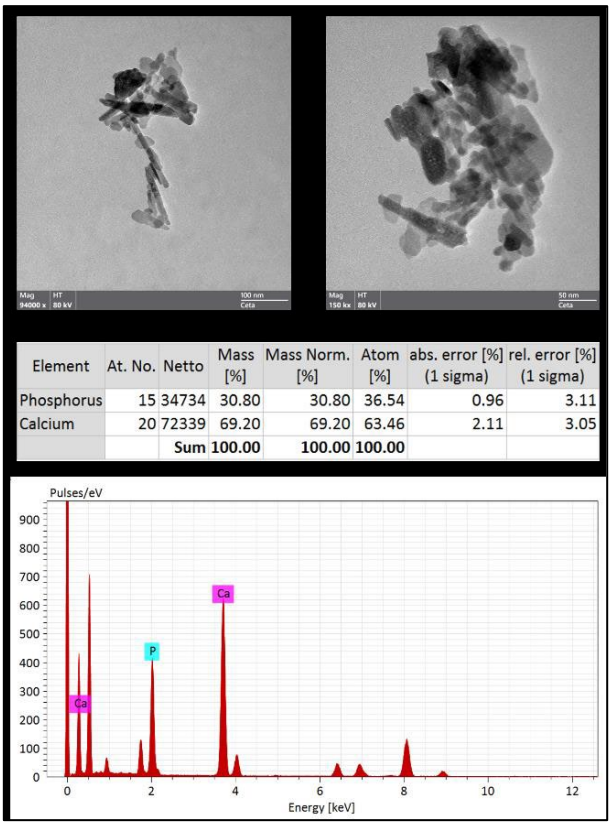

Element	At. No.	Netto	Mass [%]	Mass Norm. [%]	Atom [%]	abs. error [%] (1 sigma)	rel. error [%] (1 sigma)
Phosphorus	15	34734	30.80	30.80	36.54	0.96	3.11
Calcium	20	72339	69.20	69.20	63.46	2.11	3.05
		Sum	**100.00**	**100.00**	**100.00**		

Figure 11: Analysis of HAP-NP in the form of PhPC-2022-3 by TEM-EDX. A) Representative images of HAP-NP at magnification of 94 kx and 150 kx are presented. EDX analysis of the sample showing B) the data associated to the identification of calcium and phosphorus elements and C) the signal spectrum.

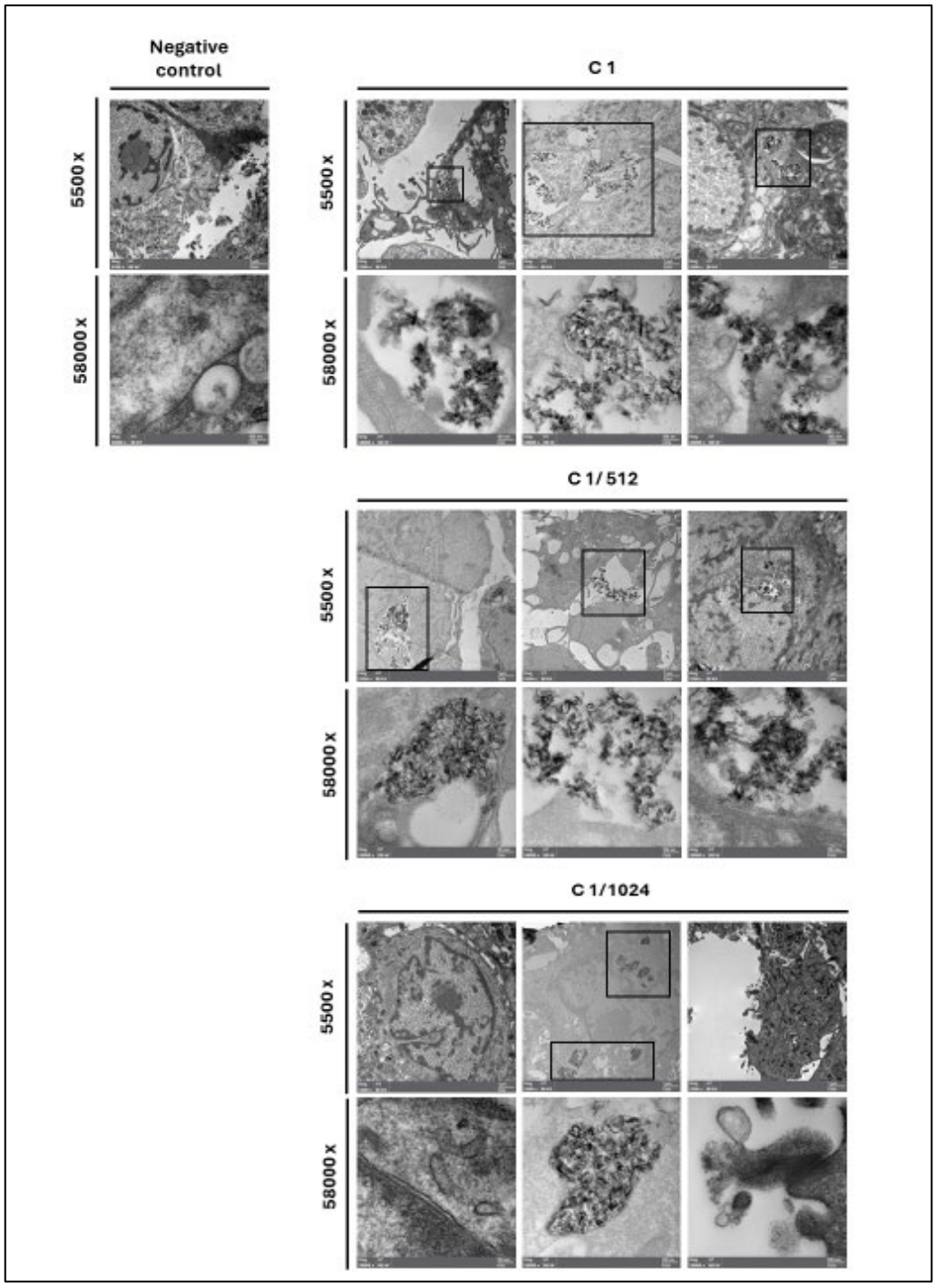

Figure 12: Representative micrographs of HOE tissues treated with different concentrations of HAP-NP (C1, C1/512 and C1/1024) as well as the negative control, obtained at 5500 x and 58000 x. Clusters of HAP-NP are indicated by boxes.

Element	At. No.	Netto	Mass [%]	Mass Norm. [%]	Atom [%]	abs. error [%] (1 sigma)	rel. error [%] (1 sigma)
Calcium	20	2376	65.87	65.87	59.86	2.93	4.45
Phosphorus	15	1328	34.13	34.13	40.14	1.85	5.42
		Sum	**100.00**	**100.00**	**100.00**		

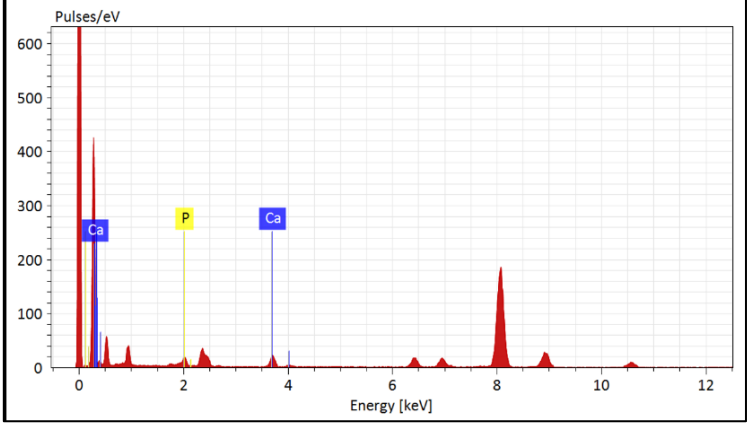

Figure 13: EDX analysis for a tissue sample treated with HAP-NP (C1). A) Associated data and B) signal spectra for the elements calcium and phosphorus are shown.

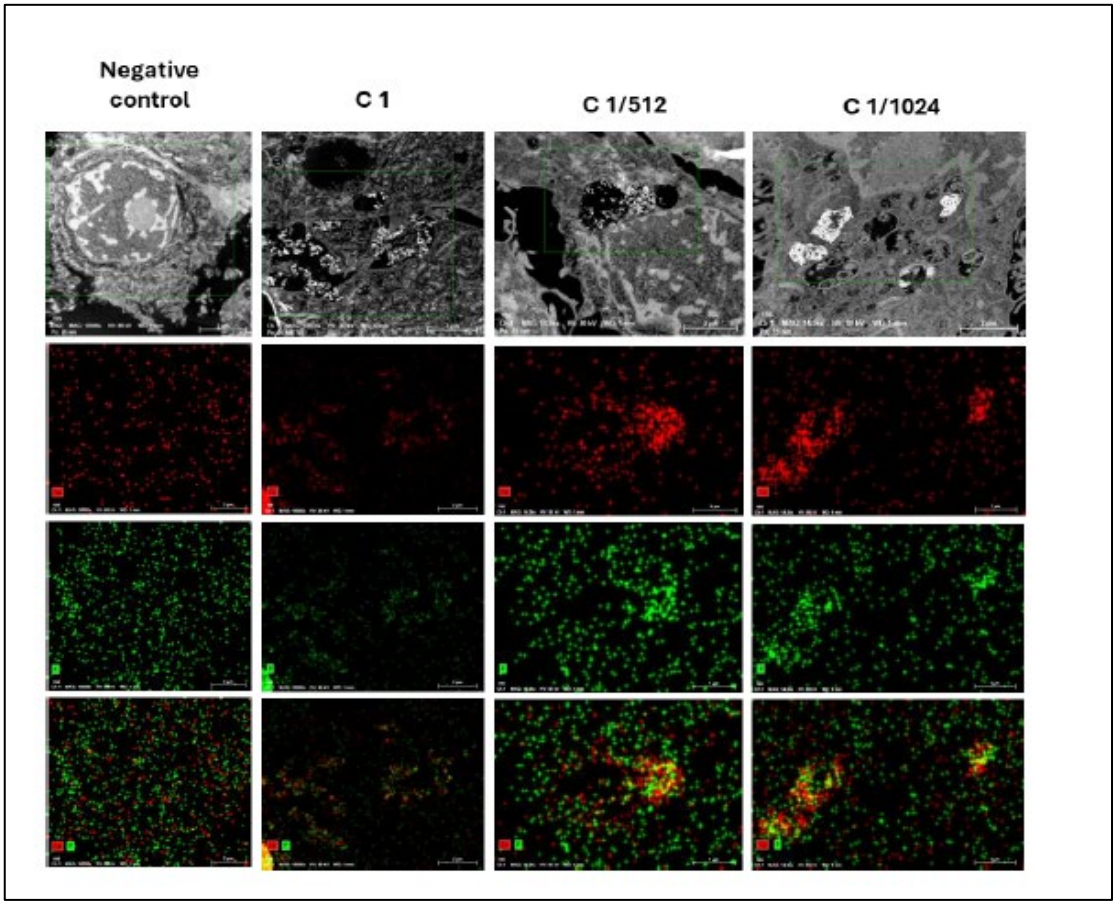

Figure 14: TEM images (upper row) for each of the experimental groups (negative control, C1, C1/512 and C1/1024) with EDX mapping in the green boxes for the elements phosphorus (green) and calcium (red).

Conclusions from the Applicant

1. Biocompatibility of HAP-NP: The assessment of hydroxyapatite nanoparticles (HAP-NP) using LDH activity, MTT assay, and IL-1α release indicates that the tested concentrations of HAP-NP are biocompatible with human oral epithelium (HOE) tissues. A treatment over 48 h with the test item did not affect cell viability or increase cytotoxicity. Additionally, no inflammatory response was observed, as indicated by the IL-1α marker.

2. Histological Observations: Histological analysis revealed that HOE tissues treated with the lowest concentration of HAP-NP (C1/1024 ≙ 0.046 mg/mL) exhibited a normal tissue architecture similar to the negative control. Tissues treated with higher concentrations (C1 ≙ 47.3 mg/mL and C1/512 ≙ 0.092 mg/mL) demonstrated minor or moderate epithelial changes, possibly attributed to processing artifacts, as neither a dose-response nor any correlation to the biocompatibility data were seen.

3. HAP-NP staining: HAP-NP accumulation was observed predominantly at the apical side of tissues treated with the highest concentration (C1≙ 47.3 mg/mL), without significant cellular uptake or detection in lower layers of the epithelial tissue. Lower concentrations (C1/512 ≙ 0.092 mg/mL and C1/1024 ≙ 0.046 mg/mL) did not show such HAP-NP adsorption to their cell surfaces.

4. Cellular Uptake and TEM Analysis: Transmission Electron Microscopy (TEM) confirmed the uptake of particles in aggregates/agglomerates by individual cells across all tested concentrations. Energy-Dispersive X-ray Spectroscopy (EDX) enabled the identification of the observed particles as HAP-NP by analyzing the elemental composition and distribution of calcium and phosphorus within the micrographs.

Overall conclusion from the Applicant

The study concludes that HAP-NPs in the form of PhPC-2022-3 are generally biocompatible with non-keratinized human oral epithelium after 48 hours of exposure at the tested concentrations. Cellular uptake by epithelial cells was confirmed, but the observed histological and biochemical responses suggest that HAP-NP is well-tolerated.

Reference: TERCIT, 2024

SCCS comments

Hydroxyapatite PhPC-2022-3 (nano) did not induce cytotoxic effects (MTT, LDH tests) or a pro-inflammatory response (IL-1α production) in the *in vitro* human buccal mucosa model after 48 h of exposure.
The SCCS noted moderate histological changes in the epithelium after 48 h of exposure to the mid concentration of 0.092 µg/mL, and minimal changes at the highest and lowest concentrations. Although the dose ranges chosen for the study did not follow the principle of low, medium and high exposures, the changes were, however, superficial and not dose dependent, and might also be due to artefacts introduced by the histological sample preparation.
In addition, an uptake of particles in aggregates/agglomerates by individual cells across all tested concentrations was observed. As no cross-sectional images of the epithelial histological samples were provided, it was not possible to conclude on the depth of nanoparticles penetration. However, epithelial cells of the buccal mucosa are continually replaced and any cells with internalised particles will be shed out over time.
Overall, the SCCS is of the opinion that hydroxyapatite in the form of PhPC-2022-3 (nano), even when used at the highest concentration of 47.25 mg/mL, did not induce either cytotoxicity or inflammatory reactions in the buccal mucosa model after 48 h of exposure.

3.3 EXPOSURE ASSESSMENT

From the Applicant

Hydroxyapatite (nano) in the form of PhPC-2022-3 (nano) is only intended to be used in oral cosmetic products (toothpastes and mouthwashes), only exposure via the oral route will be considered. After entering the mouth, part of the cosmetic formulation comes in contact with the buccal mucosa and part of it may be ingested. Therefore, systemic exposure to hydroxyapatite (nano) may occur either via uptake by mucosal cells or by getting into the intestinal tract.

However, these aspects were appropriately investigated and can be considered as not relevant as any significant systemic exposure via the oral mucosa, via ingestion due to increasing solubility in acidic environment like gastric fluid and any cytotoxicity at the level of the oral epithelium can be excluded in line with the most recent SCCS Opinion (SCCS/1648/22, 2023) and as demonstrated by the following investigations.

The possible penetration into buccal mucosal cells was studied as a preliminary step to investigate whether hydroxyapatite (nano) can enter systemic tissues through the oral epithelium. It was histologically studied to what extent hydroxyapatite (nano) could penetrate the stratified layers in two types of three-dimensional (3-D) reconstituted human oral epithelial models, one with and one without a stratum corneum. The results showed that the nanoparticles did not penetrate the *stratum corneum* in SkinEthic HGE samples and penetrated only the outermost layer of cells in SkinEthic HOE samples without stratum corneum. There was clearly no permeation into the deeper layers of the epithelium in either tissue model.

References: Ramis *et al*., 2018; SCCS 2021, 2023a

In addition, absorption by gastric compartment and stability of an analogue hydroxyapatite (nano) form was assessed in a stability study in simulated gastric fluid (SGF) by determination of calcium content at different time points. The results confirmed that the material would solubilize in the gastric fluid if ingested. Therefore, there should not be any issue of nano-related concerns over its safety following ingestion. As it was concluded that systemic exposure to hydroxyapatite (nano) following cosmetic use in oral care products was not significant, the SCCS concluded in its opinion from 2023 (SCCS/1648/22) that only local toxicity and genotoxicity have to be assessed.

References: Ramis *et al*., 2018; SCCS 2021, 2023a

With regards to local toxicity the SCCS reported in its opinion dated 2012 (SCCS/1624/20) that to determine the biocompatibility/oral irritation on human oral epithelium of hydroxyapatite (nano), an *in vitro* model of reconstructed human oral epithelium was used after exposure to nanoparticles of an analogue nanoscaled material in the SkinEthic reconstructed Human Oral Epithelium test. This was a non-keratinizing model that was taken as the worst-case scenario. As no toxicity was revealed using this model, the SCCS concluded that no toxic effects should be expected in a keratinized model that has additional protective layers of stratum corneum. With this model it was demonstrated that the analogue hydroxyapatite (nano) material showed that after an incubation period of 48 hours the material was not cytotoxic to the mucosal cells.

References: SCCS 2021, 2023a

SCCS comment
In response to the SCCS concerns expressed in the letter to the Applicant on potential internal uptake of HAP (nano) via buccal mucosal cells as reported by Ramis *et al*. (2018) and cytotoxicity, the Applicant provided a new study on *In Vitro* Biocompatibility and Irritation of

Biomimetic Hydroxyapatite Nanoparticles on Human Oral Epithelium. The results and the SCCS assessment are described under 3.2.2.

3.3.1 Function and uses

From the Applicant

Hydroxyapatite as an ingredient is listed in the CosIng database without any reference to the nano form being used as an abrasive, for bulking and for stabilizing emulsions.
Hydroxyapatite (nano) in the form of PhPC-2022-3 (nano) is intended to be formulated and used in the following oral care products:

- Toothpaste at concentrations of up to 29.5%
- Mouthwashes at concentrations of up to 10%

In its review in 2011, Bose and Tarafder pointed out that calcium phosphates, especially in the form of hydroxyapatite (nano) and tricalcium phosphate (nano), are the most widely used bone substitutes in bone tissue engineering due to their compositional similarities to bone mineral and excellent biocompatibility. Due to their favourable properties, calcium phosphates are also used as coatings on metallic implants, calcium phosphate cements, and custom designed scaffolds to treat musculoskeletal disorders.

References: Dossier on Hydroxyapatite (nano)
KG 2023-08-09; Bose and Tarafder, 2011

Hydroxyapatite (nano) is also widely and safely used in dentistry. This application field was recently summarized by Limeback in 2022. In his expert statement he summarized that hydroxyapatite (nano) is a popular ingredient in dental products used by dentists for implant integration, bone repair, dental decay prevention, and dentin hypersensitivity treatment and is a common ingredient in consumer oral care products for daily use. Dental health care professionals and their patients have been using these products with confidence for years because the active ingredient, synthetic hydroxyapatite (nano), has been demonstrated to not only have effectiveness but also biocompatibility and safety.

Reference: Limeback, 2022

The working group of Enax *et al.* in 2002 emphasized that calcium phosphates like hydroxyapatite (nano) are generally safe as food additives, which also covers formula for babies. This conclusion is justified as e.g., hydroxyapatite (nano) is soluble in the acidic environment of the stomach, regardless of the particle size or phase. Consequently, it is present as dissolved ions after passing through the stomach. These dissolved ions cannot be distinguished from a mixture of calcium and phosphate ions that were ingested separately. Milk, including human breast milk, is a natural source of calcium and phosphate in which calcium phosphate is present as nanoscopic clusters (nanoparticles) inside casein (protein) micelles.

Reference: Enax *et al.*, 2022

In several reviews also covering potential health risks associated with nanosized calcium phosphates like hydroxyapatite (nano), Epple in 2010 and 2018 as well as Sokolova and Epple in 2021 re-iterated that these materials are well established biomaterials and used not only in many products in biomedicine, but also in toothpastes and cosmetics. This is due to their high biocompatibility and biodegradability in respect to their chemical similarity to human hard tissues like bone and teeth. This also enables the use as efficient carriers for different kinds of biomolecules, which alone are not able to enter cells. After a thorough literature review, he concluded that calcium phosphate nanoparticles as such have no inherent toxicity and that the risk associated with an exposure to nanosized calcium phosphate in doses that

are usually applied in biomedicine, health care products, and cosmetics is very low and most likely not present at all.

References: Epple *et al*., 2010, Epple, 2018; Sokolova and Epple, 2021

SCCS comment
The studies cited above indicate that hydroxyapatite might be safe. However, the materials considered do not relate to the material under assessment in this Opinion in relation to the exposure of the buccal mucosa.
In response to the SCCS concerns expressed in the letter to the Applicant on potential internal uptake of HAP (nano) via buccal mucosal cells as reported by Ramis *et al*. (2018) and cytotoxicity, the Applicant provided a new study on *In Vitro* Biocompatibility and Irritation of Biomimetic Hydroxyapatite Nanoparticles on Human Oral Epithelium. The results and the SCCS assessment are described under 3.2.2.

3.4 TOXICOLOGICAL EVALUATION

As described above, HAP (nano) is not likely to lead to any significant systemic exposure via the oral route. Considering that any unintentionally ingested HAP nanoparticles during the use of oral-care products will undergo rapid dissolution in the gastric fluid and, therefore, this should not raise any nano-specific concern over safety.

The systemic toxicity was already addressed in the previous Opinions (SCCS/1624/20 and SCCS/1648/22) and no new information was provided by the Applicant. Therefore, this evaluation is limited to potential genotoxicity and local effects.

3.4.1 Mutagenicity/genotoxicity

With the new dossier, the Applicant provided results of two new mutagenicity studies on PhPC-2022-3 (nano), i.e. hydroxyapatite (nano), i.e. an *in vitro* mammalian cell gene mutation Mouse Lymphoma Assay (MLA) and a micronucleus assay on CHO-K1 cells. As the SCCS questioned validity of the MLA study due to absence of observation of cell uptake under the test conditions of the HAP nanoparticles, the Applicant provided a third study (a gene mutation test in the *Hprt* locus of V79 cells). A summary of the SCCS evaluation of these 3 studies is provided in the paragraphs below.

3.4.1.1 Mutagenicity/genotoxicity *in vitro*

***In vitro* mammalian cell gene mutation**

The Applicant provided an *In vitro* mammalian cell gene mutation Mouse Lymphoma Assay (MLA) including investigation of particle size distribution, dispersion stability and cellular uptake.

From the Applicant (SCCS Dossier on Hydroxyapatite (nano) KG 2023-08-09; Project number: 22LA14102/MN. Evaluation of PhPC-2022-3 (nano) behaviour in terms of size distribution, dispersion and cellular uptake for Micronucleus (MN) assay. ECAMRICERT SRL. 2023).

Study Design:

Reference:	Chelab, 2023a
Date of report:	08.05.2023
Study period:	11.07.2022 – 26.10.2023
Guideline:	OECD 490 (2016) plus requirements of SCCS guidance (SCCS/1611/19 and 1628/21)
Test system:	L5178Y $TK^{+/-}$ mouse lymphoma cells
Replicates:	Duplicate cultures
Test substance:	PhPC-2022-3 (nano, i.e. hydroxyapatite (nano))
Batch (Purity):	D20469A (hydroxyapatite (nano) content: 29.5%, specified by CoA)
Vehicle:	F10 medium (Fisher's medium, 10% heat-inactivated Horse serum, 1 mM sodium pyruvate, 1% Penicillin/Streptomycin, 0.1% Pluronic F-127)
Concentrations#:	**Main MLA:** PhPC-2022-3 Without S9: 0, 0.0066, 0.0132, 0.0265, 0.0530, 0.1059 mg/mL (corresponding to hydroxyapatite (nano): 0, 0.002, 0.0039, 0.0078, 0.0156, 0.0313 mg/mL) With S9: 0, 0.0033, 0.0066, 0.0132, 0.0265, 0.0530 mg/mL (corresponding to hydroxyapatite (nano): 0, 0.0010, 0.0020, 0.0039, 0.0078, 0.0156 mg/mL)
Treatment:	4 h ±S9 24 h -S9
Expression period:	2 days
Colony counting:	After 12 days of incubation in medium containing Trifluorothymidine (TFT)
Positive controls:	-S9: Methylmethanesulphonate (MMS): 4.0, 7.5 µg/mL +S9: Cyclophosphamide monohydrate (CP): 2.5, 5 µg/mL
Negative control:	Vehicle
Statistics:	One-way ANOVA and non-parametric Post Test
GLP:	Yes
Published:	No

the tested concentrations were based on the results of a preliminary cytotoxicity test

Material and methods:

The possible mutagenic potential of PhPC-2022-3 (nano, i.e., hydroxyapatite (nano), batch: D20469A, hydroxyapatite (nano) content: 29.5%) was investigated in the mouse lymphoma assay (MLA) according to OECD 490 under GLP conditions and following SCCS guidance requirements. The test was carried out on L5178Y/$TK^{+/-}$ cell line. Cells were exposed to 5 different concentrations of the test substance at three different exposure conditions: 4 hours in the presence and in the absence of metabolic activation (4h ± S9) and 24 hours in the absence of metabolic activation (24h - S9). At the end of the expression period, the mutagenic potential of the test substance was assessed by colony counting to determine the mutant frequencies increase. Based on the results of a preliminary cytotoxicity test concentrations of 0, 0.0066, 0.0132, 0.0265, 0.0530, 0.1059 mg/mL of PhPC-2022-3 suspension (corresponding to hydroxyapatite (nano)): 0, 0.002, 0.0039, 0.0078, 0.0156, 0.0313 mg/mL) without metabolic activation (-S9) and 0, 0.0033, 0.0066, 0.0132, 0.0265, 0.0530 mg/mL (corresponding to hydroxyapatite (nano): 0, 0.0010, 0.0020, 0.0039, 0.0078, 0.0156 mg/mL) with S9 mix were selected.

Osmolality and pH of the growth medium were assessed during the preliminary cytotoxicity as well as during the main assay using reference substances with known osmolality and pH.

After the treatment and following a two-days expression period, cells were counted, and two different cell suspensions were prepared: the first culture was resuspended in F_{20} TFT medium and selected for the mutant phenotype and 2000 cells/well were plated into 96-well plates. These plates were incubated for 12 days. The second culture was prepared in F_{20} medium for viability assays and 1.6 cells/well were plated. These viability plates were incubated for 10 days. Plates were counted by a trans-luminometer to evaluate Suspension Growth (SG),

Relative Suspension Growth (RSG%), Relative Total Growth (RTG%), Cloning Efficiency (CE) and Mutant Frequency (MF).
For comparison and to demonstrate the sensitivity and validity of the test system, negative controls (treatment medium) and positive controls (Methylmethanesulphonate (MMS) without S9 and Cyclophosphamide monohydrate (CP) with S9) were examined in parallel.
In addition, the uptake of nanoparticles into the cell and/or nucleus was investigated by TEM-EDX (according to ISO 21363:2020) and DLS (according to ISO 22412:2017).

Results:
Osmolality and pH were monitored and were acceptable.
No cytotoxicity was evident at any concentration after 4 h exposure with/without S9 or 24 h without S9.
The highest concentration analysed was the lowest concentration producing a visible precipitate.
It was clearly demonstrated that the test item led to no increase of the mutation frequency at either concentration, neither in the form of incidences for small and large colonies or combined, when compared to concurrent or historical controls after 4 h ±S9 or 24 h -S9 exposures in the mouse lymphoma L5178Y/TK$^{+/-}$ cell line.

Table 11: Results of MLA assay for treatment 4 h-S9

Substance	**Final dose in flask**	**Mean SG**	**Mean RSG %**	**Mean RTG %**	**Mean MF / 10^6 cells**	**Mean SMF / 10^6 cells**	**Mean LMF / 10^6 cells**
Hydroxyapatite (nano) concentration	0.0313 mg/mL (*)	20.074	86.997	73.370	124.784	109.262	13.157
	0.0156 mg/mL	17.040	73.848	66.280	103.668	87.241	14.399
	0.0078 mg/mL	20.785	90.078	84.769	103.100	84.848	15.812
	0.0039 mg/mL	23.958	103.833	67.129	107.263	92.618	13.190
	0.002 mg/mL	20.847	90.348	72.241	118.684	102.990	13.545
Positive control (MMS)	7.5 µg/mL	11.282	48.895	30.323	739.571	597.326	75.013
	4 µg/mL	17.274	74.865	54.442	882.092	727.868	60.119
Untreated control (UC)	/	23.074	100.000	100.000	106.287	87.488	16.200
*=precipitating concentration							

Table 12: Results of MLA assay for treatment 4 h+S9

Substance	**Final dose in flask**	**Mean SG**	**Mean RSG %**	**Mean RTG %**	**Mean MF / 10^6 cells**	**Mean SMF / 10^6 cells**	**Mean LMF / 10^6 cells**
Hydroxyapatite (nano) concentration	0.0313 mg/mL (*)	20.661	88.093	92.642	69.545	59.947	8.324
	0.0156 mg/mL	20.303	86.566	89.770	57.961	53.147	4.191
	0.0078 mg/mL	20.318	86.630	86.901	60.502	52.819	6.689
	0.0039 mg/mL	22.496	95.917	118.196	54.026	45.205	7.731
	0.002 mg/mL	21.978	93.708	112.785	50.176	42.826	6.503
Positive control	5 µg/mL	6.668	28.429	10.534	900.355	721.814	91.559

(CP)	2.5 µg/mL	15.007	63.983	33.461	1119.915	896.131	67.721
Untreated control (UC)	/	23.454	100.000	100.000	64.325	55.997	7.294
*=precipitating concentration							

Table 13: Results of MLA assay for treatment 24 h-S9

Substance	**Final test dose in flask**	**Mean SG**	**Mean RSG %**	**Mean RTG %**	**Mean MF / 10^6 cells**	**Mean SMF / 10^6 cells**	**Mean LMF / 10^6 cells**
Hydroxyapatite (nano) concentration	0.0313 mg/mL (*)	56.255	74.590	92.115	34.299	30.409	3.571
	0.0156 mg/mL	78.783	104.461	106.420	38.348	35.303	2.805
	0.0078 mg/mL	73.703	97.726	91.790	50.386	44.439	5.393
	0.0039 mg/mL	65.786	87.228	90.779	40.630	35.945	4.283
	0.002 mg/mL	69.728	92.455	84.339	43.885	37.487	5.949
Positive control (MMS)	7.5 µg/mL	34.596	45.872	11.118	1523.738	1273.863	118.853
	4 µg/mL	32.772	45.872	14.598	2232.171	1755.410	110.377
Untreated control (UC)	/	75.419	100.000	100.000	51.886	44.928	6.274
*=precipitating concentration							

All validity and acceptance criteria were met and the positive as well as the negative controls showed the sensitivity and suitability of the test system.

Conclusion by the Applicant
Finally, under the conditions of reliable test conditions, the test item did not induce gene mutations in L5178Y TK+/- mouse lymphoma cell line, when tested up to precipitation concentrations. Overall, the hydroxyapatite (nano) test item was clearly negative and revealed no genotoxic potential *in vitro* in the Mouse Lymphoma Assay.

Size distribution, dispersion stability and cellular uptake for the *in vitro* Mammalian Cell Mouse Lymphoma Assay (MLA)

The detailed results for HAP (nano) particle size and aspect ratio distributions based on individual particle measurement, for all the MLA test conditions (C1, C2, C3, C4 and C5 without S9 and C1*, C2*, C3*, C4* and C5* with S9) provided by Applicant are reported in Annex C.

Study Design:

Reference:	EcamRicert, 2023c
Date of report:	03.05.2023
Guideline/guidance:	Requirements of SCCS Opinion (SCCS/1624/2020) and SCCS guidance (SCCS/1611/19)
Test system/method:	a) Particle size distribution and dispersion b) Uptake: L5178Y $TK^{+/-}$ mouse lymphoma cells
Test substance:	PhPC-2022-3 (nano, i.e. hydroxyapatite (nano))
Batch (Purity):	D20469A (hydroxyapatite (nano) content: 29.5%, specified by CoA)
Vehicle:	F10 medium (Fisher's medium, 10% heat-inactivated Horse serum, 1 mM sodium pyruvate, 1% Penicillin/Streptomycin, 0.1% Pluronic F-127)

Analytical methods:	- Transmission electron microscopy coupled with energy-dispersive X-ray spectroscopy (TEM-EDX) - Dynamic light scattering (DLS)
Concentrations:	Without S9: 0, 0.0066, 0.0132, 0.0265, 0.0530, 0.1059 mg/mL of PhPC-2022-3 suspension (corresponding to hydroxyapatite (nano): 0, C5: 0.002, C4: 0.0039, C3: 0.0078, C2: 0.0156, C1: 0.0313 mg/mL) With S9: 0, 0.0033, 0.0066, 0.0132, 0.0265, 0.0530 mg/mL of PhPC-2022-3 suspension (corresponding to hydroxyapatite (nano): 0, C5*: 0.0010, C4*: 0.0020, C3*: 0.0039, C2*: 0.0078, C1*: 0.0156 mg/mL)
GLP:	No data
Published:	No

* has been added by the SCCS to distinguish the tests without and with S9.

Material and methods:
The size distribution, dispersion and cellular uptake of PhPC-2022-3 (nano, i.e., hydroxyapatite (nano), batch: D20469A, hydroxyapatite (nano) content: 29.5%) during the MLA assay were examined according to requirements of the SCCS available at that time (SCCS/1611/19, Reference: SCCS, 2019). These investigations were performed using TEM-EDX (according to ISO 21363:2020) and DLS (according to ISO 22412:2017). Culture media and sample preparation for DLS and TEM-EDX analyses were corresponding to those described in MLA assay above compliant with OECD 490 and SCCS requirements under GLP conditions.

Results:
Focusing on the main results of this safety dossier, only the results of the highest hydroxyapatite (nano) concentrations without S9 and with S9 metabolic activation are presented as representative examples.

The results for particle size and aspect ratio distributions of all the concentrations based on individual particle measurements are listed in Annex C, Tables Annex C – 1, 2, 3, 4 and 5, for the compositions C1, C2, C3, C4 and C5 without S9, and C1*, C2*, C3*, C4* and C5* with S9 in MLA Culture Cell media.

Finally, it was demonstrated that regardless of the condition tested, median particle sizes are comparable to those of the pure (pristine) material (21.1 ± 2.9 nm for length and 12.2 ± 2.7 for width) and, even though hydroxyapatite (nano) particles are embedded in a matrix layer, their aggregation/agglomeration state does not worsen during the treatment up to 24 hours of exposure.

The following Table summarizes the particle sizes and aspect ratio as a function of the assay conditions.

Table 14: Particle sizes and aspect ratio-based on individual particle measurements of HAP NPs in the form of PhPC-2022-3 (nano) as a function of the MLA assay conditions (Summary edited by SCCS) (for details, see Annex C)

Assay conditions (MLA Test)	Median Length (nm) (TEM)	Median Width (nm) (TEM)	Median Aspect Ratio (TEM)
Pristine HAP) (nano)	21 ± 3	12 ± 3	1.51
0.0313 mg/mL, before 24 h exposure time in condition without S9	21.8 ±2.9	12.5 ± 2.7	1.58
0.0313 mg/mL, after 24 h exposure without S9 mix	20.8 ± 2.9	12.1 ± 2.7	1.50

Reference: Ref 11 22.523987.00001_FR_Attachment_3 MLA uptake

Cellular uptake and cytoplasmatic internalization

From the Applicant (SCCS Dossier on Hydroxyapatite (nano) KG 2023-08-09; Document file name: Ref 11 22.523987.00001_FR_Attachment_3 MLA uptake; Project number: 22LA14076/MLA. Evaluation of PhPC-2022-3 (nano) behaviour in terms of size distribution, dispersion and cellular uptake for Mouse Lymphoma Assay (MLA) assay. ECAMRICERT, 2023)

Cellular uptake and cytoplasmatic internalization of hydroxyapatite (nano) particles of PhPC-2022-3 (nano) during MLA assay was investigated by TEM-EDX analysing cells exposed to the test item in question at the following concentrations: one hydroxyapatite (nano) concentration inducing visible precipitates (0.0313 mg/mL without S9 and 0.0156 mg/mL with S9) and four lower concentrations (0.0156 mg/mL, 0.0078 mg/mL, 0.0039 mg/mL and 0.0020 mg/mL for condition without S9 and 0.0078 mg/mL, 0.0039 mg/mL, 0.0020 mg/mL and 0.0010 mg/mL for condition with S9).
It was shown that hydroxyapatite (nano) particles were not internalized under any of the conditions tested.

Conclusion by the Applicant on the *in vitro* Mammalian Cell Mouse Lymphoma Assay (MLA)
The test material, PhPC-2022-3 (nano, *i.e.* hydroxyapatite (nano)) is composed of calcium (Ca), phosphorus (P) and oxygen (O) and the analysed hydroxyapatite (nano) particles showed a median length of 21.1 nm and 12.2 nm, respectively.

Under conditions tested and based on TEM results, hydroxyapatite (nano) particles of PhPC-2022-3 (nano) preserved its primary particle size distribution and no changes in agglomeration/aggregation phenomena were observed at each tested concentration under any test condition.

Cellular uptake of hydroxyapatite (nano) particles of PhPC-2022-3 (nano) was also investigated at the concentrations used in the MLA assay but cytoplasmatic internalization of hydroxyapatite (nano) particles was not observed under any of the conditions tested.

SCCS comment on the *in vitro* mammalian cell Mouse Lymphoma Assay (MLA)
Since information on cellular uptake by L5178Y cells under the tested conditions was not provided, it was not possible to exclude gene mutation potential of HAP (nano). In the absence of a valid justification, a new study to exclude gene mutation potential was requested by the SCCS, that should be in accordance with the SCCS Guidance on the Safety Assessment of Nanomaterials in Cosmetics - 2nd revision (SCCS/1655/23). The SCCS also suggested to the Applicant that, if the evidence for cellular uptake would be difficult to obtain from lymphoid cells, the test would need to be carried out in another appropriate cell system in which cellular uptake had been previously demonstrated.

In response to the above SCCS comment, the Applicant provided a new study on *Hprt* mammalian cell gene mutation on V79 cells, which is summarised below.

***In vitro* Mammalian Cell gene mutation study on V79 cells**

Summary of the study by the Applicant based on Report: PhPC-2022-3: Gene Mutation Assay in Chinese Hamster V79 Cells in vitro (V79/HPRT). ICCR Study Number: 4114412. Issue Date: 19 September 2024.

Study Design:

Reference:	4114412 (Main Study, GLP) plus 4114411, RICC005 (non-GLP)
Date of report:	19.09.2024
Study period:	16.07.2024 – 01.08.2024 (Main HPRT-Study)
Guideline:	OECD Test No. 476 (2016) plus requirements of SCCS guidance (SCCS/1647/22 and SCCS/1655/23)
Test system:	V79 Chinese Hamster Cells
Replicates:	Duplicates
Test substance:	PhPC-2022-3 (nano, i.e. hydroxyapatite (nano))
Batch (Purity):	D20469A (hydroxyapatite (nano) content: 29.5%, specified by CoA)
Vehicle:	Minimal essential medium (MEM) containing Hank's salts plus 10% foetal bovine serum, 5 µg/mL neomycin, and 1% amphotericin B
Solvent	Deionised water
Concentrations[#]:	0.16, 0.41. 1.0, 2.56, 6.4, 16, 40, and 100 µg/mL (≙ PhPC-2022-3 (nano), batch: D20469A: 0.54, 1.39, 3.4, 8.7, 21.7, 54.2, 135.6, 339 µg/mL) Continued for selection: 1.0, 2.56, 6.4, 16, 100 µg/mL
Treatment:	24 h
Expression period:	7-9 days (subcultivation: 2 days after end of treatment)
Colony counting:	After 9 ± 2 days of incubation in medium containing 6-thioguanine (6TG)
Positive controls:	Ethylmethane sulfonate (EMS): 214 µg/mL
Negative control:	Vehicle with solvent
Statistics:	t-test and least squares method
GLP:	Yes (except subcontracted DLS measurement, TEM imaging, and preliminary cytotoxicity test)

[#] the highest test concentration was set based on the recommendations for *in vitro* genotoxicity testing of manufactured nanomaterials (OECD, 2022; Burgum *et al*., 2024) and justified by the results of a preliminary cytotoxicity test

Study conditions:

The potential of PhPC-2022-3 (nano, i.e., hydroxyapatite (nano), batch: D20469A, hydroxyapatite (nano) content: 29.5%) to induce gene mutations in mammalian cells was investigated at the *Hprt* locus using the Chinese hamster cell line V79. The assay was conducted according to OECD TG 476 under GLP conditions and following SCCS guidance requirements under Project No. 4114412 (Ref.: ICCR, 2024 (Annex 5)). According to the SCCS Guidance on the Safety Assessment of Nanomaterials in Cosmetics - 2nd revision (SCCS/1655/23, Ref.: SCCS, 2023b), metabolic activation by enzyme mixtures can be omitted since the test item is an inorganic and unmodified calcium phosphate that is not metabolized and practically insoluble at neutral pH. The exposure duration of 24 h was selected to expose the cells to the test item for at least one cell cycle (V79 cells approx. 16 h) to ensure sufficient conditions for cellular uptake as recommended in current guidelines. Prior to the main study, a preliminary test (Project No. 4114411) was conducted to exclude cytotoxicity and to assess the competence of the chosen cell line for uptake of hydroxyapatite (nano) under identical conditions to the subsequent genotoxicity study (Ref.: ICCR, 2024 (Annex 5)). The potential presence of hydroxyapatite (nano) in the intracellular compartments of V79 cells exposed to the test item was investigated by TEM at a subcontracted CRO (Ref.: Fraunhofer IAP, 2024 (Annex 5)). Following the recommendations for *in vitro* genotoxicity testing of manufactured nanomaterials, the highest concentration was set at 100 µg/mL, as higher concentrations of insoluble nanomaterials are considered physiologically irrelevant (OECD, 2022; Burgum *et al.*, 2024). The subsequent concentrations were defined using a dilution factor of 2.5, resulting in 100, 40, 16, 6.4, 2.56, 1.0, 0.41 and 0.16 µg/mL of PhPC-2022-3 suspension, corresponding to 339, 135.6, 54.2, 21.7, 8.7, 3.4, 1.39, and 0.54 µg/mL of the test material HAP NPs in the form of PhPC-2022-3 (nano).

After excluding cytotoxic effects by appropriate preliminary tests and successfully demonstrating cellular uptake within the relevant concentration range, the main study was

conducted under GLP and in accordance with the requirements and acceptance criteria of OECD TG 476 (Ref.: ICCR, 2024 (Annex 5)). To assess the dispersion stability of hydroxyapatite (nano) in cell culture medium over the treatment period of the study, a dynamic light scattering (DLS) measurement of the test suspensions was conducted by a subcontractor (Ref.: ZentriForce, 2024 (Annex 5)). Following treatment and an appropriate phenotypic expression period, including verification of viability by subcultivation of a small cell number in parallel culture flasks, selection for mutant cells was performed and evaluated for the highest concentration of 100 µg/mL, the lowest concentration that causes precipitation in the culture medium, and the three highest concentrations that do not cause precipitation. Negative controls (medium with solvent) and positive controls (214 µg/mL ethyl methanesulfonate (EMS)) were examined in parallel to ensure sensitivity and validity.

Cells and colonies were counted to evaluate Cloning Efficiency after treatment and expression period, Cell Density at first subcultivation, and Mutant Frequency. Please refer to the original reports for a more detailed description of the studies (Ref.: ICCR, 2024; Fraunhofer IAP, 2024; ZentriForce, 2024 (Annex 5)).

Results:

Cellular Uptake of Hydroxyapatite (nano) in V79 cells

The cytoplasmic internalization of hydroxyapatite (nano) particles of PhPC-2022-3 (nano) under *Hprt* assay conditions was investigated by TEM, analysing V79 cells treated with the test item for 24 hours. Based on the preliminary cytotoxicity test and the observed precipitation behaviour of HAP NPs (PhPC-2022-3 (nano)) in culture medium at the end of the treatment period, the cells exposed to 100 µg/mL and 6.4 µg/mL (corresponding to 339 µg/mL and 21.7 µg/mL of PhPC-2022-3 (nano), respectively) were selected and prepared for subsequent analysis using high-resolution microscopy.

Representative micrographs of the examined cells at various magnifications are presented in the annexed report (Ref.: Fraunhofer IAP, 2024 (Annex 5)). The treated V79 cells exhibit cytoplasmic vesicles containing nanoparticles, which have not been observed in untreated V79 cells in the conducting institute. The particles predominantly appear as small agglomerates/aggregates. They are morphologically consistent with those taken up by CHO cells in the previously reported Micronucleus Assay and identified as hydroxyapatite (nano), as indicated in preceding data previously submitted to the SCCS (SM I). Thus, cellular uptake under experimental conditions has been demonstrated, and the chosen cell line meets the requirements specified in the SCCS Guidance on the Safety Assessment of Nanomaterials in Cosmetics - 2nd revision (SCCS/1655/23, Ref.: SCCS, 2023b). Consequently, the *Hprt* test with V79 cells is considered suitable for evaluating the endpoint of gene mutations in mammalian cells potentially induced by hydroxyapatite (nano) in the form of PhPC-2022-3 (nano).

In vitro Mammalian Cell Gene Mutation Test using the *Hprt* gene

The main study was performed under GLP and in accordance with OECD TG 476. Osmolality and pH were monitored and were acceptable. No cytotoxicity was evident at any concentration following the 24 h treatment with the test item. Precipitation occurred during treatment period at 16 µg/mL up the highest investigated concentration. In a parallel non-GLP investigation, the stability of PhPC-2022-3 (nano) in cell culture medium during treatment was assessed using dynamic light scattering (DLS). The results indicate that there were no significant changes in the measured size distribution at the highest test concentration, the highest non-precipitating concentration at 6.4 µg/mL, or the lowest precipitating concentration of hydroxyapatite (nano) (Ref.: ZentriForce, 2024 (Annex 5)). Therefore, the hydroxyapatite (nano) is considered stable throughout the entire duration of the study.

Based on these results and the requirements of the relevant testing guidelines, the concentrations of 1.0, 2.56, 6.4, 16, and 100 µg µg/mL of PhPC-2023-3 suspension were evaluated for mutagenicity. After cultivation in medium supplemented with 11 µg/mL 6-thioguanine, no significant increases in the numbers of mutant colonies were observed after

treatment with the test item. The observed mean mutant frequency (MF) of the solvent control and all evaluated concentrations was within the 95% confidence interval of the solvent historical control data (Table 15). All validity and acceptance criteria were met and the positive as well as the negative controls showed the sensitivity and suitability of the test system.

Table 15: Results of HPRT test on V79 cells after treatment for 24 h as a function of concentration of HAP (nano)

	Conc. [µg/mL]	P	rel. CE I [%]	rel. CD [%]	rel. CE II [%]	MF	95% CI	t-test [*p* value]
	Main Experiment / 24 h treatment		mean values of culture I and II					
Solvent control			100.0	100.0	100.0	12.3	2.7 – 26.5	
Positive control (EMS)	214.0		70.9	93.3	84.5	649.2	106.3 – 598.7	**0.000[S]**
Hydroxyapatite (nano)	0.16 (0.54)[a]	-	105.2	95.3	#	#		
Hydroxyapatite (nano)	0.41 (1.39)[a]	-	108.8	88.6	#	#		
Hydroxyapatite (nano)	1.0 (3.4)[a]	-	103.2	94.2	83.7	11.6	2.7 – 26.5	n.c.
Hydroxyapatite (nano)	2.56 (8.7)[a]	-	96.2	98.2	102.4	11.9	2.7 – 26.5	n.c.
Hydroxyapatite (nano)	6.4 (21.7)[a]	-	103.4	98.8	101.0	14.2	2.7 – 26.5	0.458
Hydroxyapatite (nano)	16.0 (54.2)[a]	P	116.5	89.8	85.0	18.1	2.7 – 26.5	0.087
Hydroxyapatite (nano)	40.0 (135.6)[a]	P	109.5	104.4	#	#		
Hydroxyapatite (nano)	100.0 (339)[a]	P	103.3	88.9	87.8	16.2	2.7 – 26.5	0.198

[a] Corresponding concentration of PhPC-2022-3 (nano) in parenthesis
* statistical analysis based on the mean values of culture I and II
n.c. not calculated (mean MF ≤ MF of the solvent control)
P precipitation visible at the end of treatment
S = significant trend ($p < 0.05$)
CE I relative Cloning Efficiency after treatment
CD relative Cell Density after first subcultivation
CE II relative Cloning Efficiency after phenotypic expression period
CI Confidence Interval
MF Mutant frequency (mutant colonies per 10^6 cells)
cultures not continued as a minimum of only four analysable concentrations are required

Conclusion

It can be stated that under the experimental conditions reported, the test item did not induce gene mutations at the HPRT locus in V79 cells. Cellular uptake of the test item was confirmed, and the study results are therefore considered valid for practically insoluble nanomaterials.

Consequently, HAP NPs in the form of PhPC-2022-3 (nano) are considered to be non-mutagenic in this HPRT assay when tested in the absence of S9 mix up to the highest applied concentration of 100 µg/mL.

Cellular uptake and cytoplasmatic internalization for the *in vitro* mammalian cell gene mutation test (*Hprt*)

The TEM images and size distributions of internalised HAP (nano) particles for the various concentrations, provided by Applicant, are reported in Annex F. Below are presented overall summary on cellular uptake by the Applicant and the comment on the issue by the SCCS.

Summary by the Applicant
Cross-sections of V79 cells were analysed by chemical staining with osmium tetroxide (contrast enhancement) and ultramicrotomy with a transmission electron microscope. Two samples with different concentrations of a 29.5 % thixotropic aqueous dispersion of hydroxyapatite particles were analysed to detect the internalization of particles in V79 cells. At both concentrations of 6.4 µg/ml and 100 µg/ml, internalized particles were detected within the V79 cells. The majority of hydroxyapatite particles were found internalized in the cells. The particles are present separately or in smaller clusters in the cells. Only a limited number of hydroxyapatite particles were found outside the cells. In general, the hydroxyapatite particles were not detected in the cell nuclei.

In summary, cellular uptake of hydroxyapatite particles were detected for both concentrations of 6.4 µg/mL and 100 µg/mL and was observed exclusively in cytoplasmic vesicles but not in the nuclei.

Ref.: ICCR, 2024; Fraunhofer IAP, 2024; ZentriForce, 2024

SCCS comment on cellular uptake
Cellular uptake of HAP nanoparticles from PhPC-2022-3 (nano) was demonstrated for the lowest and highest concentrations of PhPC-2022-3 (nano). Elemental identification of the nanoparticles was not performed.

The SCCS comment on the *in vitro* mammalian cell gene mutation test on V79 cells (*Hprt* locus)

The SCCS considers the study as valid. The results were negative, as concomitantly, cellular uptake was confirmed. Hence, it can be concluded that hydroxyapatite in the form of PhPC-2022-3 (nano) did not induce gene mutations in mammalian cells.

***In vitro* Mammalian Cell Micronucleus Test (MNT)**
The Applicant provided an *in vitro* mammalian Cell Micronucleus Test (MNT), including investigation of particle size distribution, dispersion stability and cellular uptake.

Summary of the study by the Applicant based on Report:

Study Design:

Reference:	Chelab, 2023c
Date of report:	08.05.2023
Study period:	11.07.2022 – 09.11.2023
Guidelines/Methods:	OECD 487 (2016) plus requirements of SCCS guidance (SCCS/1611/19 and 1628/21)
Test system:	Chinese hamster CHO-K1 cells
Replicates:	Triplicates
Test substance:	PhPC-2022-3 (nano, i.e. hydroxyapatite (nano))
Batch (Purity):	D20469A (hydroxyapatite (nano) content: 29.5%, specified by CoA)
Vehicle:	Treatment medium: HAM'S enriched with 5 % Foetal Bovine Serum (FBS)
Concentrations#:	**Main MNT:** PhPC-2022-3 Without S9: 0, 0.0530, 0.1059, 0.2119 mg/mL (corresponding to hydroxyapatite (nano): 0, 0.0156, 0.0313, 0.0625 mg/mL) With S9: 0, 0.1059, 0.2119, 0.4237 mg/mL (corresponding to hydroxyapatite (nano): 0, 0.0313, 0.0625, 0.1250 mg/mL)
Treatment:	4 h ±S9 24 h -S9
After treatment exposure:	24 h: Cytochalasin B (cytoB): 3 µg/mL

Positive controls:	-S9: Mitomycin C (MMC): 4.7 µg/mL (4 h), 0.02 µg/mL (24 h) Colchicine (COL): 0.5 µg/mL (4 h), 0.06 µg/mL (24 h) +S9: Cyclophosphamide monohydrate (CP): 50 µg/mL (4 h)
Negative control:	Vehicle
Statistics:	ANOVA
GLP:	Yes
Published:	No
# the tested concentrations were based the results of a preliminary cytotoxicity test	

Material and methods:
The possible mutagenic potential of PhPC-2022-3 (nano, i.e., hydroxyapatite (nano), batch: D20469A, hydroxyapatite (nano) content: 29.5%) was investigated in an *in vitro* micronucleus test according to OECD 487 under GLP conditions and following SCCS guidance requirements. The assay was carried out on CHO-K1 cells. The cells were exposed to the test substance at three different treatment conditions: 4 hours in the presence and in the absence of metabolic activation (4h+S9 and 4h-S9) and 24 hours in the absence of metabolic activation (24h-S9). Based on the results of a preliminary cytotoxicity test concentrations of PhPC-2022-3 (nano) of 0, 0.0530, 0.1059, 0.2119 mg/mL (corresponding to hydroxyapatite (nano): 0, 0.0156, 0.0313, 0.0625 mg/mL) without metabolic activation and of 0, 0.1059, 0.2119, 0.4237 mg/mL (corresponding to hydroxyapatite (nano): 0, 0.0313, 0.0625, 0.1250 mg/mL) with metabolic activation were selected. Osmolality and pH of the growth medium were assessed during the preliminary cytotoxicity as well as during the main assay using reference substances with known osmolality and pH. For comparison and to demonstrate the sensitivity and validity of the test system, negative controls (treatment medium) and positive controls (Mitomycin C (MMC) and Colchicine (COL) without S9 and Cyclophosphamide monohydrate (CP) with S9) were examined in parallel. After the treatment with the test substance, cells were grown for a period sufficient to allow the formation of micronuclei in interphase cells. During this period, cells were exposed to Cytochalasin B to permit the selective analysis of micronucleus frequency in cells that have completed one mitosis. Micronuclei formation was investigated by using a microscope after cell staining with Giemsa. At least 1000 cells/plate, for a total of 3000 cells per concentration tested, were scored for the evaluation of the micronuclei.

In addition, the uptake of hydroxyapatite (nano) into the cell and/or nucleus was investigated by TEM-EDX (according to ISO 21363:2020) and DLS (according to ISO 22412:2017.

Results:
Osmolality and pH were monitored and were acceptable.
No cytotoxicity was evident at any concentration after 4 h exposure with/without S9 or 24 h without S9.
The highest concentration analysed was the lowest concentration producing a visible precipitate.
The obtained results demonstrated clearly that the test item did not lead to an increased frequency of micronuclei, when compared to concurrent or historical controls and thus, indicating no chromosome damaging potential in the form of numerical (aneuploidy) or structurally (clastogenic) chromosomal aberrations in exposed CHO-K1 cells. Details for the results are presented in the tables below:

Table 16: Results of Micronuclei counting for treatment 4 h – S9

Treatment		**Mean Cytostasis %**	**Mean Micronuclei frequency**	**% MN**	**Induction factor (IF)**
Negative control	Treatment medium	/	13.7	1.4	-
Positive control	COL (0.5 µg/ml)	- 3.7	40.3	4.0	2.9

	MMC (4.7 µg/ml)	25.9	67.7	6.8	4.9
Hydroxyapatite (nano)	0.0625 mg/mL*	3.7	10.7	1.1	0.8
	0.0313 mg/mL	0.0	9.7	1.0	0.7
	0.0156 mg/mL	3.7	10.0	1.0	0.7
*=precipitating concentration					

Table 17: Results of Micronuclei counting for treatment 4 h + S9

Treatment		**Mean Cytostasis %**	**Mean Micronuclei frequency**	**% MN**	**Induction factor (IF)**
Negative control	Treatment medium	/	12.7	1.3	/
Positive control	CP (50 µg/ml)	22.2	56.0	5.6	4.3
Hydroxyapatite (nano)	0.125 mg/mL*	- 50.0	11.7	1.2	0.9
	0.0625 mg/mL	- 50.0	8.7	0.9	0.7
	0.0313 mg/mL	- 16.7	11.3	1.1	0.8

*=precipitating concentration

Table 18: Results of Micronuclei counting for treatment 24 h - S9

Treatment		**Mean Cytostasis %**	**Mean Micronuclei frequency**	**% MN**	**Induction factor (IF)**
Negative control	Treatment medium	/	13.0	1.3	/
Positive control	COL (0.06 µg/ml)	- 22.2	37.0	3.7	2.8
	MMC (0.2 µg/ml)	11.1	93.7	9.4	7.2
Hydroxyapatite (nano)	0.0625 mg/mL*	3.7	13.3	1.3	1.0
	0.0313 mg/mL	0.0	11.3	1.1	0.8
	0.0156 mg/mL	0.0	9.7	1.0	0.8

*=precipitating concentration

All validity and acceptance criteria were met and the positive as well as the negative controls showed results indicating the sensitivity and suitability of the test system.

Conclusion
Under the conditions of reliable test conditions, the test item did not induce an increased frequency of micronucleus formation and thus is considered to induce no chromosome destruction and/or gains or losses, when tested with and without metabolic activation up to precipitation concentrations in CHO-K1 cells. Thus, the hydroxyapatite (nano) test material in the form of PhPC-2022-3 (nano) was considered to possess neither a clastogenic nor an aneugenic potential.

Size distribution, dispersion stability and cellular uptake for the *in vitro* mammalian cell micronucleus test (MNT)

The detailed elements on the size and aspect ratio distribution based on individual particle measurements of HAP NPs in the form of PhPC-2022-3 (nano) provided by Applicant for all the MNT test conditions are reported in Annex D, Tables Annex D-1, 2, and 3 for the compositions C1, C2 and C3 without S9 and C1*, C2* and C3* with S9 in MNT Culture Cell media.

Study Design:

Reference:	EcamRicert, 2023f
Date of report:	26.04.2023
Guideline:	Requirements of SCCS Opinion (SCCS/1624/2020) and SCCS guidance (SCCS/1611/19)
Test system/method:	a) Particle size distribution and dispersion b) Uptake: Chinese hamster CHO-K1 cells
Test substance:	PhPC-2022-3 (nano, i.e. hydroxyapatite (nano))
Batch (Purity):	D20469A (hydroxyapatite (nano) content: 29.5%, specified by CoA)
Vehicle:	Treatment medium: HAM'S enriched with 5 % Foetal Bovine Serum (FBS)
Analytical methods:	- Transmission electron microscopy coupled with energy-dispersive X-ray spectroscopy (TEM-EDX) - Dynamic light scattering (DLS, Zetasizer nanoZS Zen 3600, Malvern)
Concentrations:	Without S9: 0, 0.0530, 0,1059, 0.2119 mg/mL (corresponding to hydroxyapatite (nano): 0, C3: 0.0156, C2: 0.0313, C1: 0.0625 mg/mL) With S9: 0, 0.1059, 0.2119, 0.4237 mg/mL (corresponding to hydroxyapatite (nano): 0, C3*: 0.0313, C2*: 0.0625, C1*: 0.1250 mg/mL)
GLP:	No data
Published:	No

* has been added by the SCCS to distinguish the tests without and with S9.

Material and methods:
The size distribution, dispersion and cellular uptake of PhPC-2022-3 (nano, i.e., hydroxyapatite (nano), batch: D20469A, hydroxyapatite (nano) content: 29.5%) during the MNT assay were examined according to requirements of the SCCS available at that time (SCCS/1611/19, Reference: SCCS, 2019). These investigations were performed using TEM-EDX (according to ISO 21363:2020) and DLS (according to ISO 22412:2017). Culture media and sample preparation for DLS and TEM-EDX analyses were corresponding to those described in MNT assay above compliant with OECD 487 and SCCS requirements under GLP conditions.

Results:
Focusing on the main results of this safety dossier, only the results of the highest hydroxyapatite (nano) concentrations in the form of PhPC-2022-3 (nano) without S9 and with S9 metabolic activation are presented as representative examples.

The results are summarized in the following Table 19:

Table 19: Particle sizes and aspect ratio as a function of the MNT conditions (Summary edited by SCCS) (for details, see Annex D)

Assay Condition **(MNT)**	**Median length (nm) (TEM)**	**Median width**	**Aspect ratio (TEM)**
Pristine HAP (nano)	21 ± 3	12 ± 3	1.51
0.0625 mg/mL producing visible precipitates in CHO-K1 cell culture medium without S9 before exposure time	22.2 ± 2.9	12.4 ± 2.7	1.72 ± 0.27

0.0625 mg/mL producing visible precipitates in CHO-K1 cell culture medium without S9 after 24 h exposure time	22.1 ± 2.9	12.6 ± 2.7	1.75 ± 0.24

Cellular uptake and cytoplasmatic internalization for the *in vitro* mammalian cell micronucleus test (MNT)

The TEM images and size distributions of internalised HAP (nano) particles for the various concentrations, provided by Applicant, are reported in Annex E. Below are presented overall summary on cellular uptake by the Applicant and the comment by the SCCS on the aspect ratio of internalized HAP (nano) particles.

Conclusion from the Applicant
The test material, PhPC-2022-3 (nano, i.e. hydroxyapatite (nano)) is principally composed of calcium (Ca), phosphorus (P) and oxygen (O) and the analysed hydroxyapatite (nano) particles showed a median length of 21.1 nm and 12.2 nm, respectively.

Under conditions of the investigations and based on TEM results, hydroxyapatite (nano) particles of PhPC-2022-3 (nano) preserved its primary particle size distribution and no changes in agglomeration/aggregation phenomena were observed at each tested concentration under any test condition.
Cellular uptake of hydroxyapatite (nano) particles of PhPC-2022-3 (nano) was also investigated at the concentrations used in the MNT and cytoplasmic internalization of hydroxyapatite (nano) was observed in all test conditions. The size of internalized particles was comparable with hydroxyapatite (nano) particles to those of the pure (pristine) form.

SCCS comments on the aspect ratio of internalized HAP (nano) particles in the *in vitro* mammalian cell micronucleus test (MNT)
The characterisation data of the internalised HAP (nano) particles in the *in vitro* mammalian cell micronucleus test (MNT) indicate that the AR 90th percentile was equal to or greater than 3, which is regarded as the threshold between rod shape and fibre shape:
AR 90th percentile = 3.91, (C2 24h – S9) – 24h exposure - 0.0313 mg/mL without S9
AR 90th percentile = 3.35, (C3 24h – S9) – 24 h exposure – 0.0156 mg/mL without S9
AR 90th percentile = 3.24, (C3* 4h + S9) – 4h exposure – 0.0313 mg/mL with S9

These data indicate that whilst most (90th percentile) of the internalised particles are rod shaped, a fraction of the internalised HAP (nano) particles in the three MNT conditions listed above can be considered to be at the borderline between rod and fibre shapes.

For these 3 conditions listed above, for which the AR 90th percentiles of the internalized HAP (nano) particles are larger than 3, these AR 90th percentiles of internalised HAP (nano) particles are larger than the ones of HAP (nano) particles in the same MNT conditions (see Table below).

Table 21: Aspect ratio 90th percentile of particles in culture cell media and of internalized particles (MNT conditions)

Reference	MNT conditions	AR 90th percentile of particles in culture cell media	AR 90th percentile of internalized particle
C2 – S9 before 24h	Before exposure – 0.0313 mg/mL without S9	2.68	
C2 24h – S9	24h exposure - 0.0313 mg/mL without S9	2.39	3.91
C3 – S9 before 24h	Before exposure – 0.0156 mg/mL without S9	2.82	
C3 24h – S9	24 h exposure – 0.0156 mg/mL without S9	3.01	3.35
C*3 + S9 before exposure	Before exposure – 0.0313 mg/mL with S9	3.04	
C3* 4h + S9	4h exposure – 0.0313 mg/mL with S9	2.96	3.24

* has been added by the SCCS to distinguish the tests without and with S9.

References: Dossier on Hydroxyapatite (nano) KG 2023-08-09; Document file name: Ref 14 22523987.0002_FR_Attachment_3-1_complete MNT Uptake, Project number: 22LA14102/MN. Evaluation of PhPC-2022-3 (nano) behavior in terms of size distribution, dispersion and cellular uptake for Micronucleus (MN) assay. ECAMRICERT SRL. 2023

SCCS comment on the *in vitro* micronucleus test on CHO-K1 cells
In the opinion of the SCCS the study is valid and the results are considered negative with demonstration of cellular uptake. Hence, it could be confirmed that hydroxyapatite PhPC-2022-3 (nano) does not induce chromosomal damage in mammalian cells.

3.4.1.2 Overall comment on mutagenicity/genotoxicity

From the Applicant
Hydroxyapatite (nano) in the form of PhPC-2022-03 (nano) was thoroughly investigated for its possible mutagenic/genotoxic potential *in vitro* according to most appropriate internationally accepted guidelines under GLP conditions and following SCCS guidance requirements for testing nanoscaled materials.

Mouse Lymphoma Assay (MLA)
The test was carried out according to OECD 490 on the L5178Y/TK$^{+/-}$ cell line. The treatment consisted of a sufficiently high number of concentrations up to the lowest concentrations inducing precipitation but no cytotoxicity. After treatment and following a sufficient two-days expression period, the cells were further processed and analysed for the required endpoints. Study design and methodology were compliant with OECD testing and reporting requirements as well as with the recommended SCCS guidance. All quality and acceptability criteria were met, and no obvious deviations were evident.

It was clearly demonstrated that the test item led to no increase of the mutation frequency at either concentration, neither in the form of incidences for small and large colonies or combined, when compared to concurrent or historical controls after 4 h ±S9 or 24 h -S9 exposures. Under the conditions of reliable test conditions, the test item did not induce gene mutations in L5178Y TK+/- mouse lymphoma cell line, when tested up to precipitating but non-cytotoxic concentrations. Therefore, the hydroxyapatite (nano) test item was clearly negative and revealed no genotoxic potential *in vitro* in the Mouse Lymphoma Assay.

In addition, the analysed hydroxyapatite (nano) particles showed a median length of 21.1 nm and 12.2 nm, respectively and preserved its primary particle size distribution. No changes in agglomeration/aggregation were observed at each tested concentration under any test

condition. Cellular uptake was SCCS-compliantly investigated but cytoplasmatic internalization of hydroxyapatite (nano) particles was not observed, although the selected and examined concentrations were requirement compliant and a sufficient exposure duration covering two-days expression was given. Apparently, cells in suspension may have a different internalization capability for minerally structures then adherent cells as can be deduced from results obtained from the Micronucleus Test. In any case, all investigations should be considered as sufficiently valid to indicate that hydroxyapatite (nano) possess no genotoxic potential in this test system.

In this respect it is important to mention that in the last SCCS Opinion from 2023 (SCCS/1648/22, Reference: SCCS, 2023a) it is reported that cellular uptake of an analogue hydroxyapatite (nano) material by L5178Y TK+/- mouse lymphoma cells, tested in the same laboratory under practically identical conditions, was only detected at the highest test concentration after 24 h exposure in the absence of S9, while in the MNT performed, cellular uptake was also demonstrated in all tested conditions as in our experimental conditions. The SCCS finally assessed both the MLA and MNT, including the cellular uptake investigations, as valid and the same is considered justified for the MLA and MNT presented in this dossier.

Micronucleus Test (MNT)
The test was carried according to OECD 487 on CHO-K1 cells. Again, the treatment consisted of a sufficient high number of concentrations up to the lowest concentrations inducing precipitation but no cytotoxicity. After the exposure cells were grown for a period sufficient to allow the formation of micronuclei in interphase cells and exposed to Cytochalasin B to permit the selective analysis of micronucleus frequency in cells that have completed one mitosis. Study design and methodology were compliant to OECD testing and reporting requirements as well as to the recommended SCCS guidance. All quality and acceptability criteria were met, and no obvious deviations were evident.

The results obtained clearly indicated that the test item did not induce an increased frequency of micronucleus formation when compared to concurrent or historical controls after 4 h ±S9 or 24 h -S9 exposures. Thus, no induction of chromosome destruction and/or gains or losses was evident, when tested with and without metabolic activation up to precipitation but no cytotoxicity inducing concentrations in CHO-K1 cells. Thus, also in this test system hydroxyapatite (nano) was clearly negative and neither a clastogenic nor an aneugenic potential was evident *in vitro* in the Micronucleus Test.

In addition, the analysed hydroxyapatite (nano) particles showed a median length of 21.1 nm and 12.2 nm, respectively and preserved its primary particle size distribution. No changes in agglomeration/aggregation were observed at each tested concentration under any test condition.

Cellular uptake was SCCS-compliantly investigated and cytoplasmic internalization of hydroxyapatite (nano) particles was observed in all test conditions. The size of internalized particles was not substantially different from those of the pure (pristine) form.
Overall, when the possible *in vitro* genotoxic potential of hydroxyapatite (nano) HAP (nano) in the form of PhPC-2022-03 was investigated according to nano-material specific conditions requested by the SCCS, all quality and acceptability criteria were met, and the analytical methodology used comprised the current state of the art procedures and knowledge.

Based on comprehensive analytical investigations, appropriate testing concentrations were established that fulfilled the nano material testing requirements, as the highest concentrations induced acceptable precipitation, while no cytotoxicity was induced. Analyses performed prior to and after the respective *in vitro* genotoxicity tests demonstrated that the primary particle size distribution or changes in agglomeration/aggregation phenomena were not observed at each tested concentration.

In the testing guideline compliant *in vitro* mutagenicity tests, it was clearly shown that the test item was not able to induce gene mutations in L5178Y TK+/- mouse lymphoma cells, when tested up to precipitation concentrations in the mammalian cell Mouse Lymphoma Assay. It was also demonstrated that it was not possible to induce structural or numerical chromosomal damage in CHO-K1 cells, when tested up to precipitation concentrations and including a non-precipitating concentration, all of them leading to cellular uptake in the mammalian cell Micronucleus test.

Finally, using appropriate state of the art nano material specific methodology, it was clearly shown that hydroxyapatite (nano) revealed no genotoxic potential *in vitro*. It induced neither gene mutations nor structural or numerical chromosomal damage.

It is important to note that in the last SCCS Opinion from 2023 (SCCS/1648/22, Reference: SCCS, 2023a) the same conclusion was drawn for an analogue hydroxyapatite (nano) material, tested in the same laboratory under practically identical conditions. Thus, the same conclusion is considered justified for the MLA and MNT studies presented in this dossier.

Overall assessment by the Applicant
Based on the comprehensive and SCCS-compliant data presented in both the SM I and the current SM II, it is justified to conclude that hydroxyapatite (nano) does not possess any genotoxic potential.

Overall SCCS comment on mutagenicity/genotoxicity
Hydroxyapatite in the form of PhPC-2022-3 (nano) was tested in two mammalian cell gene mutation assays (one MLA test of limited reliability and one valid *Hprt* test on V79 cells with negative result) and one valid micronucleus test on CHO-K1 cells with negative result. In all 3 studies, the same batch of PhPC-2022-3 (nano) was tested. Cellular uptake was demonstrated in the *Hprt* and micronucleus tests.
Based on the outcome of these studies, the SCCS is of the opinion that hydroxyapatite in the form of PhPC-2022-3 (nano) does not raise a concern for mutagenicity.

3.5 SAFETY EVALUATION (INCLUDING CALCULATION OF THE MOS)

From the Applicant
A calculation of the systemic exposure dose (SED) and margin of safety (MoS) is considered as not relevant for the following reasons:
a) After a thorough data evaluation of analogue hydroxyapatite (nano) forms, the SCCS in its opinion SCCS/1624/20 in 2021 concluded that
"*Based on the available data, the SCCS concludes that hydroxyapatite (nano) under the conditions of uses in cosmetic products would not have:*
- any significant systemic exposure via the oral mucosa
- any significant systemic exposure via ingestion (due to solubility in gastric fluid)
- any cytotoxicity at the level of the oral epithelium after 48h exposure"
b) This conclusion was re-iterated in the SCCS Opinion SCCS/1648/22 in 2023
c) This safety dossier demonstrated clearly that hydroxyapatite (nano) as physicochemically characterized and specified in this dossier clearly revealed the absence of any genotoxic potential.
d) Finally, and in line with the SCCS conclusion, the MoS calculation was not regarded as relevant for this safety dossier, as the systemic hydroxyapatite (nano) exposure could be only negligible, if any may occur.

SCCS comment
In the SCCS Opinion from 2021 (SCCS/1624/20), it was concluded that based on the available data, HAP (nano) under the conditions of uses in cosmetic products would not have:
- any significant systemic exposure via the oral mucosa,
- any significant systemic exposure via ingestion (due to solubility in gastric fluid),

- any cytotoxicity at the level of the oral epithelium after 48h exposure.

In its latest Opinion from 2023 (SCCS/1648/22), the SCCS focused on the genotoxicity of the HAP (nano). Based on the data provided at the SCCS request, the conclusion drawn by the SCCS was that HAP (nano) as specified in the 2023 Opinion[4] (at concentrations up to 10% in toothpaste, and up to 0.465% in mouthwash) did not have genotoxicity potential. Also, as the systemic exposure could be considered only negligible, the MoS calculation was not considered relevant for the previous evaluation.

Based on the new data provided along with the current submission (IV), the conclusion drawn by the SCCS is that HAP (nano) as specified in this Opinion[5] (at concentrations up to 29.5% in toothpaste, and up to 10% in mouthwash) does not have genotoxicity potential. The provided data showed that HAP (nano) did not induce cytotoxic effects (MTT, LDH tests) or a pro-inflammatory response (IL-1α production) in the *in vitro* human buccal mucosa model after 48 h of exposure.

In addition, the systemic exposure to HAP particles through oral route is considered negligible, if any. Although some cell uptake of HAP (nano) was shown in the cells of buccal mucosa model, it is considered that epithelial cells of the oral mucosa are continuously replaced, and any cells containing particles can be expected to be shed out. In addition, any unintentionally ingested HAP (nano) particles will undergo rapid and complete dissolution under acidic conditions in the stomach.
In consideration of all these aspects, the MoS calculation was not considered relevant for this evaluation.

3.6 DISCUSSION

Physicochemical Properties
Hydroxyapatite (nano) (PhPC-2022-3 (nano)) is fully synthetic and inorganic in nature and consists of rod-shaped particles with median primary particle length and width of 21 nm and 12 nm, respectively, a volume specific surface area of 269 m^2/cm^3 and a zeta-potential of -29.5 ± 1.4 mV.

Hydroxyapatite (nano) is known to be insoluble or practically insoluble in water at neutral pH but is increasingly soluble in water with lower pH. Below a pH value of approximately 5.5 a dissolution of hydroxyapatite can be observed which leads to the release of calcium ions, (hydrogen)phosphate ions, and water.

The tested hydroxyapatite (nano) was reported to be stable for at least 18 months.

Exposure and Toxicokinetics
Hydroxyapatite (nano) in oral cosmetic products comes into contact with the buccal mucosa, and part of it may potentially be accidentally swallowed. Due to the significantly increased solubility of hydroxyapatite (nano) in acidic environments and the absence of any toxicological concern of the resulting calcium and phosphate ions, the systemic availability of hydroxyapatite (nano) can be considered negligible.
Potential penetration through the multilayered oral mucosal epithelium was investigated using an *in vitro* epithelial model tissue. The experiments reported in this submission focused on non-keratinized epithelial models as worst-case scenario. The results demonstrated uptake of

[4] Composed of rod-shaped particles of which at least 95.8% (in particle number) have an aspect ratio of less than 3, and the remaining 4.2% have an aspect ratio not exceeding 4.9; and the particles are not coated or surface modified.
[5] Composed of rod-shaped particles of which at least 87% (in particle number) have aspect ratio equal to or less than 3, and the remaining 13% have an aspect ratio not exceeding 9; and the particles are not coated or surface modified.

particles in aggregates/agglomerates by individual cells across all tested concentrations. However, it was not possible to conclude on the depth of nanoparticles penetration.

Toxicological Evaluation

Given that systemic exposure to hydroxyapatite (nano) following cosmetic use in oral cosmetic products is negligible, the SCCS concluded in its opinion (SCCS/1648/22) that only local cytotoxicity on the oral mucosa and mammalian cell genotoxicity need to be assessed.

Cytotoxicity on the oral mucosa:

The studies reported in this submission using non-keratinized buccal mucosa models revealed some histological changes which were superficial and not dose-dependent, and might also be due to artefacts introduced by the histological sample preparation. Therefore, even when used at the highest concentration of 47.25 mg/mL, PhPC 2022-3 (nano) did not induce either cytotoxicity (MTT, LDH tests) or pro-inflammatory reactions (IL-1α production) in the buccal mucosa model after 48 h of exposure. Even if some internalization of the nanoparticles was observed, no cytotoxicity was associated with it. Further support for no cytotoxic potential of the exposure to the nanoparticles, may be the physiological turnover of the epithelial cells of the buccal mucosa which are continually replaced and that any cells with internalized particles will be shed out over time.

Mammalian cell mutagenicity:

Hydroxyapatite (nano) revealed no genotoxic potential *in vitro*. However, since the unequivocal evidence of cellular uptake of the test item was demonstrated for the *in vitro* chromosomal aberration/clastogenicity assay and not for the *in vitro* mammalian cell gene mutation assay under the chosen test conditions, the latter toxicological endpoint was further investigated in a new study using a different test system according to OECD TG 476. The new study revealed negative results.

In summary, the mutagenicity hydroxyapatite in the form of PhPC-2022-3 (nano) was tested in two mammalian cell gene mutation assays (one MLA test of limited reliability and one valid *Hprt* test on V79 cells with negative result) and one valid micronucleus test on CHO-K1 cells with negative result. In all 3 studies, the same batch of PhPC-2022-3 (nano) was tested. Cellular uptake was demonstrated in the *Hprt* and micronucleus tests.

Based on the outcome of these studies, the SCCS is of the opinion that hydroxyapatite in the form of PhPC-2022-3 (nano) does not raise a concern for mutagenicity.

MoS calculation

Based on the new data provided with the current submission, the conclusion drawn by the SCCS is that HAP (nano), as specified in this Opinion, does not have mutagenicity potential.

Also, as the systemic exposure could be considered negligible, the MoS calculation was not considered relevant for this evaluation.

4. CONCLUSION

1. In view of the above, and taking into account the scientific data provided, does the SCCS consider Hydroxyapatite (nano) safe when used in toothpaste up to a maximum concentration of 29.5 % and in mouthwash up to a maximum concentration of 10 % according to the specifications as reported in the submission, taking into account reasonably foreseeable exposure conditions?

   Based on the data provided, the SCCS considers hydroxyapatite (nano) safe when used at concentrations up to 29.5% in toothpaste, and up to 10% in mouthwash.

   This conclusion is based on the available evidence, which shows that hydroxyapatite (nano) does not pose a mutagenic hazard or cytotoxicity or inflammatory effects even when tested at high concentrations in a buccal mucosa cell model. Any uptake of hydroxyapatite (nano) by buccal mucosa is considered negligible, and the epithelial cells with internalised particles will be shed out over time as they are continually replaced. Also, any unintentionally ingested HAP nanoparticles during the use of oral-care products will undergo rapid dissolution in the gastric fluid and therefore do not raise any nano-specific concern over safety.

   This safety evaluation only applies to the hydroxyapatite (nano) that have the following characteristics:
   - composed of rod-shaped particles of which at least 87% (in particle number) have aspect ratios equal to or less than 3, and the remaining 13% have aspect ratios not exceeding 9.
   - the HAP particles are not coated or surface modified.
   - the Opinion is related to HAP particles with max length of the HAP nanoparticles in the present Opinion, i.e. 122 ± 43 nm.

2. Alternatively, what is according to the SCCS the maximum concentration considered safe for use of Hydroxyapatite (nano) in cosmetic products?

   /

3. Does the SCCS have any further scientific concerns with regard to the use of Hydroxyapatite (nano) in oral cosmetic products?

   This Opinion is not applicable to any hydroxyapatite (nano) that is composed of, or contains, needle-shaped particles.

5. MINORITY OPINION

None.

6. REFERENCES

1. Bose S and Tarafder (2012) Calcium phosphate ceramic systems in growth factor and drug delivery for bone tissue engineering: A review, Acta Biomateralia, 8, 1401-1421
2. Budenheim (2022) Certficate of analysis, PhPC-2022-3 (nano), hydroxyapatite aqueous suspension, Batch D20469A, 22 August 2022, unpublished, confidential business information (CBI), Appendix 3 to Enax *et al*., 2023, unpublished, confidential business information (CBI)
3. Budenheim (2023) Statement of information regarding Tricalcium phosphate (Hydroxyapatite), 19 July 2023, unpublished, confidential business information (CBI)
4. Chelab (2023a) Report - L5178Y Tk+/- Mouse Lymphoma Mutation Assay (MLA) according to OECD 490:2016 and SCCS requirements on "PhPC-2022-3 nano-hydroxyapatite. aqueous suspension (solid (active) content: 29.5% w/w", batch No. D20469A, CAS No. 1306-06-5, Final Report No. 22.523987.0001, Chelab Srl., Resana, Italy, 08 May 2023, unpublished, confidential business information (CBI)
5. Chelab (2023b) Attachment 4 to the report of Chelab No. 22.523987.0001, 2023a – Study Plan 22.523987.0001, L5178Y Tk+/- Mouse Lymphoma Mutation Assay (MLA) according to OECD 490:2016 and SCCS requirements on "PhPC-2022-3 nano-hydroxyapatite. aqueous suspension (solid (active) content: 29.5% w/w", batch No. D20469A, CAS No. 1306-06-5, Chelab Srl., Resana, Italy, 08 May 2023, unpublished, confidential business information (CBI)
6. Chelab (2023c) Report – Test for *in vitro* mammalian Cell Micronucleus test according to OECD 487:2016 (Microscope Method) and SCCS requirements on "PhPC-2022-3 nano-hydroxyapatite. aqueous suspension (solid (active) content: 29.5% w/w", batch No. D20469A, CAS No. 1306-06-5, Final Report No. 22.523987.0002, Chelab Srl., Resana, Italy, 08 May 2023, unpublished, confidential business information (CBI)
7. Chelab (2023d) Attachment 4 to the report of Chelab No. 22.523987.0002, 2023c – Study Plan 22.523987.0002, Test for *in vitro* mammalian Cell Micronucleus test according to OECD 487:2016 (Microscope Method) and SCCS requirements on "PhPC-2022-3 nano-hydroxyapatite. aqueous suspension (solid (active) content: 29.5% w/w", batch No. D20469A, CAS No. 1306-06-5, Chelab Srl., Resana, Italy, 08 May 2023, unpublished, confidential business information (CBI)
8. CosIng (2023) European Commission database for information on cosmetic substances and ingredients, Hydroxyapatite, CAS 1306-06-5, 2023, https://ec.europa.eu/growth/tools-databases/cosing/details/34479
9. EcamRicert (2023a) Attachment 1 to the report of Chelab No. 22.523987.0001, 2023a – Particle size characterization and stability of nanohydroxyapatite in cell culture media used for genotoxicity tests, Project No.: 22LA14074-22LA14075-22LA14097, 05 August 2022, unpublished, confidential business information (CBI)
10. EcamRicert (2023b) Attachment 2 to the report of Chelab No. 22.523987.0001, 2023a – Particle size characterization and stability of nanohydroxyapatite in cell culture media used for genotoxicity tests, Project No.: 22LA14074-22LA14075-22LA14097/Preliminary characterization, 27 April 2023, unpublished, confidential business information (CBI)
11. EcamRicert (2023c) Attachment 3 to the report of Chelab No. 22.523987.0001, 2023a – Evaluation of PhPC-2022-3 (nano) behavior in terms of size distribution, dispersion and cellular uptake for Mouse Lymphoma Assay (MLA), Project No.: 22LA14076/MLA, 03 May 2023, unpublished, confidential business information (CBI)
12. EcamRicert (2023d) Attachment 1 to the report of Chelab No. 22.523987.0002, 2023c – Particle size characterization and stability of nanohydroxyapatite in cell culture media used for genotoxicity tests, Project No.: 22LA14074-22LA14075-22LA14097, 05 August 2022, unpublished, confidential business information (CBI)
13. EcamRicert (2023e) Attachment 2 to the report of Chelab No. 22.523987.0002, 2023c – Particle size characterization and stability of nanohydroxyapatite in cell culture media used for genotoxicity tests, Project No.: 22LA14074-22LA14075-22LA14097/ Preliminary characterization, 27 April 2023, unpublished, confidential business information (CBI)

14. EcamRicert (2023f) Attachment 3 to the report of Chelab No. 22.523987.0002, 2023c – Evaluation of PhPC-2022-3 (nano) behavior in terms of size distribution, dispersion and cellular uptake for Micronucleus (MN) assay, Project No.: 22LA14102/MN, 26 April 2023, unpublished, confidential business information (CBI)
15. EcamRicert (2023g) Report – Aspect ratio of the nanohydroxyapatite particles constituting PhPC-2022-3 (nano), Project No.: 22LA14074, 29 June 2023, unpublished, confidential business information (CBI)
16. ECHA (2022) Appendix for nanoforms applicable to the Guidance on Registration and Substance Identification Version 2.0, DOI: 10.2823/40
17. Enax J, Lettmann J, Meyer F, Schulze zur Wiesche E (2023) Dossier on the safety of hydroxyapatite (nano) for the use in cosmetic oral care products, Part 1: Physicochemical characterization of a representative hydroxyapatite (nano) product, Annex 2, unpublished, confidential business information (CBI)
18. Enax J, Meyer F, Schulze zur Wiesche E, Epple M (2022) On the application of calcium phosphate micro- and nanoparticles as food additive, Nanomaterials, 12, 4075, 1-11
19. Epple M (2018) Review of potential health risks associated with nanoscopic calcium phosphate, Acta Biomaterialia 77, 1-14
20. Epple M (2022) Report - Physicochemical analysis of a nanohydroxyapatite suspension, University of Duisburg Essen, Essen, Germany 06 June 2022, Appendix 3 to Enax *et al*., 2023, unpublished, confidential business information (CBI)
21. Epple M, Ganesan K, Heumann R, Klesing J, Kovtun A, Neumann S, Sokolova V (2010) Application of calcium phosphate nanoparticles in biomedicine, J. Materials Chemistry, 20, 18-23
22. Fejerskov O and Kidd E (2009) *Dental Caries: The Disease and its Clinical Management*. Wiley, Handbook, 2009.
23. Fraunhofer (2022) Analysis of a hydroxylapatite suspension - PhPC-2022-3 (nano) #D20469A, Report No. 6662_6675_rev01, Fraunhofer IKTS, Department Sintering and Characterization, Laboratory for particle and suspension characterization, Dresden, Germany, 29 August 2022, Appendix 2 to Enax *et al*., 2023, unpublished, confidential business information (CBI)
24. Fraunhofer (2023) Analysis of a hydroxylapatite suspension - PhPC-2022-3 (nano) #D20469A, 09.03.2022, Report No. 6984, Zeta Potential, Fraunhofer IKTS, Department Sintering and Characterization, Laboratory for particle and suspension characterization, Dresden, Germany, 27 July 2023, unpublished, confidential business information (CBI)
25. Fraunhofer IAP (2024), Research Report, TEM investigation of hydroxyapatite nanoparticles in biological cell cultures (V79), Fraunhofer Institute for Applied Polymer Research (IAP), Potsdam, Germany, 20 August 2024, Annex 2 of ICCR Study Number 4114412, unpublished, confidential business information (Annex 5)
26. Limeback H (2022) Hydroxyapatite (nano) application in dentistry and its safety: an expert opinion, Professor Emeritus, Faculty of Dentistry, University of Toronto, Canada, 26 June 2022, Appendix 4 to Enax *et al*., 2023, unpublished, confidential business information (CBI)
27. Microbiological CoA (2022) Certificate of analysis, PhPC-2022-3, batch D20469A, Quality Control Department, Dr. Kurt Wolff GmbH & Co. KG, Bielefeld, Germany, 11 November 2022, unpublished, confidential business information (CBI)
28. Ramis JM, Coelho CC, Cordoba A, Quadros PA, Monjo M (2018) Safety Assessment of Nano-Hydroxyapatite as an Oral Care Ingredient according to the EU Cosmetics Regulation, Cosmetics 5, 1-13
29. SCCS (2016). Scientific Committee on Consumer Safety, Opinion on Hydroxyapatite (nano), revision 16 March 2016, SCCS/1566/15
30. SCCS (2018). Checklist for applicants submitting dossiers on cosmetic ingredients to be evaluated by the SCCS, revised version 16 May 2018, SCCS/1588/17
31. SCCS (2021). Scientific Committee on Consumer Safety. Opinion on Hydroxyapatite (nano), adopted 30 – 31 March 2021, SCCS/1624/20
32. SCCS (2023a). Scientific Committee on Consumer Safety. Opinion on Hydroxyapatite (nano), adopted 21 – 22 March 2023, SCCS/1648/22

33. SCCS (2023b). Scientific Committee on Consumer Safety. Notes of Guidance for the testing of cosmetic ingredients and their safety evaluation 12th revision, 15 May 2023, SCCS/1647/22
34. SCCS (2023c). Scientific Committee on Consumer Safety. Guidance on the Safety Assessment of Nanomaterials in Cosmetics. 2nd revision, 6 June 2023. SCCS/1655/23
35. Sokolova V and Epple M (2021) Biological and Medical Applications of Calcium Phosphate Nanoparticles, Chem. Eur. J., 27, 7411-7488
36. TERCIT (2024), Report No. 202400112-01, In Vitro Biocompatibility and Irritation of Biomimetic Hydroxyapatite Nanoparticles on Human Oral Epithelium, Group of Cell Therapy and Tissue Engineering, University of Balearic Islands, Palma, Spain, 18 September 2024, unpublished, confidential business information (Annex 4)
37. ZentriForce (2024), Final Technical Report, DLS Accelerated Stability Study, Project Code RICC005, Version 1.0, ZentriForce Pharma Research GmbH, Heidelberg, Germany, 16 September 2024, Annex 3 of ICCR Study Number 4114412, unpublished, confidential business information (Annex 5)

Disclosure of details of unpublished references has been agreed by the Applicant.

7. Annex A: Hydroxyapatite (HAP) Nano

From: SCCS Dossier on Hydroxyapatite (nano) 2023-08-09_signed: Safety assessment on hydroxyapatite (nano) in cosmetic products

Ref 15 22-007867_Aspect Ratio-signed
Aspect ratio of the nanohydroxyapatite particles constituting PhPC-2022-3 (nano)

Figure Annex A.1 (a, b and c) report representative transmission electron microscopy (TEM) micrographs of PhPC-2022-3 (nano) diluted in ultrapure water to a final concentration of nanohydroxyapatite of 59 ng hydroxyapatite (nano)/mL (dilution factor: 5000x). Primary particles are rod-shaped with rounded edges, and they form ellipsoidal/spheroidal aggregates/agglomerates made of tens to hundreds of particles. EDX analysis confirms the presence of calcium (Ca), phosphorous (P), and oxygen (O) as constitutive elements of hydroxyapatite. Signals of carbon (C) and nickel (Ni) in the spectrum are due to the carbon-coated nickel grid used as sample support. To define number-based primary particle size distribution, both length and width were independently measured. The three independent distribution curves are reported in Figure Annex A.1e, Figure Annex A.1g and Figure Annex A.1i, while their descriptive parameters in Figure Annex A.1f, Figure Annex A.1h and Figure Annex A.1j.

The median particle length and width obtained on a significant number of measured particles (≥ 500 particles) are 21 nm and 12 nm, respectively.

Thus, the median value of both dimensions in the detected particles falls within the range 1-100 nm, the analysed hydroxyapatite (nano) in the form of PhPC-2022-3 (nano) was confirmed to represent a nanoscaled material.

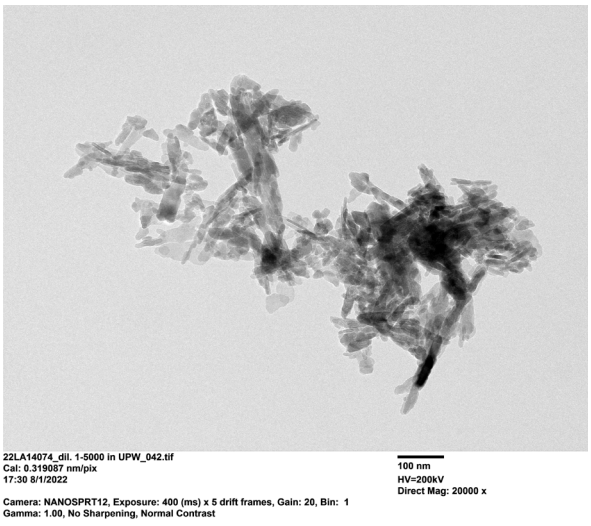

(a)

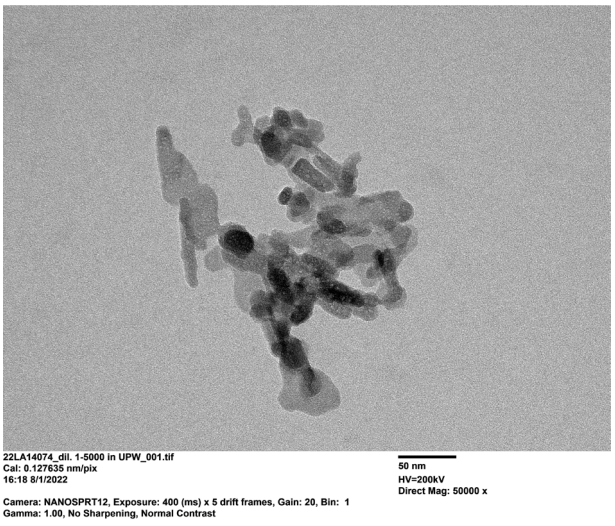

(b)

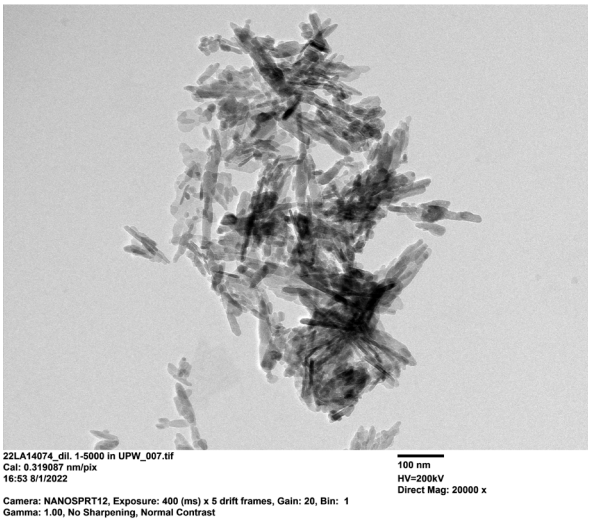

(c)

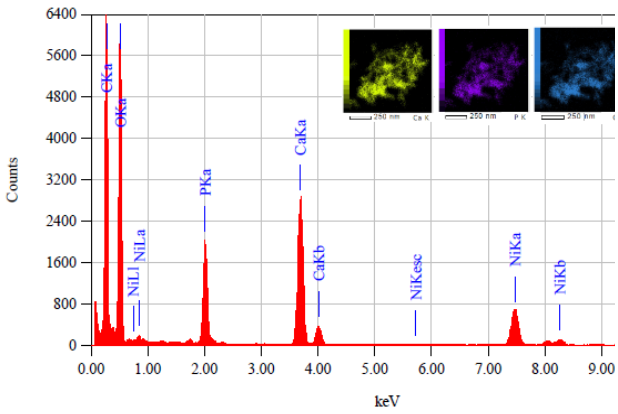

(d)

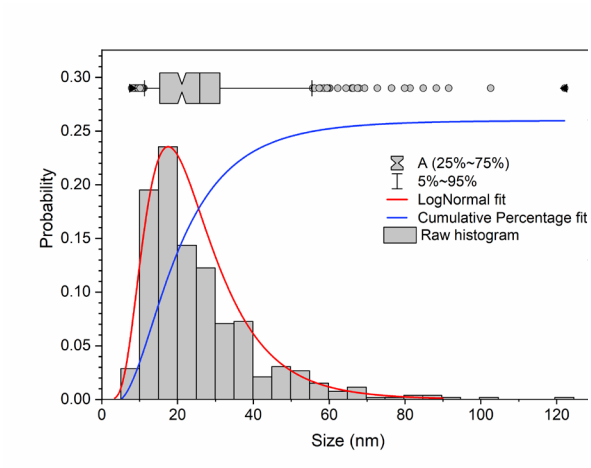

(e)

Dimensional Parameters - Length	Value
Analyzed particles	522
Minimum size (nm)	8 ± 1
First quartile (nm)	15 ± 2
Median (nm)	21 ± 3
MAD (nm)	6.9 ± 0.9
Average (nm)	26 ± 2
Standard deviation (nm)	15 ± 5
Third quartile (nm)	31 ± 3
Maximum size (nm)	122 ± 43
D10 (nm)	12 ± 2
D50 [median] (nm)	21 ± 3
D90 (nm)	47 ± 5

(f)

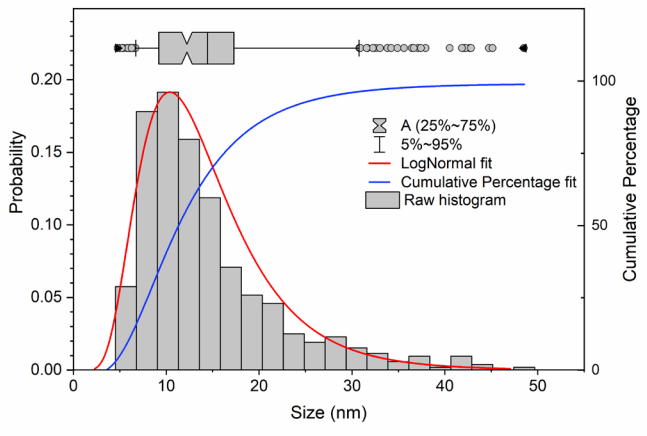

(g)

Dimensional Parameters - Width	Value
Analyzed particles	522
Minimum size (nm)	4.8 ± 0.6
First quartile (nm)	9 ± 2
Median (nm)	12 ± 3
MAD (nm)	3.5 ± 0.8
Average (nm)	14 ± 2
Standard deviation (nm)	8 ± 3
Third quartile (nm)	17 ± 3
Maximum size (nm)	49 ± 17
D10 (nm)	7 ± 1
D50 [median] (nm)	12 ± 3
D90 (nm)	25 ± 4

(h)

Figure Annex A.1: Transmission electron microscopy (TEM) number-based primary particle size distribution of hydroxyapatite (nano) in the form of PhPC-2022-3 (nano) diluted 1:5000 in ultrapure water. TEM micrographs at magnitude (a) 20000x, (b) 50000x, (c) 20000x. (d) EDX spectrum of particles. Signals of Carbon (C) and Nickel (Ni) in the spectrum are due to the carbon-coated nickel grid used as sample support. (e) Number-based particle size

distribution of particles' length and (f) its descriptive dimensional parameters. (g) Number-based particle size distribution of particles' width and (h) its descriptive dimensional parameters. Parameters are reported as value ± standard deviation. The uncertainty is expressed with two significant figures and decimal places of the values are reported accordingly.

References: EcamRicert, 2023b and 2023e

Aspect ratio

The descriptive parameters of particle AR distribution were produced and reported as minimum, first quartile, median, median absolute deviation (MAD), mean, standard deviation, third quartile, maximum and 10th, 50th and 90th percentiles. The 10th, 50th and 90th percentile values correspond to the minimum threshold below which 10 %, 50 % and 90 % of the particles in the distribution have an aspect ratio smaller than these values, respectively. Therefore the 50th percentile corresponds to the median value of the aspect ratio.

The ratio between length (measured as the longest dimension) and its associated width (measured as the smallest dimension perpendicular to length) was calculated producing the AR of each individual particle analyzed by TEM-EDX.

Figure Annex A.2 reports graphical representation and descriptive parameters of AR distribution calculated for hydroxyapatite (nano) individual particles. In the analyzed particles, AR ranges from 1.00 (lower limit) to 8.97 (upper limit) with median (i.e., 50th percentile) ± MAD of 1.51 ± 0.26. Average ± standard deviation is 1.96 ± 1.19. AR values corresponding to 10th and 90th percentile are 1.19 and 3.31 respectively, indicating that 10 % and 90 % of particles have AR smaller than these values. The aspect ratio analysis in this respect demonstrated that at least 87.2% (in particle number) had an aspect ratio of less than 3, while the remaining 12.8% had an aspect ratio greater that 3 but not exceeding 8.97, when calculated on a significant number of hydroxyapatite (nano) particles (522).

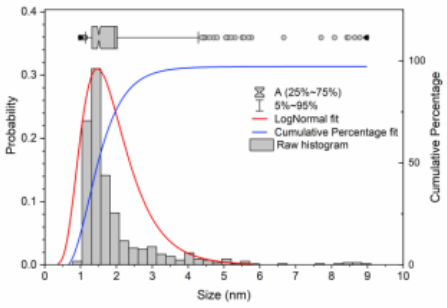

(a)

AR Descriptive parameters	
Number of particles	522
Minimum	1.00
First quartile	1.32
Median	1.51
MAD	0.26
Average	1.96
Standard deviation	1.19
Third quartile	2.02
Maximum	8.97
10th percentile	1.19
50th percentile	1.51
90th percentile	3.31
% of particles with AR ≥ 3.0	12.8 %
Fit parameters	
R^2	0.97
μ	1.44
σ	0.26

(b)

Figure Annex A.2: (a) Graphical representation of the Aspect Ratio (AR) distribution for hydroxyapatite (nano) particles of PhPC-2022-3 (nano). (b) Descriptive parameters of the AR distribution

Reference: EcamRicert, 2023g

Table Annex A – 1: Summary of the particle size and aspect ratio distribution of pristine HAP (nano) particles (edited by SCCS according to the above provided information by Applicant)

Materials	**Median Length**	**Median Width**	**Length (Min – Max)**	**Width (Min – Max)**	**AR Average**	**AR Median**	**Max AR**	**AR Third quartile**	**AR 90th percentile**
Pristine	21 ± 3	12 ± 3	8 ± 1 122 ± 43	4.8 ± 0.6 49 ± 17	1.96	1.51 ± 0.26	8.97	2.02	3.31*

8. Annex B: Hydroxyapatite (nano) in Cell Culture Media

From: Ref 9 22.523987.00001_FR_Attachment_1 PSD gentox: Particle size characterization and stability of nanohydroxyapatite in cell media used for genotoxicity tests

From the Applicant
The particle size distribution of dispersed hydroxyapatite (nano) in the form of PhPC-2022-3 (nano) in cell culture media used for genotoxicity tests was analyzed by TEM and DLS.

Besides the morphological analysis, the primary aim was the selection of appropriate concentrations of the subsequently performed Micronucleus Test (MNT) and Mouse Lymphoma Assay (MLA).

For the DLS analysis, the samples were diluted in the cell culture media used for the MNT and MLA with and without metabolic activation (S9) reagent. Cell culture media as such were used as blank. In the presence of comparable average particle sizes between two consecutive dilutions, the one with higher reproducibility among replicates (i.e., lower relative standard deviation) was selected as the first visible precipitate-free dispersion to be used for genotoxicity tests, and no further dilutions were applied. TEM analyses of the most suitable concentrations were also performed, with the aim of assessing particle size and aggregation/agglomeration state of hydroxyapatite (nano) particles.

Table Annex B.1.: Concentrations of PhPC-2022-3 (nano) and corresponding concentrations of hydroxyapatite (nano)

PhPC-2022-3 (nano) concentration (mg/mL)	Hydroxyapatite (nano) concentration (mg/mL)
1.6949	0.5000
0.8475	0.2500
0.4237	0.1250
0.2119	0.0625
0.1059	0.0313
0.0530	0.0156
0.0265	0.0078
0.0132	0.0039
0.0066	0.0020

a) Results for Hydroxyapatite (nano) in Micronucleus Test (MNT) Medium without S9:

From the Applicant
The average curves obtained for blank (i.e., the cell culture medium without PhPC-2022-3 (nano) (NC)) and PhPC-2022-3 (nano) at different concentrations are reported in Figure Annex B.1.

The average hydrodynamic diameter corresponding to the main population of particles of each tested condition is reported in Table Annex B.2, which also reports the presence or absence of visible precipitates.

It was shown that concentrations from 0.25 mg/mL to lower values were characterized by similar mean sizes (hydrodynamic diameter around 400 nm) but 0.0313 mg/mL dispersion showed a better reproducibility among replicates (i.e., lower relative standard deviation). Therefore, it was considered as the first stable and suitable concentration of hydroxyapatite

(nano) in MNT cell culture medium without S9 to be used for the subsequent test.

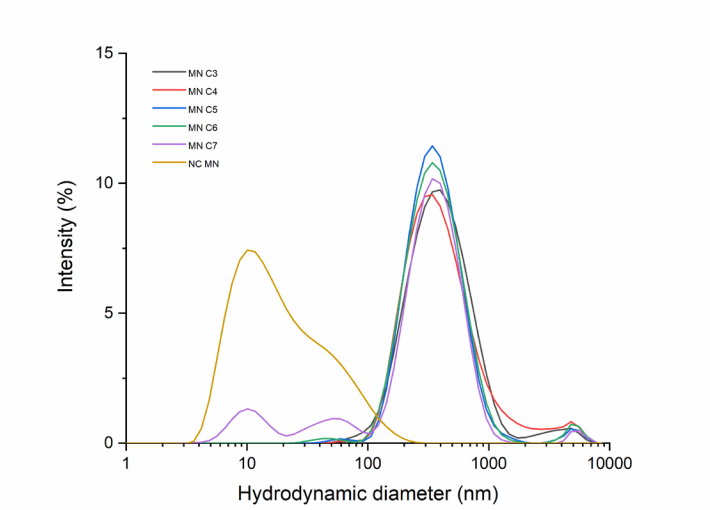

Figure Annex B.1: Dynamic Light Scattering (DLS) particle size distribution of PhPC-2022-3 (nano) (each curve is the average of 5 instrumental replicates) dispersed in Micronucleus Test (MNT) cell culture medium without S9 at different concentrations and blank (NC)

Table Annex B.2: Dynamic Light Scattering (DLS) particle size distribution parameters of the analysed dispersions in Micronucleus Test (MNT) cell culture medium without S9 (each value obtained from 5 replicates). The last column reports if dispersion presents visible precipitates. $RSD_{\%}$ = percentage relative standard deviation.

Hydroxyapatite (nano) concentration (mg/mL)	Hydrodynamic diameter of main peak (average ± standard deviation, nm)	Visible precipitates
0.5000	437 ± 46 ($RSD_{\%}$ = 11%)	Yes
0.2500	401 ± 19 (RSD% = 5%)	Yes
0.1250	395 ± 51 (RSD% = 13%)	Yes
0.0625	395 ± 30 (RSD% = 8%)	Yes
0.0313	393 ± 14 (RSD% = 4%)	No

Representative micrographs of PhPC-2022-3 (nano) in MNT cell culture medium without S9 at concentration 0.0313 mg/mL are reported in Figure Annex B.2. As shown, the agglomeration/aggregation state of hydroxyapatite (nano) particles in MNT culture medium without S9 was comparable to the particles of the pure hydroxyapatite (nano) particles (see above Figure Annex A.1).

To obtain primary particle size distribution, both length and width were independently measured, and the distribution curves are shown in Figure Annex B.2(c) and Figure Annex B.2(e), while their descriptive parameters are reported in Figure Annex B2(d) and Figure Annex B.2(f).

The median particle length and width obtained on a significant number of measured particles (≥ 500 particles) were 21 nm and 13 nm, respectively.

The aspect ratio of particles – calculated as the ratio of median length to median width – was 1.62.

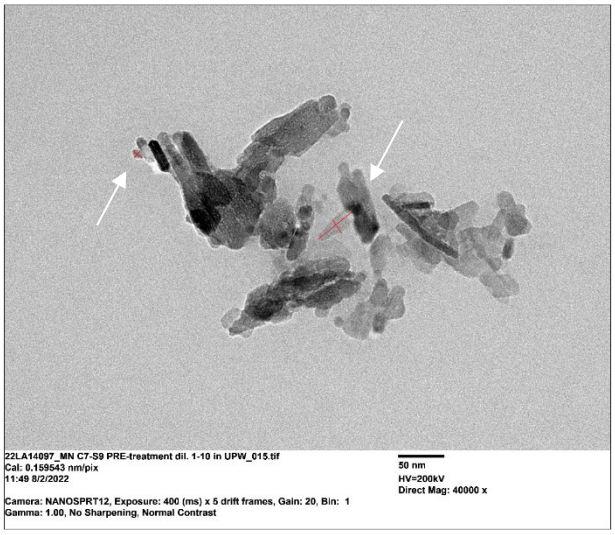

(a)

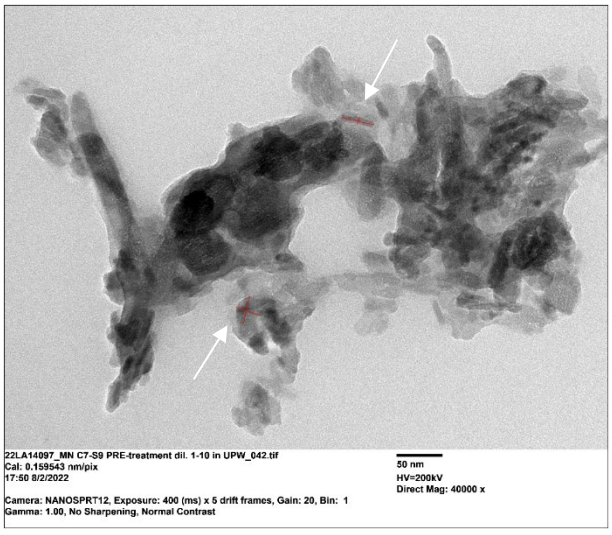

(b)

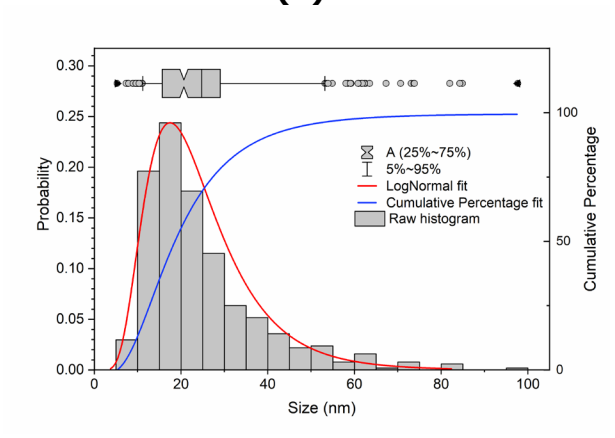

(c)

Dimensional Parameters - Length	Value
Analyzed particles	504
Minimum size (nm)	5.3 ± 0.7
First quartile (nm)	16 ± 2
Median (nm)	21 ± 3
MAD (nm)	6.0 ± 0.8
Average (nm)	25 ± 2
Standard deviation (nm)	14 ± 4
Third quartile (nm)	29 ± 3
Maximum size (nm)	98 ± 34
D10 (nm)	13 ± 2
D50 [median] (nm)	21 ± 3
D90 (nm)	43 ± 4

(d)

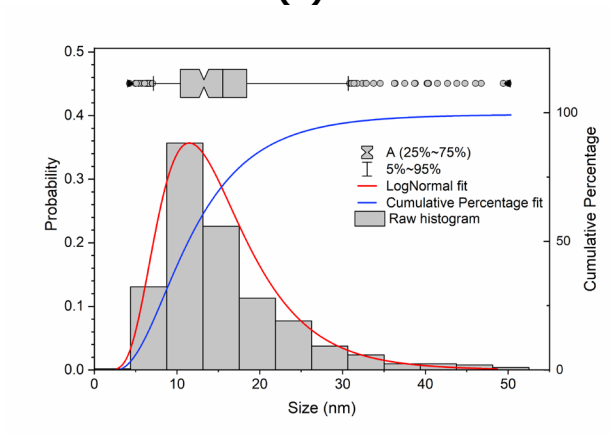

(e)

Dimensional Parameters - Width	Value
Analyzed particles	504
Minimum size (nm)	4.3 ± 0.5
First quartile (nm)	10 ± 2
Median (nm)	13 ± 3
MAD (nm)	3.5 ± 0.8
Average (nm)	16 ± 2
Standard deviation (nm)	8 ± 3
Third quartile (nm)	18 ± 3
Maximum size (nm)	50 ± 18
D10 (nm)	8 ± 1
D50 [median] (nm)	13 ± 3
D90 (nm)	26 ± 4

(f)

Figure Annex B.2: Transmission Electron Microscopy (TEM) number-based primary particle size distribution of hydroxyapatite (nano) at concentration 0.0313 mg/mL in MNT cell culture medium without S9. (a,b) TEM micrographs at magnitude of 40000x with shown (as red lines) length and width of representative particles of sample. (c) Number-based particle size distribution of particles' length and (d) its descriptive dimensional parameters. (e) Number-based particle size distribution of particles' width and (f) its descriptive dimensional parameters. Data are expressed as value ± standard deviation.

b) Results for Hydroxyapatite (nano) in Micronucleus Test (MNT) Medium with S9:

On the basis of the obtained DLS data, however, it was not possible to identify a suitable concentration for genotoxicity test in MNT cell culture medium with S9. Therefore, TEM analysis was performed on the first concentration without visible precipitates: 0.0625 mg/mL (C6).

Representative TEM micrographs of PhPC-2022-3 (nano) in MNT cell culture medium with S9 at concentration 0.0625 mg/mL are shown in Figure Annex B.3. Matrix embeds primary particles (Figure Annex B.3(a)) that are aggregated/agglomerated as in the pristine material and the other tested conditions. To obtain primary particle size distribution, both length and width were independently measured, and the distribution curves are reported in Figure Annex B.3(c) and Figure Annex B.3(e), while their descriptive parameters are reported in Figure Annex B.3(d) and Figure Annex B.3(f).

The median particle length and width obtained on a significant number of measured particles (≥ 500 particles) are 22 nm and 12 nm, respectively.

The aspect ratio of particles – calculated as the ratio of median length to median width – is 1.83.

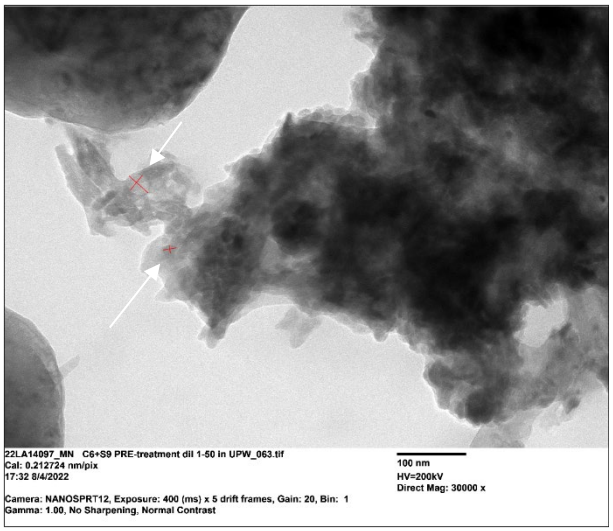

(a)

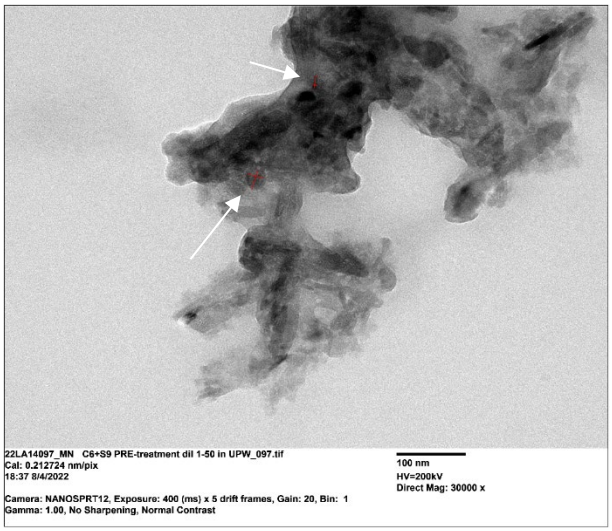

(b)

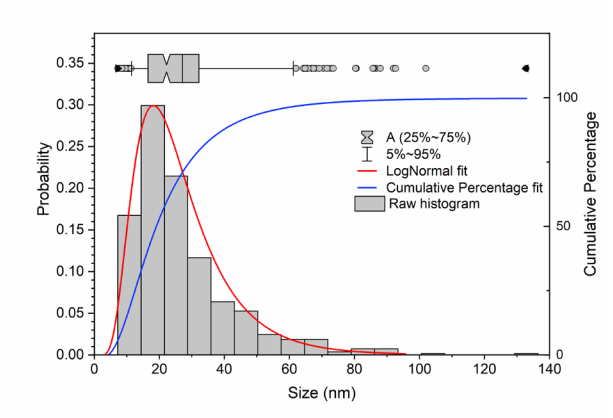

(c)

Dimensional Parameters - Length	Value
Analyzed particles	531
Minimum size (nm)	7.2 ± 0.9
First quartile (nm)	17 ± 2
Median (nm)	22 ± 3
MAD (nm)	7.1 ± 0.9
Average (nm)	27 ± 3
Standard deviation (nm)	16 ± 5
Third quartile (nm)	32 ± 3
Maximum size (nm)	133 ± 46
D10 (nm)	12 ± 2
D50 [median] (nm)	22 ± 3
D90 (nm)	48 ± 5

(d)

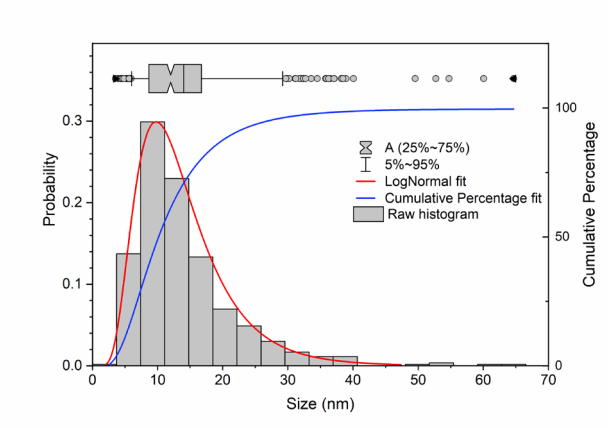

(e)

Dimensional Parameters - Width	Value
Analyzed particles	531
Minimum size (nm)	3.5 ± 0.4
First quartile (nm)	9 ± 2
Median (nm)	12 ± 3
MAD (nm)	3.7 ± 0.8
Average (nm)	14 ± 2
Standard deviation (nm)	8 ± 3
Third quartile (nm)	17 ± 3
Maximum size (nm)	65 ± 23
D10 (nm)	7 ± 1
D50 [median] (nm)	12 ± 3
D90 (nm)	24 ± 4

(f)

Figure Annex B.3: Transmission Electron Microscopy (TEM) number-based primary particle size distribution of hydroxyapatite (nano) at concentration of 0.0625 mg/mL in Micronucleus Test (MNT) cell culture medium with S9. (a,b) TEM micrographs at magnitude 30000x with shown (as red lines) length and width of representative particles of sample. (c) Number-based particle size distribution of particles' length and (d) its descriptive dimensional parameters. (e) Number-based particle size distribution of particles' width and (f) its descriptive dimensional parameters. Data are expressed as value ± standard deviation.

c) Results for Hydroxyapatite (nano) in Mouse Lymphoma Assay (MLA) Medium without S9:

The average curves for size distribution obtained for blank (i.e., cell culture medium without PhPC-2022-3 (nano) (NC)) and PhPC-2022-3 (nano) at different concentrations are reported in Figure Annex B.4.

The average hydrodynamic diameter corresponding to the main population of particles for each test condition is reported in Table Annex B.3, which also reports the presence or absence of visible precipitates.

It was shown that a significant increase of blank signal for dilutions from 0.0313 mg/mL was present. The blank signal was characterized by a broad peak from 5 nm to 2 µm and it hampers the possibility of using DLS for concentrations lower than 0.0156 mg/mL (i.e., 0.0078 mg/mL) and 0.0039 mg/mL in Figure Annex B.4). The 0.0313 mg/mL dispersion showed a better reproducibility among replicates (i.e., lower relative standard deviation). Therefore, it was considered as the first stable and suitable concentration of hydroxyapatite (nano) in MLA cell culture medium without S9 to be used for the subsequent test.

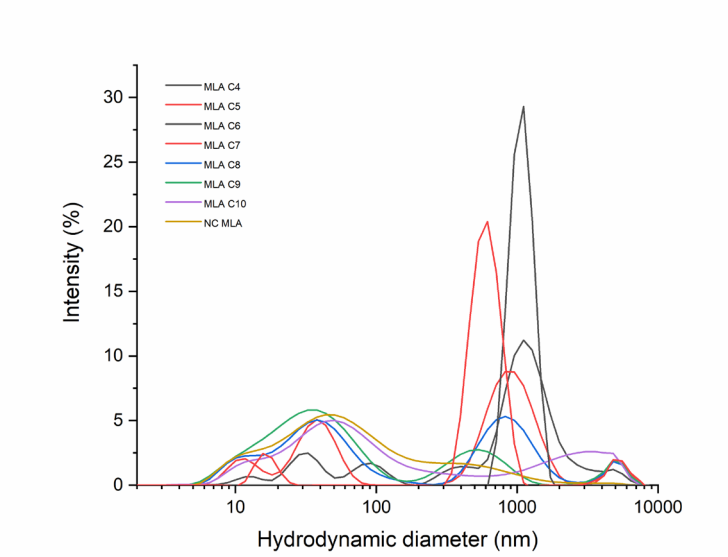

Figure Annex B.4: Dynamic Light Scattering (DLS) particle size distribution of PhPC-2022-3 (nano) (each curve is the average of 5 replicates, except for 0.1250 mg/mL which is average of 4 replicates) in Mouse Lymphoma Assay (MLA) cell culture medium without S9 at different concentrations and blank (NC).

Table Annex B.3: Dynamic Light Scattering (DLS) particle size distribution parameters of the analysed dispersions in Mouse Lymphoma Assay (MLA) cell culture medium without S9 (each value obtained from 5 replicates, except for 0.1250 mg/mL which is obtained from 4 replicates). The last column reports if dispersions present visible precipitates. RSD% = percentage relative standard deviation.

Hydroxyapatite (nano) concentration (mg/mL)	Hydrodynamic diameter of main peak (average ± standard deviation, nm)	Visible precipitates
0.2500	1083 ± 96 (RSD% = 9 %)	Yes
0.1250	612 ± 23 (RSD% = 4 %)	Yes
0.0625	1195 ± 102 (RSD% = 9 %)	Yes
0.0313	944 ± 69 (RSD% = 7 %)	Yes
0.0156	912 ± 116 (RSD% = 13 %)	No
0.0078	38 ± 2 (RSD% = 5 %)	No
0.0039	80 ± 13 (RSD% = 17 %)	No

Representative TEM micrographs of PhPC-2022-3 (nano) in MLA cell culture medium without S9 at concentration 0.0156 mg/mL are reported in Figure Annex B.5. Particles are embedded into matrix (Figure Annex.5a), though they are visible and well distinguishable from surroundings. As for the pristine product, in the presence of MLA cell culture medium without S9 particles are aggregated/agglomerated (Figure Annex B.5b).

To obtain primary particle size distribution, both length and width were independently measured, and the distribution curves are reported in Figure Annex B.5c and Figure Annex B.5e, while their descriptive parameters are reported in Figure Annex B.5d and Figure Annex B.5f.

The median particle length and width obtained on a significant number of measured particles (≥ 500 particles) were 20 nm and 12 nm, respectively.

The aspect ratio of particles – calculated as the ratio of median length to median width – was 1.67.

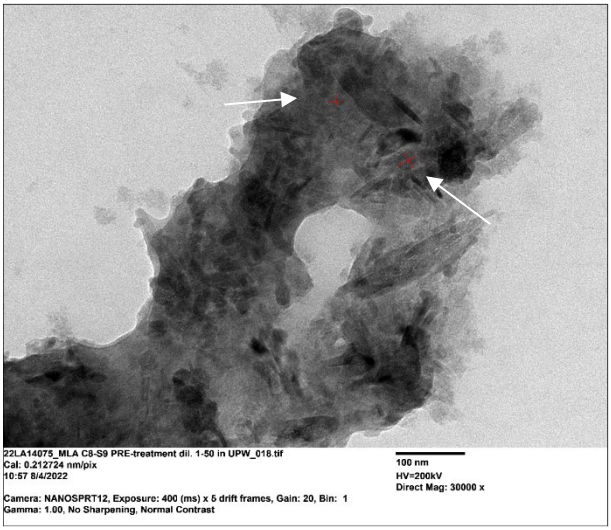

(a)

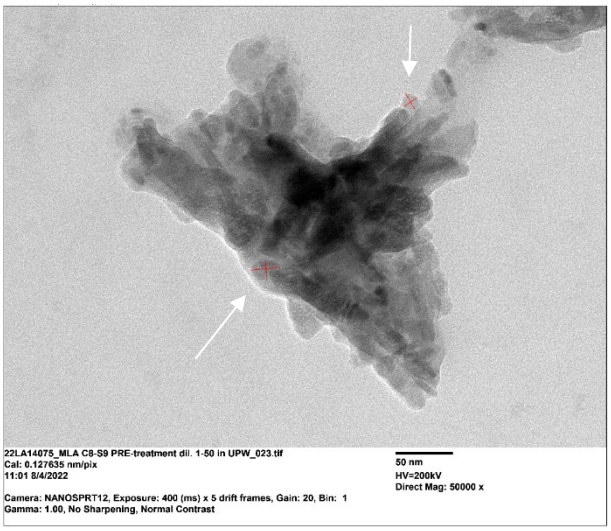

(b)

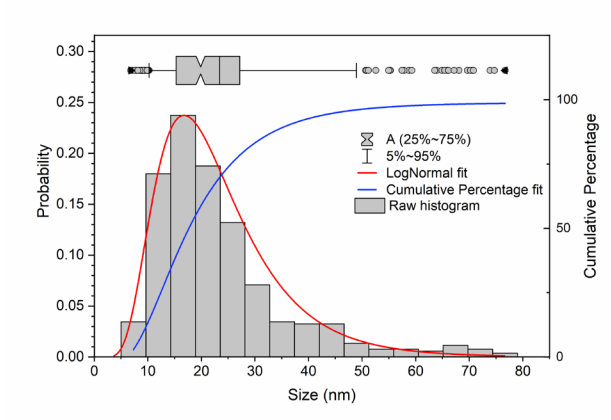

(c)

Dimensional Parameters - Length	Value
Analyzed particles	522
Minimum size (nm)	6.8 ± 0.8
First quartile (nm)	15 ± 2
Median (nm)	20 ± 3
MAD (nm)	5.6 ± 0.8
Average (nm)	23 ± 2
Standard deviation (nm)	13 ± 4
Third quartile (nm)	27 ± 3
Maximum size (nm)	77 ± 27
D10 (nm)	12 ± 2
D50 [median] (nm)	20 ± 3
D90 (nm)	40 ± 4

(d)

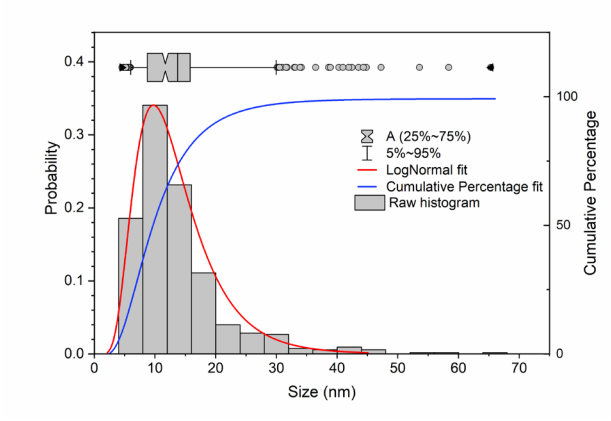

(e)

Dimensional Parameters - Width	Value
Analyzed particles	522
Minimum size (nm)	4.5 ± 0.6
First quartile (nm)	9 ± 2
Median (nm)	12 ± 3
MAD (nm)	3.3 ± 0.8
Average (nm)	14 ± 2
Standard deviation (nm)	8 ± 3
Third quartile (nm)	16 ± 3
Maximum size (nm)	65 ± 23
D10 (nm)	7 ± 1
D50 [median] (nm)	12 ± 3
D90 (nm)	23 ± 3

(f)

Figure Annex B.5: Transmission Electron Microscopy (TEM) number-based primary particle size distribution of hydroxyapatite (nano) at concentration 0.0156 mg/mL in Mouse Lymphoma Assay (MLA) cell culture medium without S9. TEM micrograph at magnitude 30000x (a) and 50000x (b) with shown (as red lines) length and width of representative particles of sample. (c) Number-based particle size distribution of particles' length and (d) its

descriptive dimensional parameters. (e) Number-based particle size distribution of particles' width and (f) its descriptive dimensional parameters. Data are expressed as value ± standard deviation.

d) Results for Hydroxyapatite (nano) in Mouse Lymphoma Assay (MLA) Medium with S9:

On the basis of the obtained DLS data, it was not possible to identify a suitable concentration for genotoxicity test in MLA cell culture medium with S9 as the DLS signal was highly unstable and not reproducible probably due to available aggregate/agglomerates. Therefore, TEM analysis was performed on 0.0078 mg/mL as the first concentration without visible precipitates.

Representative TEM micrographs of PhPC-2022-3 (nano) in MLA cell culture medium with S9 at concentration 0.0078 mg/mL are reported in Figure Annex B.6. As shown here, the aggregation/agglomeration state of hydroxyapatite (nano) particles in MLA cell culture medium with S9 was comparable to the particles of the pure hydroxyapatite (nano) particles (see above Figure Annex A.1).

To obtain size distribution of primary particles, both length and width were independently measured, and the distribution curves are reported in Figure Annex B.6c and Figure Annex B.6e, while their descriptive parameters are reported in Figure Annex B.6d and Figure Annex B.6f.

The median particle length and width obtained on a significant number of measured particles (≥ 500 particles) are 24 nm and 14 nm, respectively.

The aspect ratio of particles – calculated as the ratio of median length to median width – is 1.71.

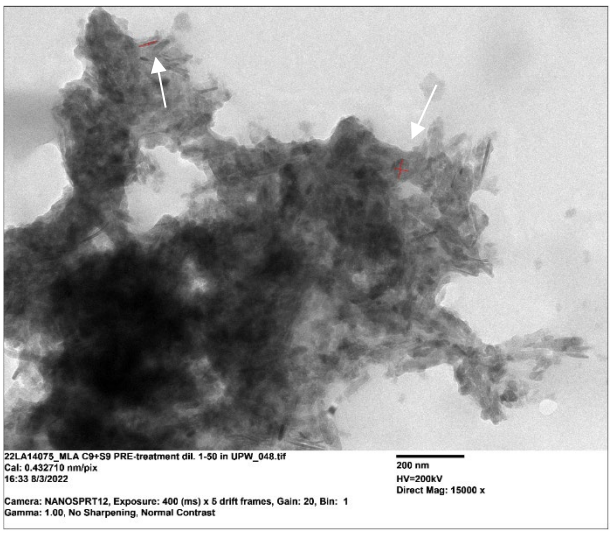

(a)

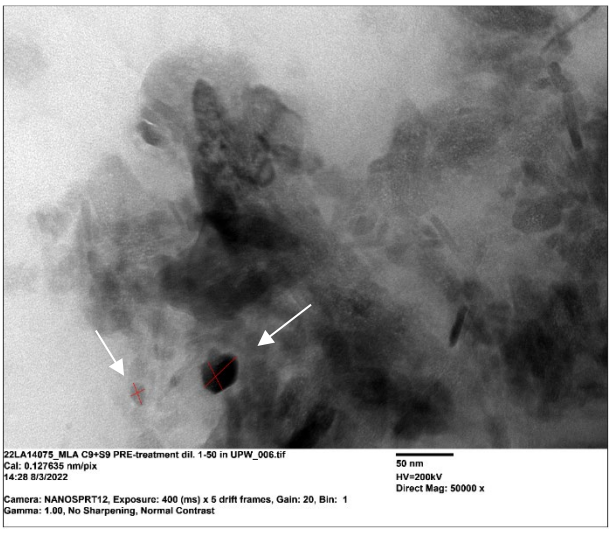

(b)

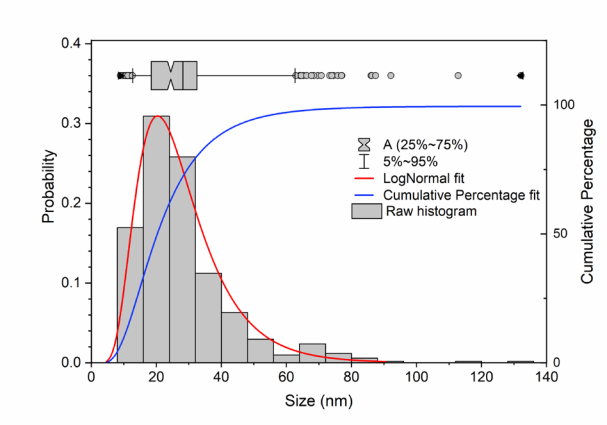

(c)

Dimensional Parameters - Length	Value
Analysed particles	507
Minimum size (nm)	9 ± 1
First quartile (nm)	18 ± 2
Median (nm)	24 ± 3
MAD (nm)	6.8 ± 0.9
Average (nm)	28 ± 2
Standard deviation (nm)	15 ± 5
Third quartile (nm)	32 ± 3
Maximum size (nm)	132 ± 46
D10 (nm)	14 ± 2
D50 [median] (nm)	24 ± 3
D90 (nm)	46 ± 4

(d)

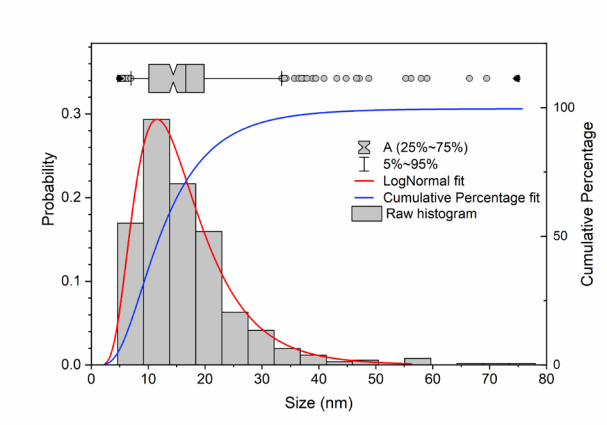

(e)

Dimensional Parameters - Width	Value
Analysed particles	507
Minimum size (nm)	5.0 ± 0.6
First quartile (nm)	10 ± 2
Median (nm)	14 ± 3
MAD (nm)	4.7 ± 0.8
Average (nm)	17 ± 2
Standard deviation (nm)	9 ± 3
Third quartile (nm)	20 ± 3
Maximum size (nm)	75 ± 26
D10 (nm)	8 ± 1
D50 [median] (nm)	14 ± 3
D90 (nm)	27 ± 4

(f)

Figure Annex B.6: Transmission Electron Microscopy (TEM) number-based primary particles size distribution of hydroxyapatite (nano) at concentration of 0.0078 mg/mL in Mouse Lymphoma Assay (MLA) cell culture medium with S9. TEM micrographs at magnitude (a) 15000x, (b) 50000x with shown (as red lines) length and width of representative particles of sample. (c) Number-based particle size distribution of particles' length and (d) its descriptive dimensional parameters. (e) Number-based particle size distribution of particles' width and (f) its descriptive dimensional parameters. Data are expressed as value ± standard deviation.

References: EcamRicert, 2023b and 2023e

Finally, it can be concluded that hydroxyapatite (nano) predominantly retained its agglomeration/aggregation state in cell culture media.
Stable conditions with no visible precipitates were identified. In the presence of MNT cell culture medium without S9, particles were stable without forming precipitates at a concentration of 0.0313 mg/ml.
In the presence of MLA cell culture medium without S9 the first concentration considered stable and without precipitates was 0.0156 mg/ml. DLS analysis was not suitable to define hydroxyapatite (nano) stability in cell culture media with S9 as the DLS signal was highly unstable and not reproducible probably due to available aggregate/agglomerates. Therefore, the two conditions without visible precipitates were selected for TEM analysis, i.e., 0.0625 mg/mL for MNT cell culture medium with S9; and 0.0078 mg/mL for MLA cell culture medium with S9, respectively.
Based on these findings, the respective stable concentrations without forming precipitates were selected for the MNT and MLA studies reported.

9. Annex C: Size Distribution, Dispersion Stability and Cellular Uptake for the *in vitro* Mammalian Cell Mouse Lymphoma Assay (MLA)

From Ref. 11 22.523987.00001_FR_Attachment_3 MLA uptake: Evaluation of PhPC-2022-3 (nano) behavior in terms of size distribution, dispersion and cellular uptake for Mouse Lymphoma Assay (MLA) assay.

Material and methods:
The size distribution, dispersion and cellular uptake of PhPC-2022-3 (nano, i.e., hydroxyapatite (nano), batch: D20469A, hydroxyapatite (nano) content: 29.5%) during the MLA assay were examined according to requirements of the SCCS available at that time (SCCS/1611/19, Reference: SCCS, 2019). These investigations were performed using TEM-EDX (according to ISO 21363:2020) and DLS (according to ISO 22412:2017). Culture media and sample preparation for DLS and TEM-EDX analyses were corresponding to those described in MLA assay above compliant with OECD 490 and SCCS requirements under GLP conditions.

DLS was only used to have qualitative information on system stability during MLA assay. While the peaks in the negative controls (blank) are due to cell culture medium components such as serum proteins, peaks observed in pre- and post-treatment media are due to the PhPC-2022-3 (nano) particles.

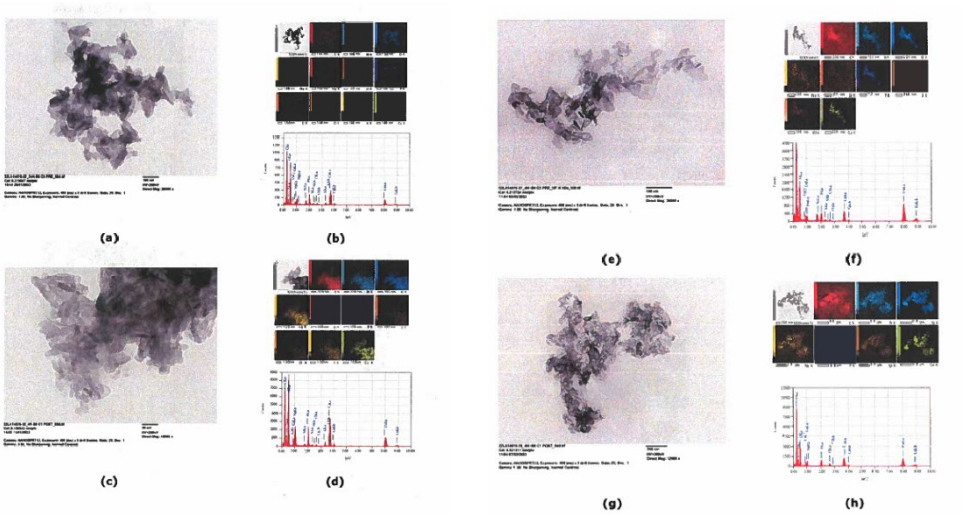

Figure Annex C.1: Representative TEM images and corresponding EDX spectra of nanohydroxyapatite particles in MLA cell culture medium. Condition without S9 before (a, b) and after (c, d) exposure. Condition with S9 before (e, f) and (g,h) after exposure.

Results:
Focusing on the main results of this safety dossier, only the results of the highest hydroxyapatite (nano) concentrations without S9 and with S9 metabolic activation are presented as representative examples. The results for all the concentrations are reported below in Tables Annex C-1, 2, 3, 4, and 5.

a) Dynamic Light Scattering (DLS) results for PhPC-2022-3 (nano)-containing cell culture medium at the lowest concentration inducing visible precipitation after 4 h – S9 or 24 h – S9 (0.0313 mg/mL) and after 4 h + S9 (0.0156 mg/mL).

The comparison of pre- and post-treatment samples of 0.0313 mg/mL at 4 h - S9 test condition (Figure Annex C.1 (a)) shows that peaks after 4 h incubation are slightly shifted towards smaller particles probably due to partial precipitation of larger aggregates/agglomerates. Samples of 0.0313 mg/mL at 24 h – S9 test condition before and after treatment (Figure Annex C.1 (c)) present overlapping peaks ascribable to PhPC-2022-3 (nano). However, the particulate

form of the blank (i.e., cell culture medium) does not allow to attribute the signal to the hydroxyapatite (nano)-particles with certainty.
In the condition with S9 (0.0156 mg/mL at 4 h + S9 in Figure Annex C.1 (b) the particulate form of the blank hampers the possibility to investigate any changes of PhPC-2022-3 (nano) behaviour during the experiment.

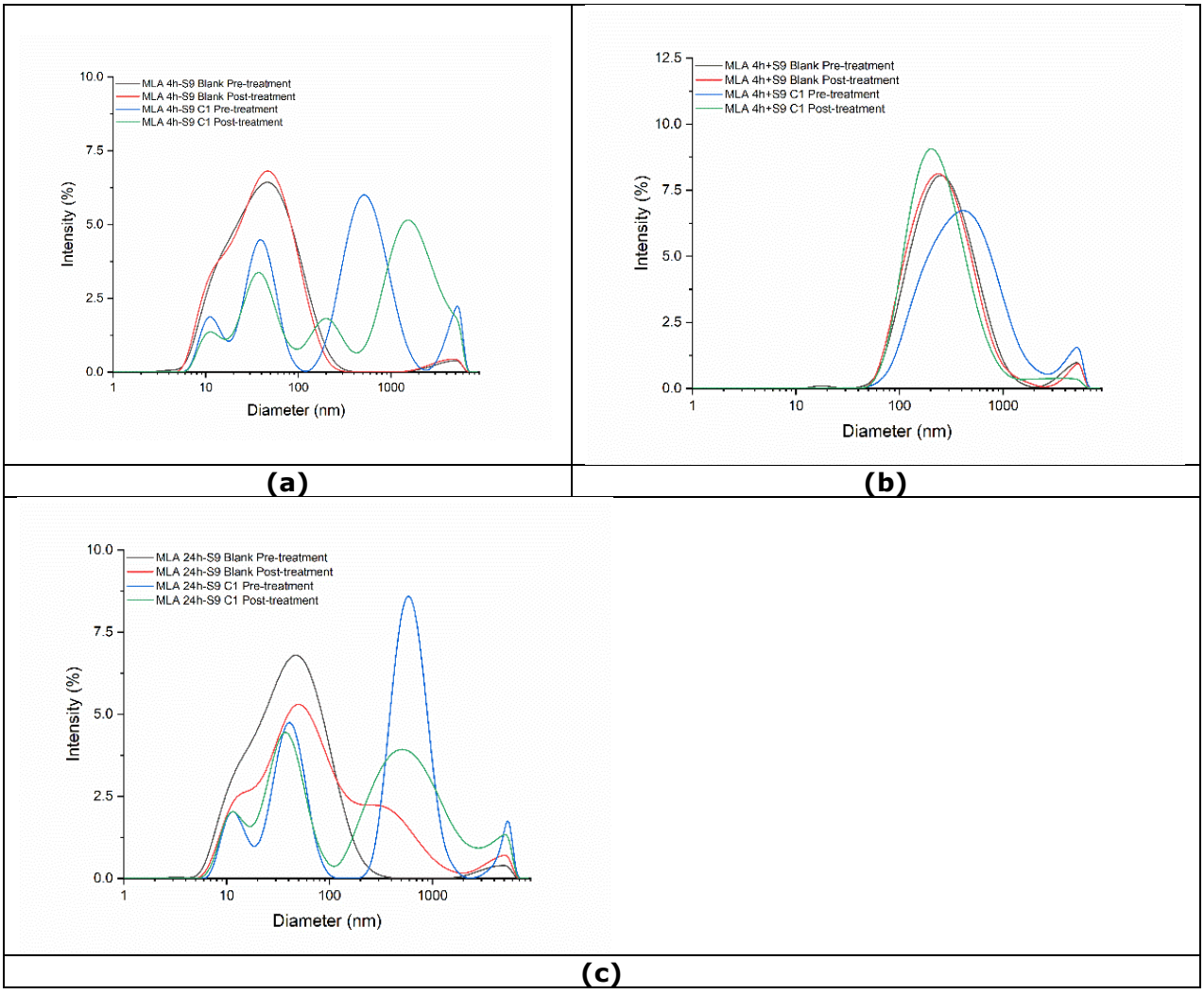

Figure Annex C.2. Size distribution curves by Dynamic Light Scattering (DLS) of PhPC-2022-3 (nano) at concentration that produces visible precipitates (0.0313 mg/mL for condition without S9 and 0.0156 mg/mL for condition with S9) before (blue curve) and after (green curve) exposure to the conditions 4 h – S9 (a), 4 h + S9 (b), and 24 h - S9 (c). Size distributions of cell culture medium (Blank) before (black curve) and after exposure (red curve) are also reported.

b) Transmission Electron Microscopy (TEM) micrographs, size and aspect ratio (AR) distributions and their corresponding descriptive parameters of hydroxyapatite (nano) particles before 24 h exposure time in condition without S9 (0.0313 mg/mL)

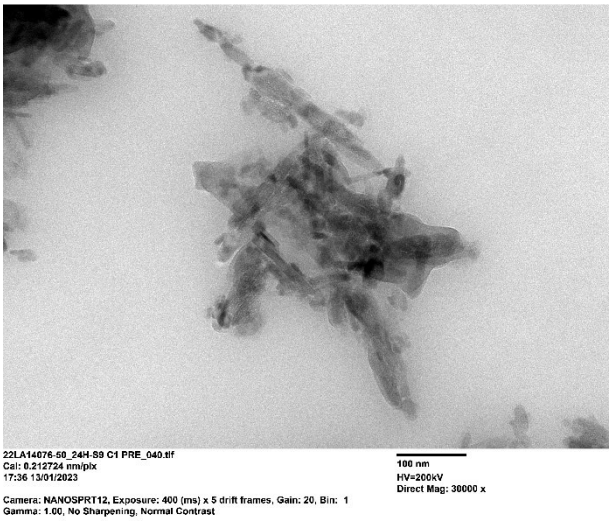

(a)

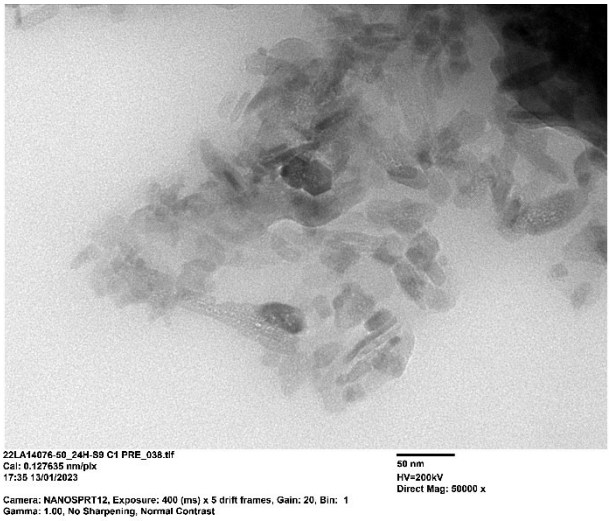

(b)

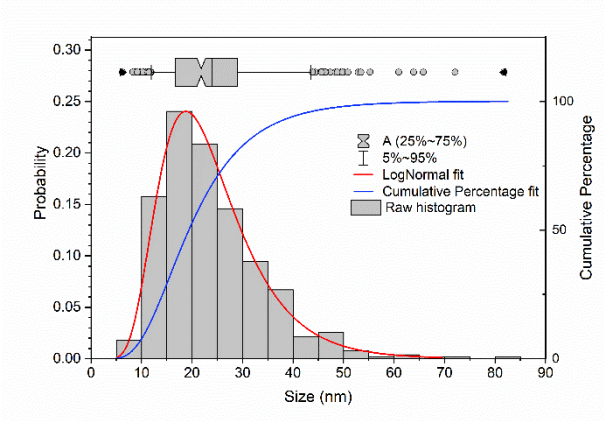

(c)

Dimensional Parameters - Length	Value
Analysed particles	507
Minimum size (nm)	6.21 ± 0.77
First quartile (nm)	16.6 ± 2.0
Median (nm)	21.8 ± 2.9
MAD (nm)	5.93 ± 0.84
Average (nm)	23.9 ± 2.4
Standard deviation (nm)	10.3 ± 3.4
Third quartile (nm)	29.0 ± 3.3
Maximum size (nm)	82 ± 29
Mode (nm)	18.4 ± 7.1
10^{th} percentile (nm)	13.2 ± 1.7
50^{th} percentile [median] (nm)	21.8 ± 2.9
90^{th} percentile (nm)	37.0 ± 4.1

(d)

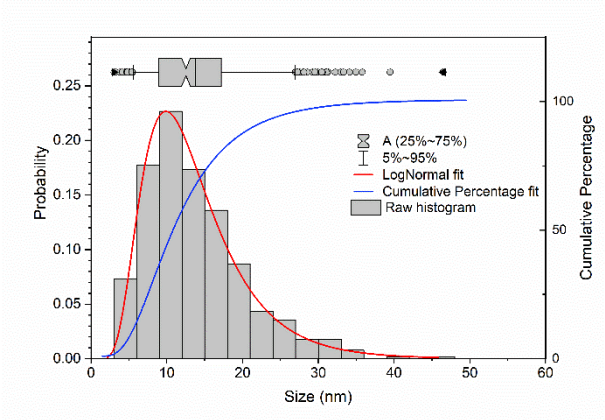

Dimensional Parameters - Width	Value
Analyzed particles	507
Minimum size (nm)	3.02 ± 0.37
First quartile (nm)	9.0 ± 1.8
Median (nm)	12.5 ± 2.7
MAD (nm)	4.05 ± 0.84
Average (nm)	13.8 ± 2.1
Standard deviation (nm)	6.6 ± 2.2
Third quartile (nm)	17.2 ± 3.1
Maximum size (nm)	46 ± 16
Mode (nm)	9.9 ± 6.5
10^{th} percentile (nm)	6.74 ± 0.86
50^{th} percentile [median] (nm)	12.5 ± 2.7
90^{th} percentile (nm)	23.4 ± 3.5

(e)

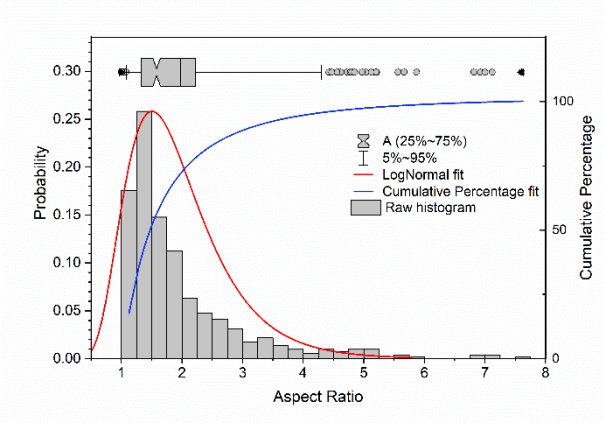

(f)

Aspect ratio	Value
Analyzed particles	507
Minimum	1.00
First quartile	1.33
Median	1.58
MAD	0.34
Average	1.97
Standard deviation	1.05
Third quartile	2.22
Maximum size	7.60
Mode	1.33
10th percentile	1.16
50th percentile [median]	1.58
90th percentile	3.33

(g) **(h)**

Figure Annex C.3. Representative Transmission Electron Microscopy (TEM) micrographs (a, b), size distribution curve and descriptive parameters for particles' length (c, d), size distribution curve and descriptive parameters for particles' width (e, f), AR distribution and descriptive parameters (g, h) of hydroxyapatite (nano) at a concentration of 0.0313 mg/mL producing visible precipitates in L5178Y/TK+/- cell culture medium without S9 before 24h exposure time (22LA14076-50). Size parameters are reported as value ± standard deviation. The uncertainty of size values is expressed with two significant figures and dimensions of the values are reported accordingly.

c) Transmission Electron Microscopy (TEM) micrographs, size and aspect ratio (AR) distributions and their descriptive parameters of 0.0313 mg/mL of hydroxyapatite (nano) after 24 h exposure without S9 mix

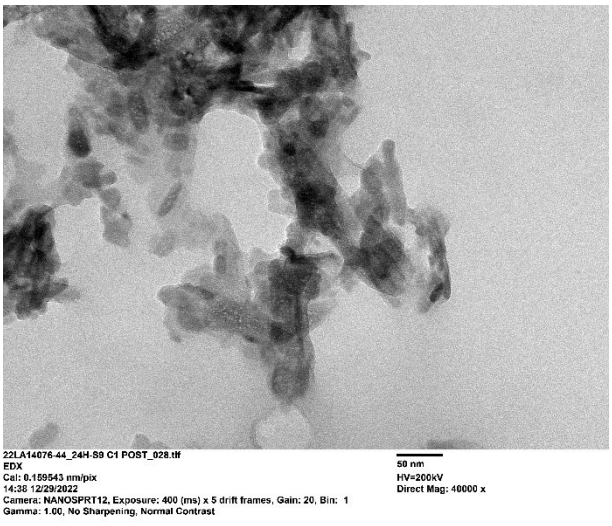

(a)

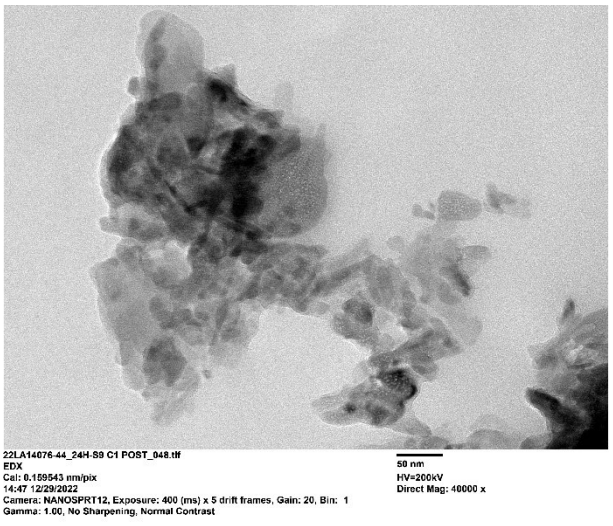

(b)

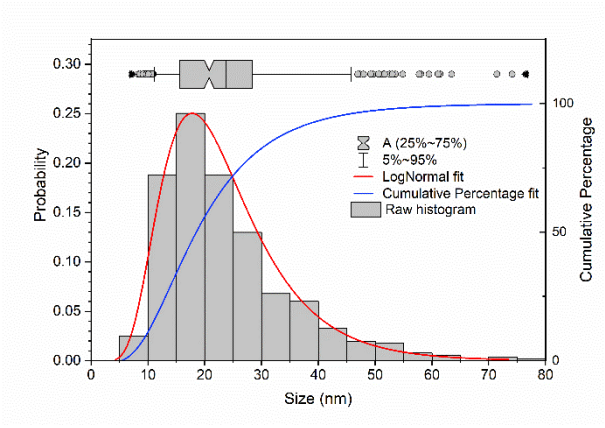

(c)

Dimensional Parameters - Length	Value
Analysed particles	515
Minimum size (nm)	7.13 ± 0.88
First quartile (nm)	15.5 ± 2.0
Median (nm)	20.8 ± 2.9
MAD (nm)	5.98 ± 0.84
Average (nm)	23.7 ± 2.4
Standard deviation (nm)	11.3 ± 3.7
Third quartile (nm)	28.4 ± 3.3
Maximum size (nm)	77 ± 27
Mode (nm)	17.1 ± 7.0
10th percentile (nm)	12.4 ± 1.6
50th percentile [median] (nm)	20.8 ± 2.9
90th percentile (nm)	39.0 ± 4.2

(d)

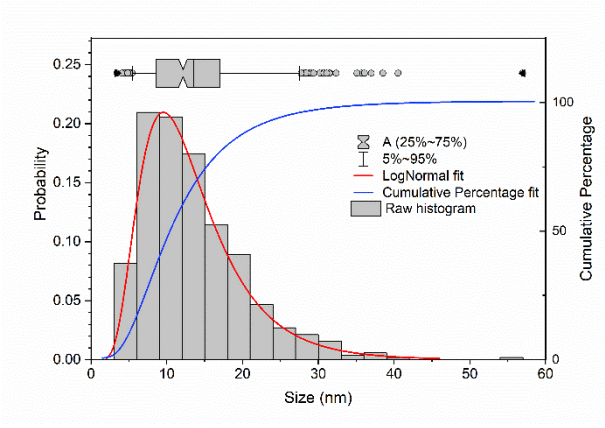

(e)

Dimensional Parameters - Width	Value
Analysed particles	515
Minimum size (nm)	3.41 ± 0.42
First quartile (nm)	8.6 ± 1.7
Median (nm)	12.1 ± 2.7
MAD (nm)	4.10 ± 0.84
Average (nm)	13.5 ± 2.1
Standard deviation (nm)	6.9 ± 2.3
Third quartile (nm)	17.0 ± 3.1
Maximum size (nm)	57 ± 20
Mode (nm)	9.3 ± 6.5
10th percentile (nm)	6.35 ± 0.81
50th percentile [median] (nm)	12.1 ± 2.7
90th percentile (nm)	22.5 ± 3.5

(f)

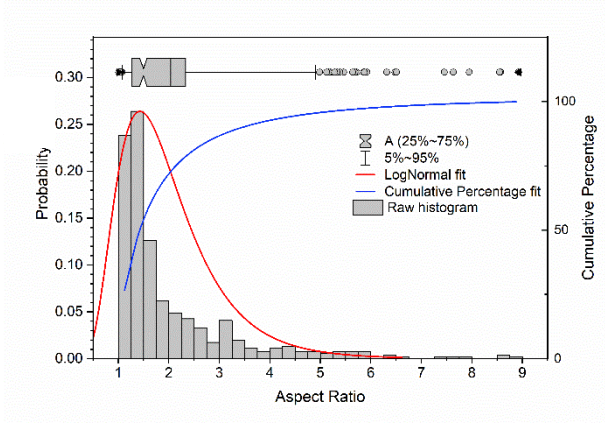

(g)

Aspect ratio	Value
Analysed particles	515
Minimum	1.00
First quartile	1.27
Median	1.50
MAD	0.32
Average	2.04
Standard deviation	1.29
Third quartile	2.33
Maximum size	8.93
Mode	1.26
10th percentile	1.13
50th percentile [median]	1.50
90th percentile	3.72

(h)

Figure Annex C.4. Representative Transmission Electron Microscopy (TEM) micrographs (a, b), size distribution curve and descriptive parameters for particles' length (c, d), size distribution curve and descriptive parameters for particles' width (e, f), AR distribution and descriptive parameters (g, h) of hydroxyapatite (nano) at a concentration producing visible

precipitates in L5178Y/TK$^{+/-}$ cell culture medium without S9 after 24 h exposure time (0.0313 mg/mL at 24 h – S9, 22LA14076-44). Size parameters are reported as value ± standard deviation. The uncertainty of size values is expressed with two exemplary figures and dimensions of the values are reported accordingly.

Table Annex C – 1: Particle size and aspect ratio for the C1 (0.0313 mg/mL) without S9 an C1* (0.0156 mg/mL) with S9 concentration **–** MLA conditions (summarized information provided by SCCS from Ref 11 22.523987.00001_FR_Attachment_3 MLA uptake)

Conditions (MLA tests)	Median Length	Median Width	Length (Min – Max)	Width (Min – Max)	AR Average	AR Median	Max AR	AR Third quartile	AR 90th percentile
Pristine	21 ± 3	12 ± 3	8 ± 1 122 ± 43	4.8 ± 0.6 49 ± 17	1.96	1.51 ± 0.26	8.97	2.02	3.31*
C1 - S9 before 4h exposure time	21.3 ± 2.9	12.9 ± 2.7	8.1 ± 1.0 63 ± 22	3.14 ± 0.39 45 ± 16	1.95	1.50 ± 0.30	9.69	2.13	3.57
C1 - S9 before 24 h exposure time	21.8 2.9 ±	12.5 ± 2.7	6.21 ± 0.77 82 ± 29	3.02 ± 0.37 46 ± 16	1.97	1.58 ± 0.34	7.60	2.22	3.33
C1 4h – S9	22.5 ± 2.9	11.5 ± 2.7	8.02 ± 0.99 85 ± 30	4.47 ± 0.55 41 ± 14	2.16	1.68 ± 041	13.64	2.39	3.80
C1 24h – S9	20.8 ± 2.9	12.1 ± 2.7	7.13 ± 0.88 77 ± 27	3.41 ± 0.42 57 ±20	2.04	1.50 ± 0.32	8.93	2.33	3.72
C1* 0h + S9 before exposure	21.5 ± 2.9	11.6 ± 2.7	8.2 ± 1.0 80 ± 28	3.36 ± 0.41 50 ± 17	2.08	1.70 ± 0.36	8.59	2.36	3.55
C1* 4h + S9	22.0 ± 2.9	12.4 ± 2.7	8.0 ± 1.0 107 ± 37	4.71 ±0.58 46 ± 16	1.92	1.74 ± 0.27	8.93	2.09	2.74

Table Annex C – 2: Particle size and aspect ratio for the C2 (0.0156 mg/mL) without S9 and C2* (0.078 mg/mL) with S9 concentrations – MLA conditions (summarized information provided by SCCS from Ref 11 22.523987.00001_FR_Attachment_3 MLA uptake)

Conditions (MLA tests)	Median Length	Median Width	Length (Min – Max)	Width (Min - Max	AR Average	AR Median	Max AR	AR Third quartile	AR 90th percentile
Pristine	21 ± 3	12 ± 3	8 ± 1 122 ± 43	4.8 ± 0.6 49 ± 17	1.96	1.51 ± 0.26	8.97	2.02	3.31*
C2 – S9 before 4h	23.6 ± 3.0	12.7 ± 2.7	7.55 ± 0.93 75 ± 26	4.09 ± 0.50 46 ± 16	2.01	1.75 ± 0.31	8.47	2.13	2.87
C2 – S9 before 24h	21.4 ±2.9	13.7 ± 2.7	10.4 ± 1.3 107 ± 37	4.09 ± 0.50 54 ± 19	1.69	1.54 ± 0.16	8.56	1.75	2.10
C2 4h – S9	21.2 ± 2.9	13.1 ± 2.7	10.3 ± 1.3 75 ± 26	4.58 ± 0.56 44 ± 15	1.74	1.55 ± 0.21	6.72	1.83	2.28
C2 24 – S9	22.1 ± 2.9	11.5 ± 2.7	6.93 ± 0.85 70 ± 25	3.31 ±0.41 42 ± 15	2.09	1.88 ±0.38	6.86	2.37	3.02
C2 + S9 before exposure	22.3 ± 2.9	10.8 ±2.6	6.68 ± 0.82 93 ± 32	3.92 ± 0.48 48 ± 17	2.50	1.89 ± 0.57	10.35	2.99	4.47
C2 4h + S9	23.5 ± 3.0	12.4 ± 2.7	7.23 ± 0.89 115 ± 40	4.20 ± 0.52 87 ± 31	2.02	1.69 ± 0.31	9.23	2.16	3.08

Table Annex C – 3: Particle size and aspect ratio for the C3 (0.0078 mg/mL) without S9 and C3* (0.0039 mg/mL) with S9 concentrations – MLA conditions (summarized information provided by SCCS from Ref 11 22.523987.00001_FR_Attachment_3 MLA uptake)

Conditions (MLA tests)	Median Length	Median Width	Length (Min – Max)	Width (Min - Max	AR Average	AR Median	Max AR	AR Third quartile	AR 90th percentile
Pristine	21 ± 3	12 ± 3	8 ± 1 122 ± 43	4.8 ± 0.6 49 ± 17	1.96	1.51 ± 0.26	8.97	2.02	3.31*
C3 – S9 before 4h exposure	21.4 ± 2.9	11.4 ± 2.7	6.73 ± 0.83 93 ± 32	3.48 ± 0.43 45 ± 16	1.99	1.82 ± 0.30	8.38	2.19	2.72
C3 – S9 before 24h exposure	20.2 ± 2.9	11.0 ± 2.6	7.7 ± 1.0 76 ± 27	3.07 ± 0.38 41 ± 14	2.11	1.67 ± 0.43	8.13	2.51	3.66
C3 4h – S9	22.7 ± 2.9	12.5 ± 2.7	6.97 ± 0.86 106 ± 37	4.02 ± 0.50 62 ± 22	1.92	1.73 ± 0.26	6.86	2.10	2.74
C3 24h – S9	21.1 ± 2.9	13.5 ± 2.7	9.6 ± 1.2 74 ± 26	5.53 ± 0.68 38 ± 13	1.63	1.53 ± 016	5.54	1.70	2.03
C3* 0h + S9 before exposure	21.0 ± 2.9	10.6 ± 2.6	6.93 ± 0.85 79 ± 28	3.22 ± 0.40 46 ± 16	2.34	1.78 ± 0.49	11.97	2.67	4.07
C3* 4h + S9	20.2 ± 2.9	11.0 ± 2.6	9.8 ± 1.2 56 ± 20	4.25 ± 0.52 33 ± 11	1.88	1.75 ± 0.26	3.68	3.13	2.58

Table Annex C – 4: Particle size and aspect ratio for the C4 (0.0039 mg/mL) without S9 and C4* (0.0020 mg/mL) with S9 concentrations – MLA conditions (summarized information provided by SCCS from Ref 11 22.523987.00001_FR_Attachment_3 MLA uptake)

Conditions (MLA tests)	Median Length	Median Width	Length (Min – Max)	Width (Min - Max	AR Average	AR Median	Max AR	AR Third quartile	AR 90th percentile
Pristine	21 ± 3	12 ± 3	8 ± 1 122 ± 43	4.8 ± 0.6 49 ± 17	1.96	1.51 ± 0.26	8.97	2.02	3.31*
C4 – S9 before 4h exposure	20.4 ± 2.9	11.3 ± 2.6	7.55 ± 0.93 70 ± 24	4.04 ± 0.50 45 ± 16	2.03	1.57 ± 0.35	11.25	2.35	3.76
C4 – S9 before 24h exposure	21.4 ± 2.9	14.0 ± 2.7	9.8 ± 1.2 67 ± 24	5.74 ± 0.71 39 ± 14	1.55	1.49 ± 0.13	3.62	1.64	1.84
C4 4h – S9	11.7 ± 2.9	12.6 ± 2.7	1.4 ± 1.2 172 ± 25	4.20 ± 0.52 42 ± 15	2.00	1.52 ± 0.30	8.83	2.08	3.54
C4 24h – S9	20.4 ± 2.9	11.2 ± 2.6	7.35 ± 0.91 120 ± 42	3.84 ± 0.47 71 ± 25	2.17	1.56 ± 0.33	8.61	2.53	4.15
C4* 0h + S9 before exposure	21.8 ±2.9	11.1 ± 2.6	7.67 ± 0.95 69 ± 24	4.04 ± 0.50 44 ± 15	2.17	1.71 ± 0.39	10.30	2.39	3.56
C4* 4h + S9	21.4 ± 2.9	12.3 ± 2.7	8.5 ± 1.0 66 ± 23	4.36 ± 0.54 36 ± 12	1.83	1.72 0.26±	5.06	2.04	2.44

Table Annex C – 5: Particle size and aspect ratio for the C5 (0.0020 mg/mL) without S9 and C5* (0.0010 mg/mL) with S9 concentrations – MLA conditions (summarized information provided by SCCS from Ref 11 22.523987.00001_FR_Attachment_3 MLA uptake)

Conditions (MLA tests)	Median Length	Median Width	Length (Min – Max)	Width (Min - Max	AR Average	AR Median	Max AR	AR Third quartile	AR 90th percentile
Pristine	21 ± 3	12 ± 3	8 ± 1 122 ± 43	4.8 ± 0.6 49 ± 17	1.96	1.51 ± 0.26	8.97	2.02	3.31*
C5 – S9 before 4h exposure	21.8 ± 2.9	14.3 ± 2.7	7.8 ± 1.0 101 ± 35	4.24 ± 0.52 73 ± 25	1.65	1.48 ± 0.17	7.89	1.69	2.15
C5 – S9 before 24h exposure	21.4 ± 2.9	10.7 ± 2.6	8.3 ± 1.0 77 ± 27	3.52 ± 0.43 38 ± 13	2.26	1.75 ± 0.48	8.87	2.70	4.09
C5 4h – S9	22.4 ± 2.9	11.8 ± 2.7	7.8 ± 1.0 63 ± 22	4.05 ± 0.50 49 ± 17	2.03	1.79 ± 0.29	9.92	2.22	2.75
C5 24h – S9	22.0 ± 2.9	11.9 ± 2.7	8.3 ± 1.0 70 ± 24	2.80 ± 0.34 40 ± 14	2.13	1.72 ± 0.46	9.52	2.49	3.65
C5* 0h + S9 before exposure	20.3 ± 2.9	11.6 ±2.7	6.40 ± 0.79 89 ± 31	3.41 ± 0.42 49 ± 17	2.01	1.64 ± 0.33	8.53	2.17	3.34
C5* 4h + S9	22.2 ± 2.9	12.1 ± 2.7	6.20 ± 0.76 86 ± 30	3.72 ± 0.46 48 ± 17	2.11	1.70 ± 0.37	10.28	2.31	3.54

10. Annex D: Size Distribution, Dispersion Stability and Cellular Uptake for the *in vitro* Mammalian Cell Micronucleus Test (MNT)

From Ref 14. 22523987.0002_FR_Attachment_3-1_complete MNT Uptake: Evaluation of PhPC-2022-3 (nano) behaviour in terms of size distribution, dispersions and cellular uptake for Micronucleus (MNT) assay

Study Design:

Reference:	EcamRicert, 2023f
Date of report:	26.04.2023
Guideline:	Requirements of SCCS Opinion (SCCS/1624/2020) and SCCS guidance (SCCS/1611/19)
Test system/method:	c) Particle size distribution and dispersion d) Uptake: Chinese hamster CHO-K1 cells
Test substance:	PhPC-2022-3 (nano, i.e. hydroxyapatite (nano))
Batch (Purity):	D20469A (hydroxyapatite (nano) content: 29.5%, specified by CoA)
Vehicle:	Treatment medium: HAM'S enriched with 5 % Foetal Bovine Serum (FBS)
Analytical methods:	- Transmission electron microscopy coupled with energy-dispersive X-ray spectroscopy (TEM-EDX) - Dynamic light scattering (DLS) (specific brand name omitted by the SCCS)
Concentrations:	Without S9: 0, 0.0530, 0,1059, 0.2119 mg/mL (corresponding to hydroxyapatite (nano): 0, 0.0156, 0.0313, 0.0625 mg/mL) With S9: 0, 0.1059, 0.2119, 0.4237 mg/mL (corresponding to hydroxyapatite (nano): 0, 0.0313, 0.0625, 0.1250 mg/mL)
GLP:	No data
Published:	No

Material and methods:
The size distribution, dispersion and cellular uptake of PhPC-2022-3 (nano, i.e., hydroxyapatite (nano), batch: D20469A, hydroxyapatite (nano) content: 29.5%) during the MNT were examined according to requirements of the SCCS available at that time (SCCS/1611/19, Reference: SCCS, 2019). These investigations were performed using TEM-EDX (according to ISO 21363:2020) and DLS (according to ISO 22412:2017). Culture media and sample preparation for DLS and TEM-EDX analyses were corresponding to those described in MNT above compliant with OECD 487 and SCCS requirements under GLP conditions.

DLS was only applied as a comparative approach to evaluate stability of particles along experimental conditions. Although no information on primary particle size could be obtained by DLS on PhPC-2022-3 (nano) dispersed in cell culture medium, DLS curves provide information on changes of system during experiments.

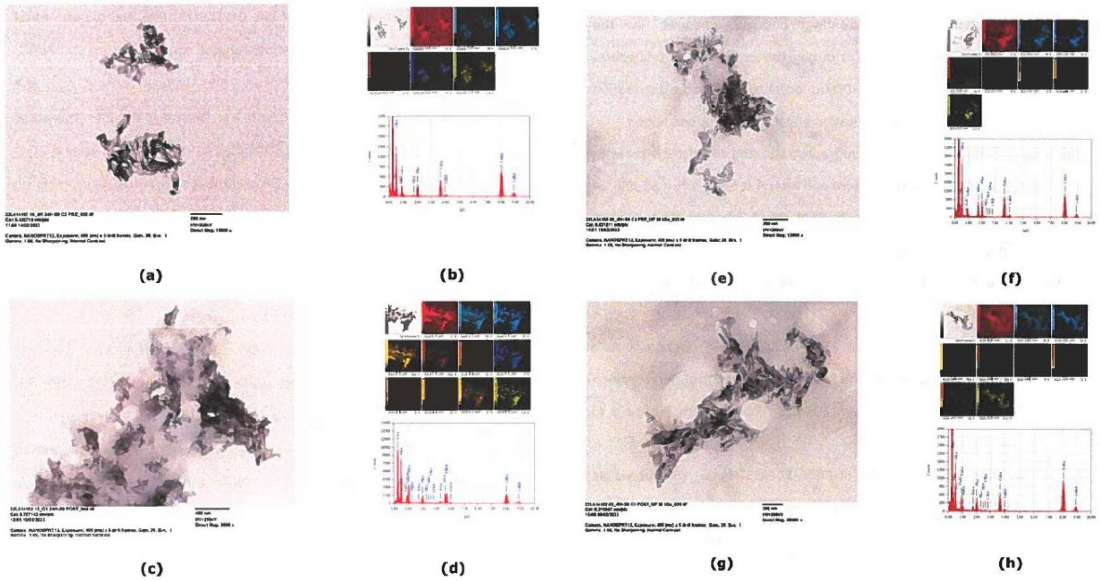

Figure Annex D.1: Representative TEM images and corresponding EDX spectra of nanohydroxyapatite particles in MNT cell culture medium. Conditions without S9 before (a, b) and after (c,d) exposure. Condition with S9 before (e, f) and (g, h) after exposure (from Ref. Ref 14 22523987.0002_FR_Attachment_3-1_complete MNT Uptake).

Results:
Focusing on the main results of this safety dossier, only the results of the highest hydroxyapatite (nano) concentrations without S9 and with S9 metabolic activation are presented as representative examples. The results of the other concentrations can be found in the comprehensive report attached.

a) Dynamic Light Scattering (DLS) results for PhPC-2022-3 (nano)-containing cell culture medium at the lowest concentration inducing visible precipitation after 4 h – S9 or 24 h – S9 (0.0625 mg/mL) and after 4 h + S9 (0.1250 mg/mL)

The comparison of pre- and post-treatment samples of samples of 0.0625 mg/mL at 4 h - S9 (Figure Annex D.1 (a)) test condition and pre- and post-treatment samples of 0.0625 mg/mL at 24 h - S9 (Figure Annex D.1 (c)) present similar peaks suggesting that PhPC-2022-3 (nano)-containing cell culture medium is stable up to 24 h incubation. After 24 h without S9 a slight shift toward smaller sizes is recorded.

The particulate form of the blank (i.e., cell culture medium) in the experimental condition 0.1250 mg/mL at 4 h + S9 (Figure Annex D.1 (b)) hampers the possibility to investigate any changes of PhPC-2022-3 (nano) behaviour during the experiment.

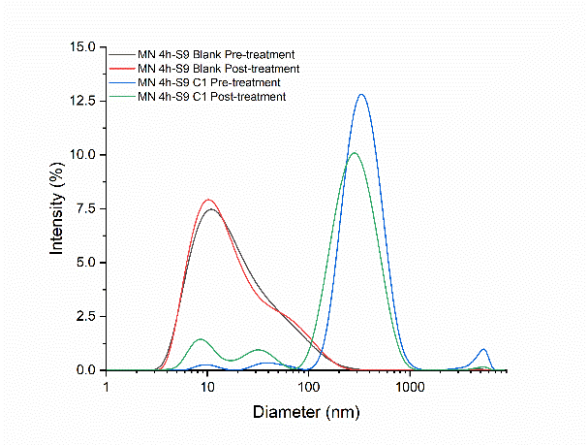

(a)

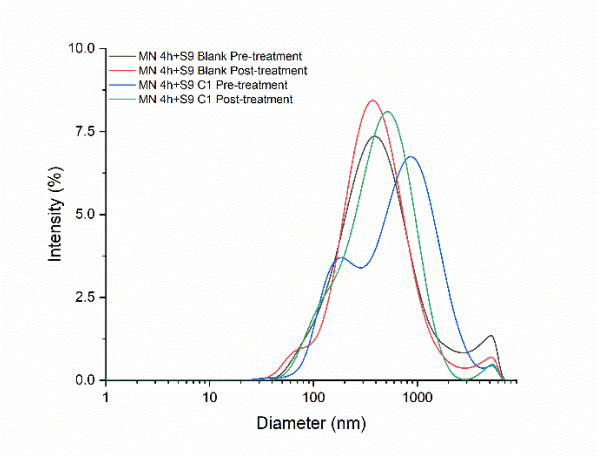

(b)

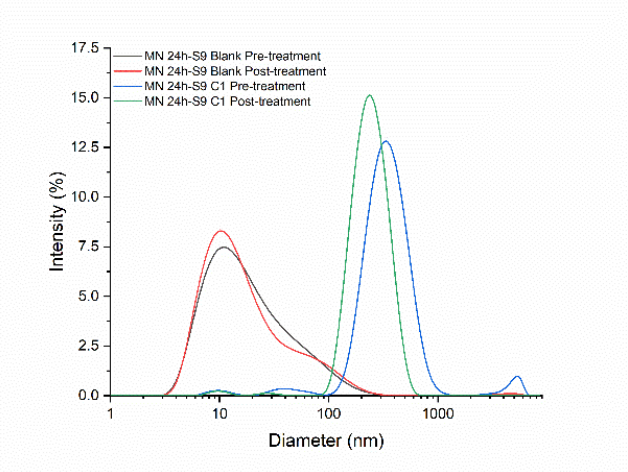

(c)

Figure Annex D.2: Size distribution curves by Dynamic Light Scattering (DLS) of PhPC-2022-3 (nano) at a concentration that produces visible precipitates (0.0625 mg/mL for condition without S9 and 0.1250 mg/mL for condition with S9) before (blue curve) and after (green curve) exposure to the conditions 4 h – S9 (a), 4 h + S9 (b), and 24 h - S9 (c). Size distributions of cell culture medium (Blank) before (black curve) and after exposure (red curve) are also reported.

b) Transmission Electron Microscopy (TEM) micrographs, size and aspect ratio (AR) distributions and their corresponding descriptive parameters of hydroxyapatite (nano) particles before 24 h exposure time in condition without S9 (0.0625 mg/mL)

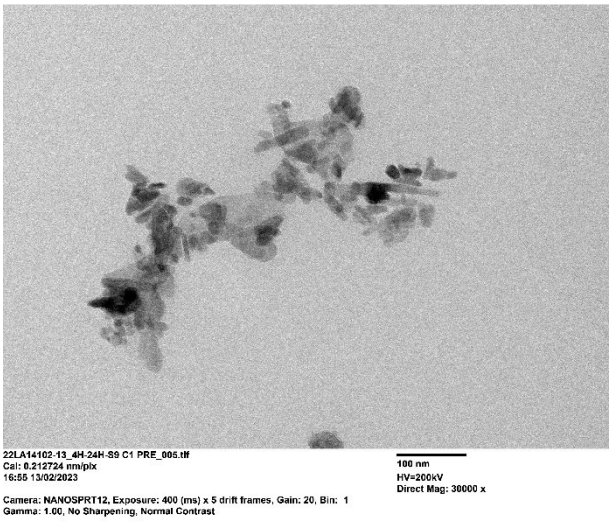

(a)

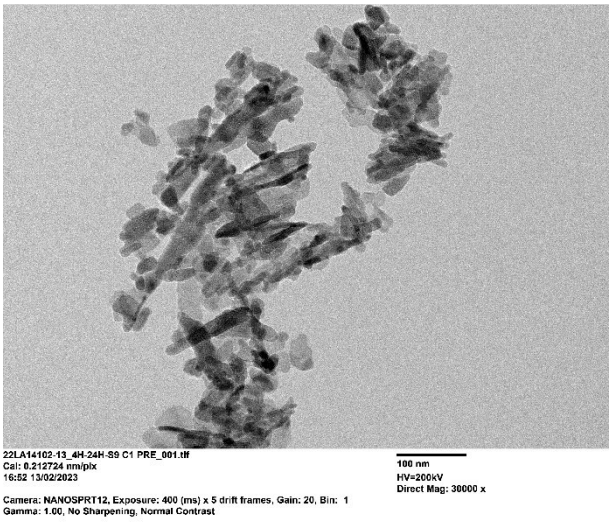

(b)

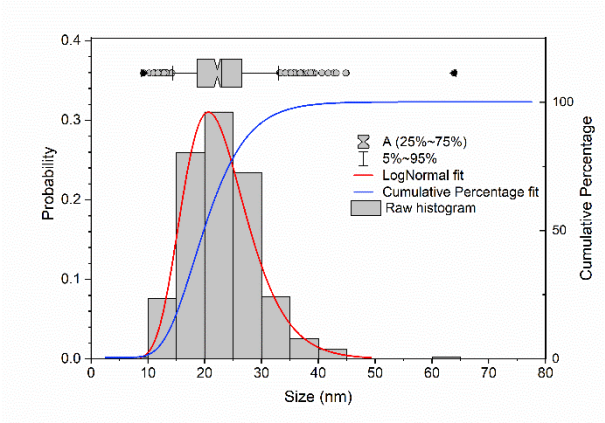

(c)

Dimensional Parameters - Length	Value
Analyzed particles	512
Minimum size (nm)	9.2 ± 1.1
First quartile (nm)	18.7 ± 2.1
Median (nm)	22.2 ± 2.9
MAD (nm)	3.84 ± 0.84
Average (nm)	23.0 ± 2.3
Standard deviation (nm)	6.3 ± 2.0
Third quartile (nm)	26.5 ± 3.2
Maximum size (nm)	64 ± 22
Mode (nm)	21.0 ± 7.2
10^{th} percentile (nm)	15.6 ± 2.0
50^{th} percentile [median] (nm)	22.2 ± 2.9
90^{th} percentile (nm)	30.5 ± 3.8

(d)

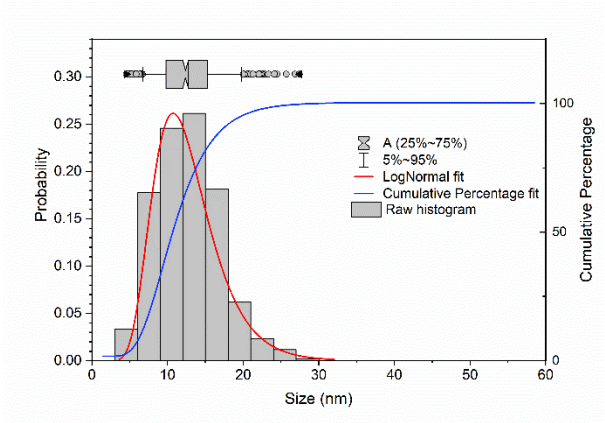

Dimensional Parameters - Width	Value
Analyzed particles	512
Minimum size (nm)	4.56 ± 0.56
First quartile (nm)	9.8 ± 1.8
Median (nm)	12.4 ± 2.7
MAD (nm)	2.79 ± 0.84
Average (nm)	12.7 ± 2.1
Standard deviation (nm)	4.1 ± 1.3
Third quartile (nm)	15.3 ± 3.0
Maximum size (nm)	27.4 ± 9.6
Mode (nm)	11.0 ± 6.6
10^{th} percentile (nm)	7.5 ± 1.0
50^{th} percentile [median] (nm)	12.4 ± 2.7

(e)

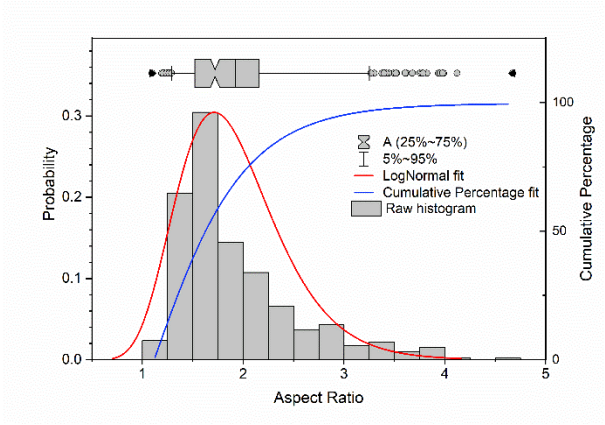

(f)

90th percentile (nm)	17.9 ± 3.3

(g)

Aspect ratio	Value
Analyzed particles	512
Minimum	1.10
First quartile	1.52
Median	1.72
MAD	0.27
Average	1.92
Standard deviation	0.60
Third quartile	2.16
Maximum	4.67
Mode	1.59
10th percentile	1.38
50th percentile [median]	1.72
90th percentile	2.80

(h)

Figure Annex D.3: Representative Transmission Electron Microscopy (TEM) micrographs (a, b), size distribution curve and descriptive parameters for particles' length (c, d), size distribution curve and descriptive parameters for particles' width (e, f), AR distribution curve and descriptive parameters (g, h) of hydroxyapatite (nano) at a concentration (0.0625 mg/mL) producing visible precipitates in CHO-K1 cell culture medium without S9 before exposure time (22LA14102-13). Size parameters are reported as value ± standard deviation. The uncertainty of size values is expressed with two significant Figures and dimensions of the values are reported accordingly.

c) Transmission Electron Microscopy (TEM) micrographs, size and aspect ratio (AR) distributions and their descriptive parameters of 0.0625 mg/mL of hydroxyapatite (nano) after 24 h exposure without S9 mix (namely 0.0625 mg/mL at 4 h – S9 and 0.0625 mg/mL at 24 h – S9)

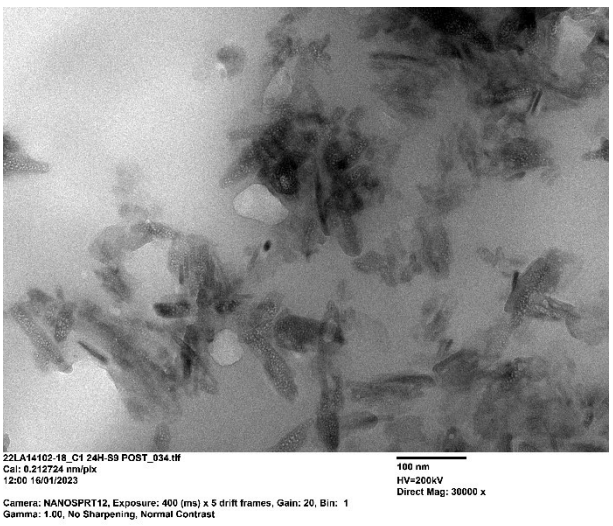

(a)

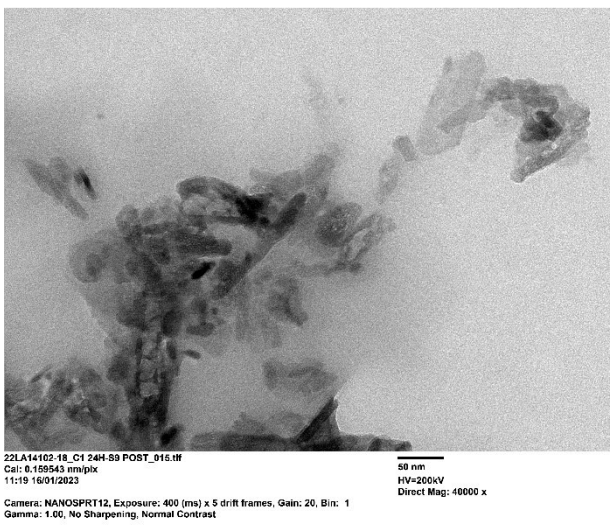

(b)

Dimensional Parameters - Length	Value
Analysed particles	510
Minimum size (nm)	8.8 ± 1.1
First quartile (nm)	17.0 ± 2.0
Median (nm)	22.1 ± 2.9

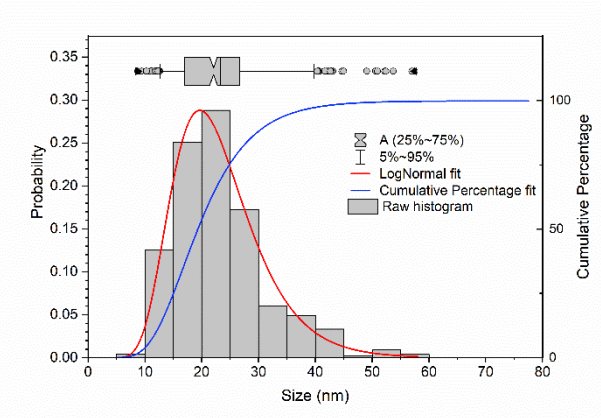

(c)

MAD (nm)	4.83 ± 0.84
Average (nm)	23.2 ± 2.4
Standard deviation (nm)	8.2 ± 2.7
Third quartile (nm)	26.7 ± 3.2
Maximum size (nm)	57 ± 20
Mode (nm)	19.6 ± 7.1
10th percentile (nm)	14.5 ± 1.8
50th percentile [median] (nm)	22.1 ± 2.9
90th percentile (nm)	34.9 ± 4.0

(d)

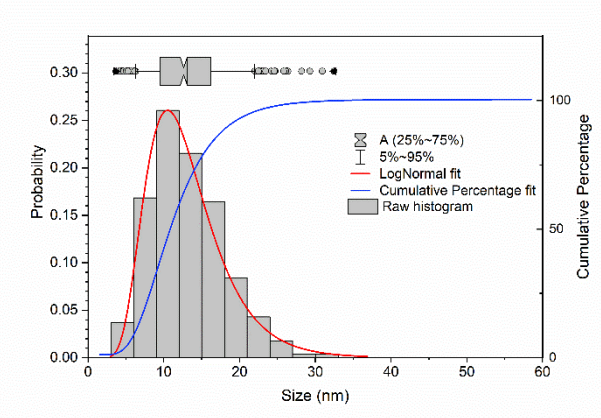

(e)

Dimensional Parameters - Width	**Value**
Analysed particles	510
Minimum size (nm)	3.69 ± 0.45
First quartile (nm)	9.5 ± 1.8
Median (nm)	12.6 ± 2.7
MAD (nm)	3.26 ± 0.84
Average (nm)	13.1 ± 2.1
Standard deviation (nm)	4.9 ± 1.6
Third quartile (nm)	16.2 ± 3.1
Maximum size (nm)	32 ± 11
Mode (nm)	10.8 ± 6.6
10th percentile (nm)	7.13 ± 0.91
50th percentile [median] (nm)	12.6 ± 2.7
90th percentile (nm)	19.6 ± 3.4

(f)

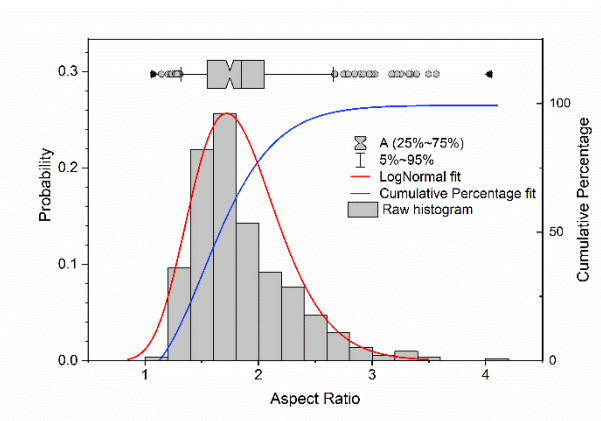

(g)

Aspect ratio	**Value**
Analysed particles	510
Minimum	1.07
First quartile	1.55
Median	1.75
MAD	0.24
Average	1.85
Standard deviation	0.44
Third quartile	2.05
Maximum	4.03
Mode	1.64
10th percentile	1.40
50th percentile [median]	1.75
90th percentile	2.45

(h)

Figure Annex D.4: Representative Transmission Electron Microscopy (TEM) micrographs (a, b), size distribution curve and descriptive parameters for particles' length (c, d), size distribution curve and descriptive parameters for particles' width (e, f), AR distribution curve and descriptive parameters (g, h) of hydroxyapatite (nano) at a concentration (0.0625 mg/mL) producing visible precipitates in CHO-K1 cell culture medium without S9 after 24 h exposure time (C1 24 h – S9, 22LA14102-18). Parameters are reported as value ± standard

deviation. The uncertainty of size values is expressed with two significant Figures and dimensions of the values are reported accordingly.

Table Annex D – 1: Particle size and aspect ratio distribution of the HAP (nano) particles for the C1 without S9 (0.0625 mg/mL) and C1* with S9 (0.1250 mg/mL) concentrations – MNT conditions *(summarized information provided by SCCS from Ref 14 22523987.0002_FR_Attachment_3-1_complete MNT Uptake)*

Conditions (MNT)	Median Length	Median Width	Length (Min – Max)	Width (Min – Max)	AR Average	AR Median	Max AR	AR Third quartile	AR 90th percentile
Pristine	21 ± 3	12 ± 3	8 ± 1 122 ± 43	4.8 ± 0.6 49 ± 17	1.96	1.51 ± 0.26	8.97	2.02	3.31*
C1 - S9 before 4h exposure time	22.2 ± 2.9	12.4 ± 2.7	9.2 ± 1.1 64 ± 22	4.56 ± 0.56 27.4 ± 9.6	1.92	1.72 ± 0.27	4.67	2.16	2.80
C1 - S9 before 24 h exposure time	22.2 ± 2.9	12.4 ± 2.7	9.2 ± 1.1 64 ± 22	4.56 ± 0.56 27.4 ± 9.6	1.92	1.72 ± 0.27	4.67	2.16	2.80
C1 4h – S9	23.3 ± 2.9	14.3 ± 2.7	9.2 ± 1.1 111 ± 39	4.85 ± 0.60 61 ± 21	1.76	1.46 ± 0.19	8.77	1.78	2.53
C1 24h – S9	22.1 ± 2.9	12.6 ± 2.7	8.8 ±1.1 57 ± 20	3.69 ± 0.45 32 ± 11	1.85	1.75 ± 0.24	4.03	2.05	2.45
C1* 0h + S9 before exposure	24.7 ± 3.0	12.7 ± 2.7	7.8 ± 1.0 59 ± 20	5.01 ± 0.62 33 ± 11	2.07	1.89 ± 0.36	4.61	2.38	2.93
C1* 4h + S9	24.9 ± 3.0	11.7 ± 2.7	9.2 ± 1.1 74 ± 26	4.03 ± 0.50 50 ± 17	2.23	2.08 ± 0.42	5.89	2.64	3.13

Table Annex D – 2: Particle size and aspect ratio distributions of HAP (nano) particles for the C2 without S9 (0.0313 mg/mL) and C2* with S9 (0.0625 mg/mL) concentrations – MNT conditions (*summarized information provided by SCCS from Ref 14 22523987.0002_FR_Attachment_3-1_complete MNT Uptake)*

Conditions (MNT)	Median Length	Median Width	Length (Min – Max)	Width (Min – Max	AR Average	AR Median	Max AR	AR Third quartile	AR 90th percentile
Pristine	21 ± 3	12 ± 3	8 ± 1 122 ± 43	4.8 ± 0.6 49 ± 17	1.96	1.51 ± 0.26	8.97	2.02	3.31*
C2 – S9 before 4h	21.6 ± 2.9	12.1 ± 2.7	7.66 ± 0.94 53 ± 19	3.99 ± 0.49 34 ± 12	1.89	1.74 ± 0.25	4.74	2.04	2.68
C2 – S9 before 24h	21.6 ± 2.9	12.1 ± 2.7	7.66 ± 0.94 53 ± 19	3.99 ± 0.49 34 ± 12	1.89	1.74 ± 0.25	4.74	2.04	2.68
C2 4h – S9	21.0 ± 2.9	12.6 ± 2.7	8.4 ±1.0 136 ± 47	3.30 ± 0.41 107 ± 37	1.72	1.54 ± 0.24	6.15	1.87	2.38
C2 24 – S9	20.3 ± 2.9	12.0 ± 2.7	9.3 ± 1.1 67 ± 23	4.29 ± 0.53 47 ± 16	1.81	1.70 ± 0.22	3.69	1.98	2.39
C2* + S9 before exposure	24.2 ± 3.0	11.7 ± 2.7	8.1 ± 1.0 51 ± 18	4.10 ± 0.51 34 ± 12	2.15	1.99 ± 0.34	6.05	2.40	3.03
C2* 4h + S9	24.6 ± 3.0	12.2 ± 2.7	8.1 ± 1.1 73 ± 25	5.02 ± 0.62 52 ± 18	2.11	1.96 ± 0.33	5.90	2.39	2.92

Table Annex D – 3: Particle size and aspect ratio distributions of HAP (nano) particles for the C3 without S9 (0.0156 mg/mL) and C3* with (0.0156 mg/mL) concentrations – MNT conditions *(summarized information provided by SCCS from Ref 14 22523987.0002_FR_Attachment_3-1_complete MNT Uptake)*

Conditions (MNT)	**Median Length**	**Median Width**	**Length (Min – Max)**	**Width (Min - Max**	**AR Average**	**AR Median**	**Max AR**	**AR Third quartile**	**AR 90th percentile**
Pristine	21 ± 3	12 ± 3	8 ± 1 122 ± 43	4.8 ± 0.6 49 ± 17	1.96	1.51 ± 0.26	8.97	2.02	3.31*
C3 – S9 before 4h exposure	22.3 ± 2.9	12.0 ± 2.7	9.6 ± 1.2 45 ± 16	4.40 ± 0.54 25.9 ± 9.1	1.96	1.79 ± 0.29	4.79	2.15	2.82
C3 – S9 before 24h exposure	22.3 ± 2.9	12.0 ± 2.7	9.6 ± 1.2 45 ± 16	4.40 ± 0.54 25.9 ± 9.1	1.96	1.79 ± 0.29	4.79	2.15	2.82
C3 4h – S9	22.9 ± 2.9	12.4 ± 2.7	11.2 ± 1.4 51 ± 18	3.81 ± 0.47 34 ± 12	1..97	1.77 ± 0.27	5.00	2.15	2.91
C3 24h – S9	22.9 ± 2.9	11.7 ± 2.7	6.66 ± 0.82 77 ± 27	2.81 ± 0.35 50 ± 18	2.12	1.84 ± 0.32	9.94	2.27	3.01
C3* 0h + S9 before exposure	22.5 ± 2.9	12.0 ± 2.7	8.7 ± 1.1 55 ± 19	3.85 ± 0.47 30 ± 11	2.06	1.83 ± 0.33	5.67	2.35	3.04
C3* 4h + S9	24.9 ± 3.0	12.9 ± 2.7	6.47 ± 0.80 91 ± 32	4.06 ± 0.50 42 ± 15	2.10	1.86 0.33	9.35	2.27	2.96

11. Annex E: Cellular Uptake and Cytoplasmatic Internalization (MNT Assay)

From Ref 14. 22523987.0002_FR_Attachment_3-1_complete MNT Uptake - searchable_Rev1: Evaluation of PhPC-2022-3 (nano) behaviour in terms of size distribution, dispersion and cellular uptake for Micronucleus (MNT) Assay

From the Applicant
Cellular uptake and cytoplasmic internalization of nanohydroxyapatite particles of PhPC-2022-3 (nano) during micronucleus assay was investigated by TEM-EDX. Regardless of the micronucleus assay condition (i.e., 4h – S9, 4h + S9, 24h – S9) and concentration (i.e., 0.1250 mg/mL, 0.0625 mg/mL, 0.0313 mg/mL, 0.0156 mg/mL of nanohydroxyapatite), it was demonstrated that cells exposed to PhPC-2022-3 (nano) internalized Ca-P-based particles consistent with nanohydroxyapatite. Representative EDX spectra of internalized particles are reported below.

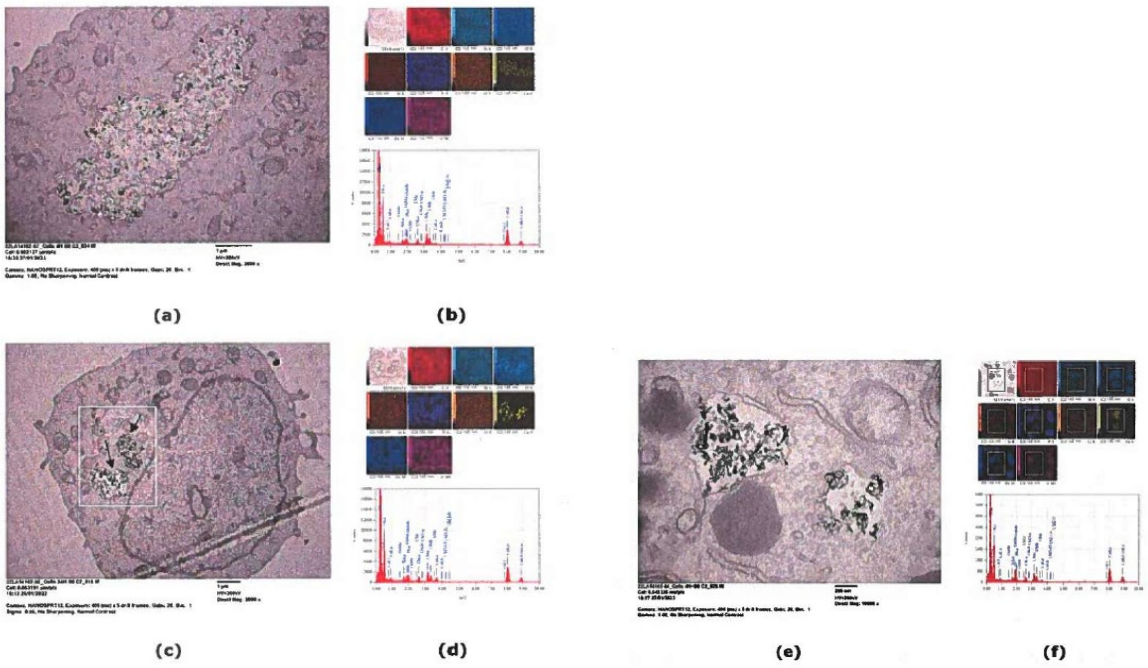

Figure Annex E.1: Representative TEM micrographs of analyzed areas and corresponding EDX spectra of nanohydroxyapatite particles in CHO-K1 cells. (a) TEM micrograph of cells treated without S9 with cytoplasmic internalization of nanohydroxyapatite particles after 4h exposure, and (b) corresponding EDX spectrum and map of nanohydroxyapatite in the cytoplasm. (c) TEM micrograph of cell treated with S9 with cytoplasmic internalization of nanohydroxyapatite particles after 24h exposure, and (d) EDX map and spectrum of nanohydroxyapatite in the cytoplasm. EDX spectrum and map were collected in the area highlighted by the rectangle in Figure Annex E.1.c. Arrows in Figure Annex E.1.c indicate nanohydroxyapatite particles. (e) TEM micrograph of cells treated with S9 with cytoplasmic internalization of nanohydroxyapatite particles, and (f) corresponding EDX map and spectrum of nanohydroxyapatite in the cytoplasm. Rectangles in the EDX map (Figure Annex E.1.f) correspond to the area in Figure Annex E.1.e. (from Ref. Ref 14 22523987.0002_FR_Attachment_3-1_complete MNT Uptake).

a) Cellular Uptake and Cytoplasmatic Internalization without S9 mix at 0.0625 mg/mL
Figure Annex E.2a-b shows representative TEM micrographs of CHO-K1 cells after 24 h exposure time to the first concentration of hydroxyapatite (nano) not producing visible precipitates without S9 (0.0625 mg/mL of hydroxyapatite (nano), 24 h – S9). Figure Annex E.2c and Figure Annex E.2e report size distribution curve for length and width of

hydroxyapatite (nano) internalized particles, respectively. Figure E.2.d and Figure E.2.f report the descriptive parameters for particles' length and width distribution, respectively. Figure Annex E.2g and Figure Annex E.2h show respectively the AR distribution curve and its corresponding descriptive parameters for hydroxyapatite (nano) internalized particles.

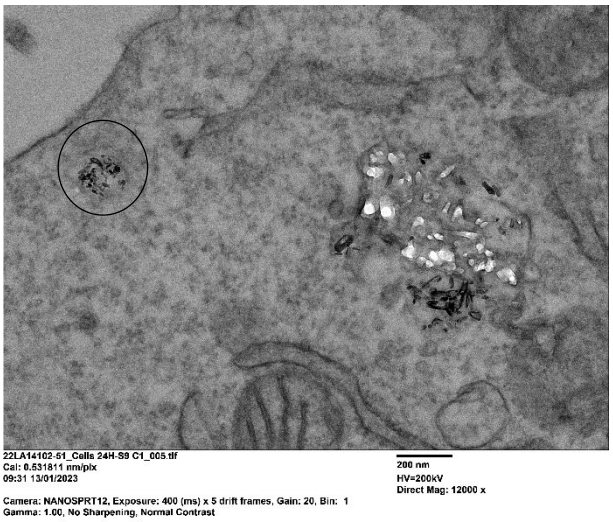

(a)

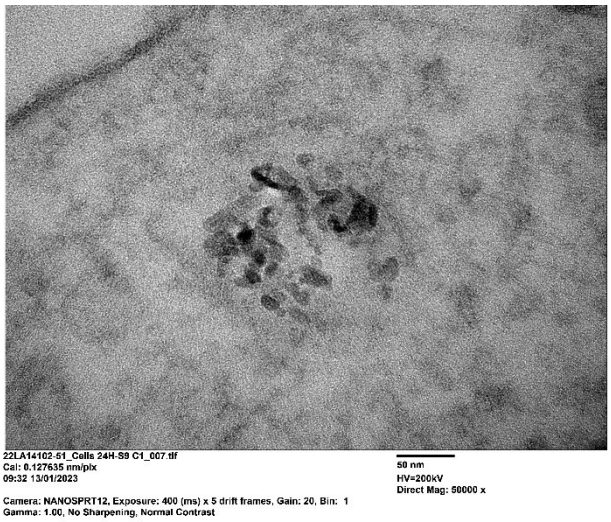

(b)50

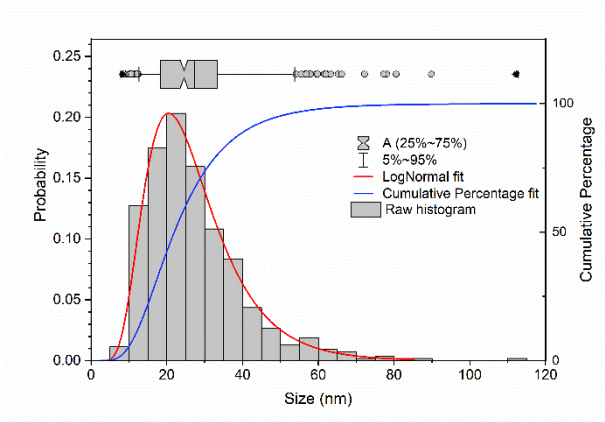

(c)

Dimensional Parameters -Length	Value
Analysed particles	526
Minimum size (nm)	8.3 ± 1.0
First quartile (nm)	18.2 ± 2.1
Median (nm)	24.5 ± 3.0
MAD (nm)	7.31 ± 0.85
Average (nm)	27.4 ± 2.5
Standard deviation (nm)	13.1 ± 4.3
Third quartile (nm)	33.2 ± 3.4
Maximum size (nm)	112 ± 39
Mode (nm)	20.0 ± 7.2
10^{th} percentile (nm)	14.2 ± 1.8
50^{th} percentile [median] (nm)	24.5 ± 3.0
90^{th} percentile (nm)	43.3 ± 4.3

(d)

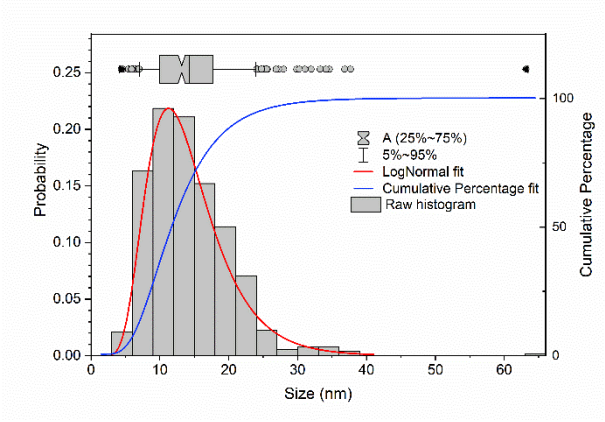

Dimensional Parameters - Width	Value
Analysed particles	526
Minimum size (nm)	4.39 ± 0.54
First quartile (nm)	9.9 ± 1.8
Median (nm)	13.2 ± 2.7
MAD (nm)	3.76 ± 0.84
Average (nm)	14.3 ± 2.1
Standard deviation (nm)	6.0 ± 2.0
Third quartile (nm)	17.7 ± 3.1
Maximum size (nm)	63 ± 22
Mode (nm)	11.1 ± 6.6
10^{th} percentile (nm)	7.8 ± 1.0
50^{th} percentile [median] (nm)	13.2 ± 2.7

(e)

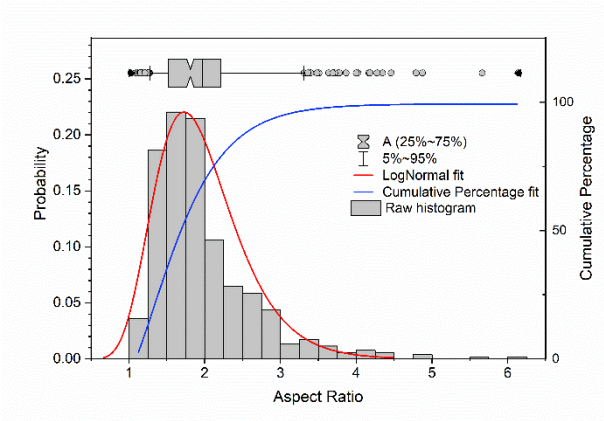

90th percentile (nm)	22.1 ± 3.5

(f)

Aspect ratio	Value
Analysed particles	526
Minimum	1.03
First quartile	1.52
Median	1.81
MAD	0.32
Average	1.97
Standard deviation	0.67
Third quartile	2.22
Maximum	6.14
Mode	1.66
10th percentile	1.35
50th percentile [median]	1.81
90th percentile	2.80

(g) **(h)**

Figure Annex E.2: Representative Transmission Electron Microscopy (TEM) micrographs at magnification 12000x (a) and 50000x (b) of CHO-K1 cells after 24 h exposure to the first concentration of hydroxyapatite (nano) not producing visible precipitates without S9 (0.0625 mg/mL at 24 h – S9, 22LA14102-51). In Panel (a) internalized particles are highlighted by the circle. Size distribution curve and its descriptive parameters for length (c, d) and width (e, f) of the internalized hydroxyapatite (nano) particles. (g, h) AR distribution curve and its corresponding descriptive parameters for the internalized hydroxyapatite (nano) particles. Size parameters are reported as value ± standard deviation. The uncertainty of size values is expressed with two significant Figures and dimensions of the values are reported accordingly.

d) Cellular Uptake and Cytoplasmatic Internalization with S9 mix at 0.1250 mg/mL

Figure Annex E.3b shows representative TEM micrographs of CHO-K1 cells after 4 h exposure time to the concentration of hydroxyapatite (nano) producing visible precipitates with S9 (0.1250 mg/mL of hydroxyapatite (nano), 4 h + S9). Figure Annex E.3c and Figure Annex E.3e report size distribution curve for length and width of hydroxyapatite (nano) internalized particles, respectively. Figure Annex E.3.d and Figure Annex E.2f report the descriptive parameters for particles' length and width distribution, respectively. Figure Annex E.3d and Figure Annex E.3f respectively show the AR distribution curve and its corresponding descriptive parameters for hydroxyapatite (nano) internalized particles.

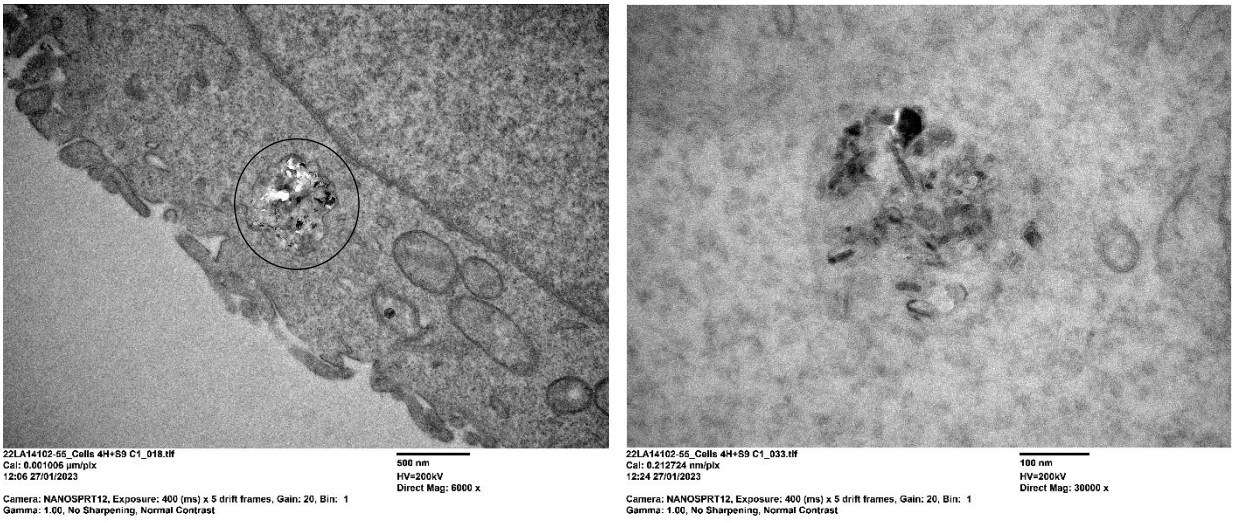

(a)

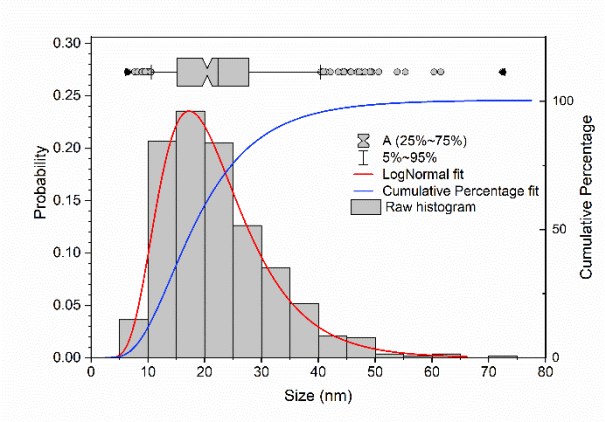

(b)

Dimensional Parameters -Length	Value
Analysed particles	522
Minimum size (nm)	6.44 ± 0.79
First quartile (nm)	15.1 ± 2.0
Median (nm)	20.5 ± 2.9
MAD (nm)	5.78 ± 0.84
Average (nm)	22.3 ± 2.3
Standard deviation (nm)	9.6 ± 3.2
Third quartile (nm)	27.8 ± 3.3
Maximum size (nm)	72 ± 25
Mode (nm)	16.8 ± 7.0
10^{th} percentile (nm)	11.9 ± 1.5
50^{th} percentile [median] (nm)	20.5 ± 2.9
90^{th} percentile (nm)	35.5 ± 4.0

(c)

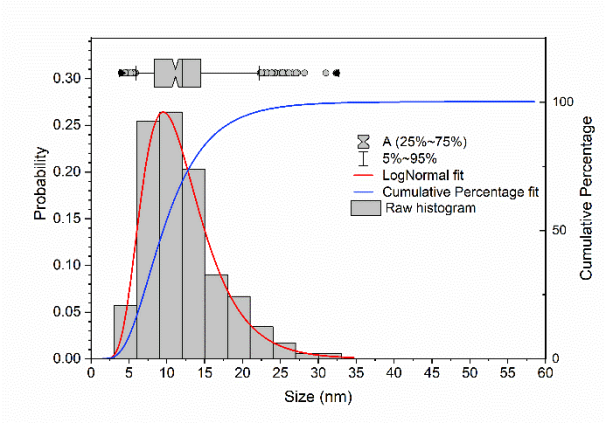

(d)

Dimensional Parameters - Width	Value
Analysed particles	522
Minimum size (nm)	4.01 ± 0.49
First quartile (nm)	8.3 ± 1.7
Median (nm)	11.1 ± 2.6
MAD (nm)	3.03 ± 0.84
Average (nm)	12.1 ± 2.1
Standard deviation (nm)	5.0 ± 1.6
Third quartile (nm)	14.5 ± 3.0
Maximum size (nm)	32 ± 11
Mode (nm)	9.3 ± 6.5
10^{th} percentile (nm)	6.68 ± 0.85
50^{th} percentile [median] (nm)	11.1 ± 2.6
90^{th} percentile (nm)	19.2 ± 3.3

(e)

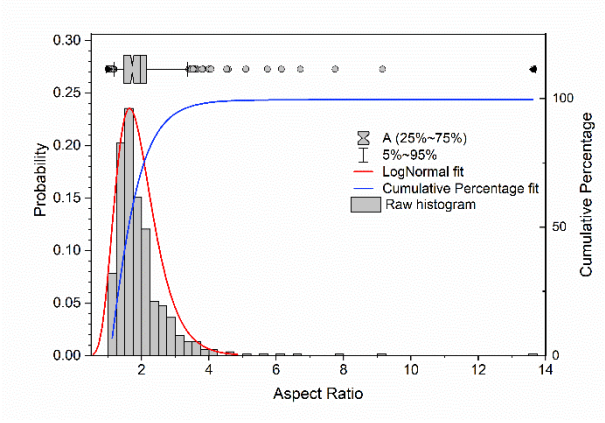

(f)

Aspect ratio	Value
Analysed particles	522
Minimum	1.01
First quartile	1.47
Median	1.72
MAD	0.31
Average	1.96
Standard deviation	0.96
Third quartile	2.14
Maximum	13.64
Mode	1.58
10^{th} percentile	1.29
50^{th} percentile [median]	1.72
90^{th} percentile	2.82

(g) **(h)**

Figure Annex E.3.: Representative Transmission Electron Microscopy (TEM) micrographs at magnification 6000x (a) and 30000x (b) of CHO-K1 cells after 4 h exposure to the concentration of hydroxyapatite (nano) producing visible precipitates with S9 (0.1250 mg/mL

at 4 h + S9, 22LA14102-55). In Panel (a) internalized particles are highlighted by the circle. Size distribution curve and its descriptive parameters for length (c, d) and width (e, f) of the internalized hydroxyapatite (nano) particles. (g, h) AR distribution curve and its corresponding descriptive parameters for the internalized hydroxyapatite (nano) particles. Size parameters are reported as value ± standard deviation. The uncertainty of size values is expressed with two significant Figures and dimensions of the values are reported accordingly.

Conclusion on Cellular uptake (by Applicant)
Cellular uptake of hydroxyapatite (nano) particles of PhPC-2022-3 (nano) was also investigated at the concentrations used in the MNT and cytoplasmic internalization of hydroxyapatite (nano) was observed in all test conditions. The size of internalized particles was comparable with hydroxyapatite (nano) particles to those of the pure (pristine) form.

Table Annex E – 1: Particle size and aspect ratio of Internalized particles for the C1, C2 and C3 without S9 and C1*, C2* and C3 with S9 concentrations – MNT conditions (summarized information provided by SCCS from Ref 14 2523987.0002_FR_Attachment_3-1_complete MNT Uptake).

Conditions (MNT)	Median Length	Median Width	Length (Min – Max)	Width (Min – Max)	AR Average	AR Median	Max AR	AR Third quartile	AR 90th percentile
Pristine	21 ± 3	12 ± 3	8 ± 1 122 ± 43	4.8 ± 0.6 49 ± 17	1.96	1.51 ± 0.26	8.97	2.02	3.31*
C1 4h – S9	20.0 ± 2.9	11.9 ± 2.7	7.14 ± 0.88 67 ± 23	4.39 ± 0.54 44 ± 15	1.71	1.67 ± 0.19	3.18	1.88	2.11
C1 24h – S9	24.5 ± 3.0	13.2 ± 2.7	8.3 ± 1.0 112 ± 39	4.39 ± 0.54 63 ± 22	1.97	1.81 ± 0.32	6.14	2.22	2.80
C1* 4h + S9	20.5 ± 2.9	11.1 ± 2.6	6.44 ± 0.79 72 ± 25	4.01 ± 0.49 32 ± 11	1.96	1.72 ± 0.31	13.64	2.14	2.82
C2 4h – S9	20.5 ± 2.9	11.5 ± 2.7	7.10 ± 0.87 57 ± 20	3.94 ± 0.49 41 ± 14	1.83	1.69 ± 0.22	5.35	1.98	2.47
C2 24h – S9	20.9 ± 2.9	10.3 ± 2.6	5.81 ± 0.72 84 ± 29	3.01 ± 0.37 47 ± 16	2.25	1.82 ± 0.43	8.05	2.53	3.91
C2* 4h + S9	20.3 ± 2.9	11.0 ± 2.6	7.51 ± 0.93 60 ± 21	4.26 ± 0.52 34 ± 12	1.96	1.82 ± 0.29	4.79	2.21	2.62
C3 4h – S9	21.0 ± 2.9	11.2 ± 2.6	7.58 ± 0.93 71 ± 25	3.75 ± 0.46 34 ± 12	1.98	1.80 ± 0.28	6.5	2.17	2.68
C3 24h – S9	21.9 ± 2.9	11.7 ± 2.7	5.01 ± 0.62 89 ± 31	4.04 ±0.50 43 ± 15	2.07	1.74 ± 0.38	8.20	2.32	3.35
C3* 4h + S9	22.0 ± 2.9	11.0 ± 2.6	6.95 ± 0.86 80 ± 28	3.05 ±0.38 49 ± 17	2.12	1.89 ± 0.40	10.10	2.35	3.24

12. Annex F: Cellular Uptake and Cytoplasmatic Internalization (gene mutations at the *Hprt* locus using the Chinese hamster cell line V79)

From Report 4114412 (ICCR, 2024; Fraunhofer IAP, 2024; ZentriForce, 2024 provided in September 2024): Report PhPC-2022-3: Gene Mutation Assay in Chinese Hamster V79 Cells *in vitro* (V79/HPRT)

This *in vitro* experiment was performed to assess the potential of the test item to induce gene mutations at the *Hprt* locus using the Chinese hamster cell line V79. Two parallel cultures were used throughout the assay.

The cellular uptake of the test item under experimental conditions of the planned study has been established in a pre-experiment (performed under non-GLP conditions ICCR Study 4114411) and was analysed by transmission election microscopy (TEM)

Cell preparation for the cellular uptake analysis via TEM (non-GLP) (page 13/69 from Report 4114412 (ICCR, 2024; Fraunhofer IAP, 2024; ZentriForce, 2024) provided in September 2024)

After 24-hour treatment and subsequent cell counting in the pre-experiment, the cells of concentrations 6.4 and 100 µg/mL were prepared for the descriptive microscopy to prove the cellular uptake of the test item.
The cells were centrifuged for approx. 10 minutes at 400x g and gently wash with prewarmed PBS.
Then the cells were centrifuged again, resuspended with the 2.5% Glutaraldehyde Fixative and incubated for approx. 15 minutes at 37°C.
After incubation, the cells were centrifuged and incubated with fresh 2.5% Glutaraldehyde Fixative for 4 hours at 4°C. The cells were centrifuged again, the supernatant was removed, and the cells were taken up in the 1.5 mL Maintenance Wash solution and stored in the refrigerator until dispatch to the lab for TEM imaging.
The prepared cells were shipped on cool packs to laboratory for TEM imaging.

The cellular uptake analysis via transmission electron microscopy (TEM) was performed under non-GLP.

As stated in the Short Report (art of Study ID 4114411, non-GLP conditions) of Fraunhofer IAP: "Cellular uptake of the test item was demonstrated for concentrations 6.4 and 100 µg/mL". (Report 4114412 (ICCR, 2024; Fraunhofer IAP, 2024; ZentriForce, 2024)).

Cell preparation for the cellular uptake analysis via TEM (non-GLP) (from Report 4114412 (ICCR, 2024; Fraunhofer IAP, 2024; ZentriForce, 2024) provided in September 2024)

TEM investigation of hydroxyapatite nanoparticles in biological cell cultures (V79)

Introduction
Detection of cellular uptake of nanoparticles of a 29.5 % thixotropic aqueous dispersion of hydroxyapatite with different concentrations in V79 cells was performed using transmission electron microscopy (TEM). Samples were prepared according to the preparation method D (method development dated March 2022).

Materials and methods

Samples:
Samples of V79 cells treated with different concentrations of a 29.5% thixotropic aqueous dispersion of hydroxyapatite were analysed (Table below).

Table 1 Samples of V79 cells with different concentrations of a 29.5% thixotropic aqueous dispersion of hydroxyapatite

Sample ID (IAP)	Sample ID (ICCR)	Test Item	Substance	Concentration
1	1.1 – 4114411	PhPC-2022-3	Hydroxyapatite	6.4 µg/mL
2	2.1 – 4114411	PhPC-2022-3	Hydroxyapatite	100 µg/mL

Table Annex F – 1: Samples of V79 cells with different concentration of a 29.5% thixotropic aqueous dispersion of hydroxyapatite

Solutions
Solutions required were prepared using the following formulation

Phosphate buffer Stock Solutions

PART 1:

200 mM disodium hydrogen orthophosphate dihydrate (Na2HPO4 . 2H2O) basic

8.9 g dissolved in 250 mL water

PART 2:

200 mM sodium dihydrogen orthophosphate monohydrate (NaH2PO4 . H2O) acidic

2.76 g dissolved in 100 mL water

Storage Buffer, Washing Buffer (LP)

34.22 g saccharose dissolved in 50 mL water (2M solution) (100 mL beaker)

128 mL part 1

38 mL part 2

mixed in a 500 mL beaker and adjusted to pH 7.3 while stirring

62.5 mL of saccharose solution transferred into 500 mL stock bottle

187.5 mL water added

165 mL of the phosphate buffer stock solution were made up to 250 mL with water and transferred in to a storage bottle.

The solution was stored at 4 °C.

Stock Solution OsO4-Contrasting

PART A

1.30231 g sodium dihydrogen orthophosphate in 50 mL water

PART B

1.4519 g sodium hydroxide in 50 mL water

PART C

0.43207 g glucose in 10 mL water.

PART D

5 mL osmium tetroxide (4 % solution)

PART E

20.75 mL part A

4.25 mL part B

Final solution

12.5 mL part E

2.5 mL part C

5 mL part D

The solution was stored at 4 °C in the dark.

Chemical staining by OsO_4 solvent exchange, embedding and preparation of ultra-thin cuts, TEM measurements.
The delivered dispersion of fixed cells (ICCR study number 4114411) were first transferred to a 1.5 mL Eppendorf tube and washed. For this purpose, the cells were pelleted in a benchtop centrifuge (11000 rpm, 3 min), the supernatant was removed with a pipette and finally buffer solution was added to redisperse the cell pellet. This procedure was repeated 2 more times.

Osmium tetroxide (OsO_4) solution was added to the cell pellet for contrast enhancement and then the cells were dispersed. The reaction was performed at 4°C in the dark for 90 min. with occasional shaking.

At the end of the reaction time, the cells were pelleted at 14000 rpm (4 min.) by centrifugation and the supernatant was removed with a pipette. Deionized wate (0.5 mL) was added to the pellet without dispersing it. After removing the water, the sample was ready for water exchange.

The cells, now in demineralized water, were gradually dehydrated using a centrifuge (Hettich EBA 35) at 2000 rpm for 2 min. For this purpose, the water was replaced by increasing ethanol concentrations, 10, 70 and 96% ethanol solutions were used. Subsequently, embedding in methacrylate was carried out by means of a 24hour UV polymerization, allowing the embedding agent to penetrate the samples. Ultra-thin cuts were prepared with a thickness of approximatively 65 nm using an ultramicrotome (LECIA EM VC7).

TEM micrographs images were recorded using a transmission electron microscope (JEOL TEM 1400 Plus) at an accelerated voltage of 120 kV.

Results:
Concentration 6.4 ug / mL 29.5% thixotropic aqueous dispersion of hydroxyapatite (sample 1)
The following figures show selected TEM-micrographs of ultra-thin section with internalized hydroxyapatite particles in V79 cells. Several samples of V79 cells that have internalized hydroxyapatite particles are presented for each sample.

The internalized particles could be identified as hydroxyapatite particles based on their morphology, crystal shape and particle size.

shape and particle size.

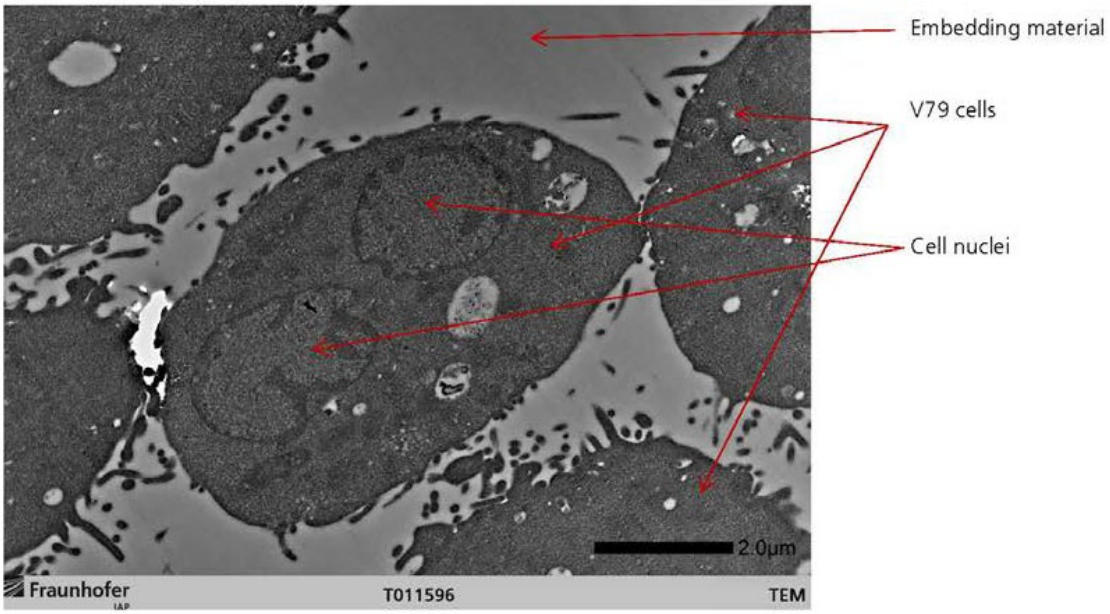

Fig.1: Sample 1, overview micrograph (cell 1), ultra-thin cut (5,000x)

Figure Annex.F.1: Sample 1, overview micrograph (cell 1), ultra-thin cut (5,000x)

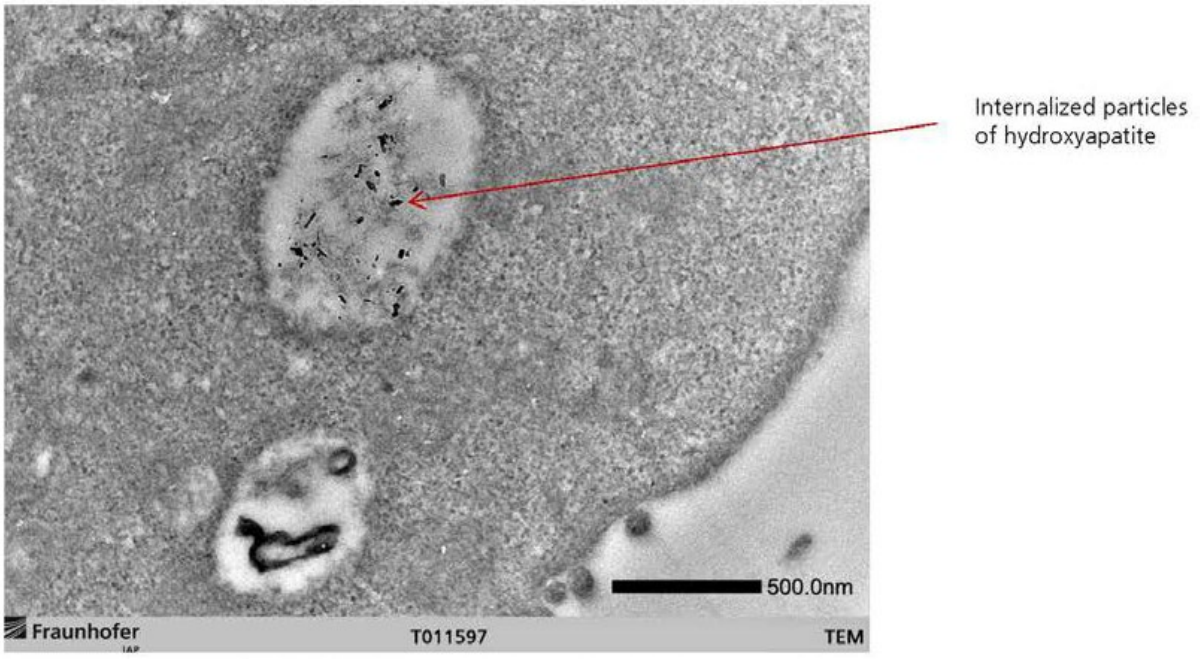

Fig.2: Sample 1, V79-cell (cell 1) with internalized particles of hydroxyapatite (20,000x)

Figure Annex.F.2: Sample 1, V79-cell (cell 1) with internalized particles of hydroxyapatite (20,000x)

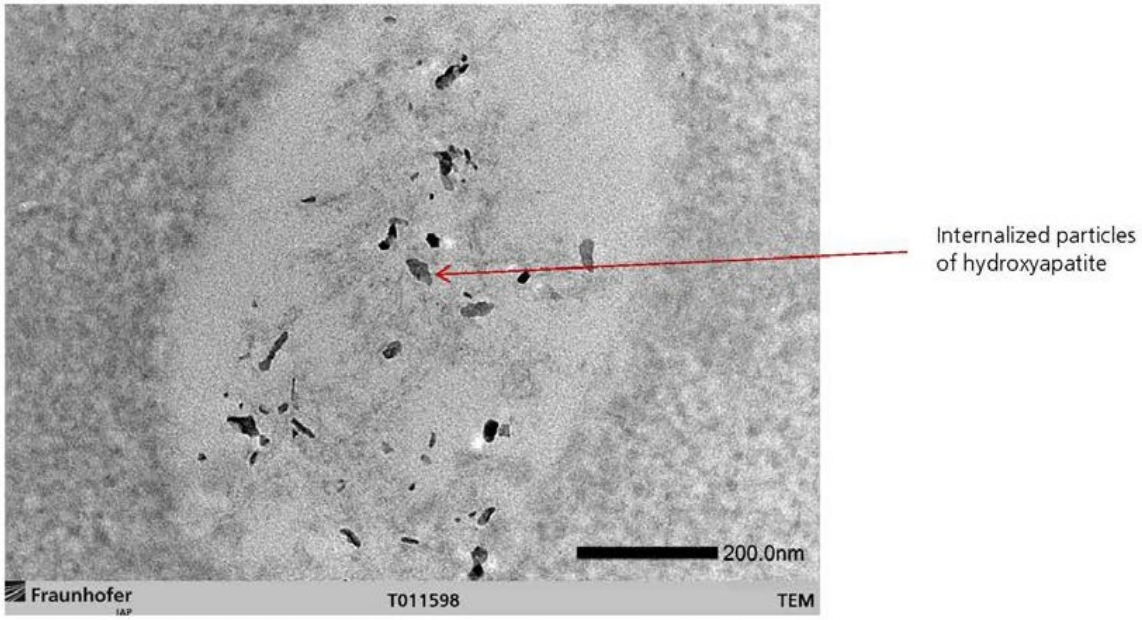

Fig.3: Sample 1, V79-cell (cell 1) with internalized particles of hydroxyapatite (50,000x)

Figure Annex.F.3: Sample 1, V79-cell (cell 1) with internalized particles of hydroxyapatite (50,000x)

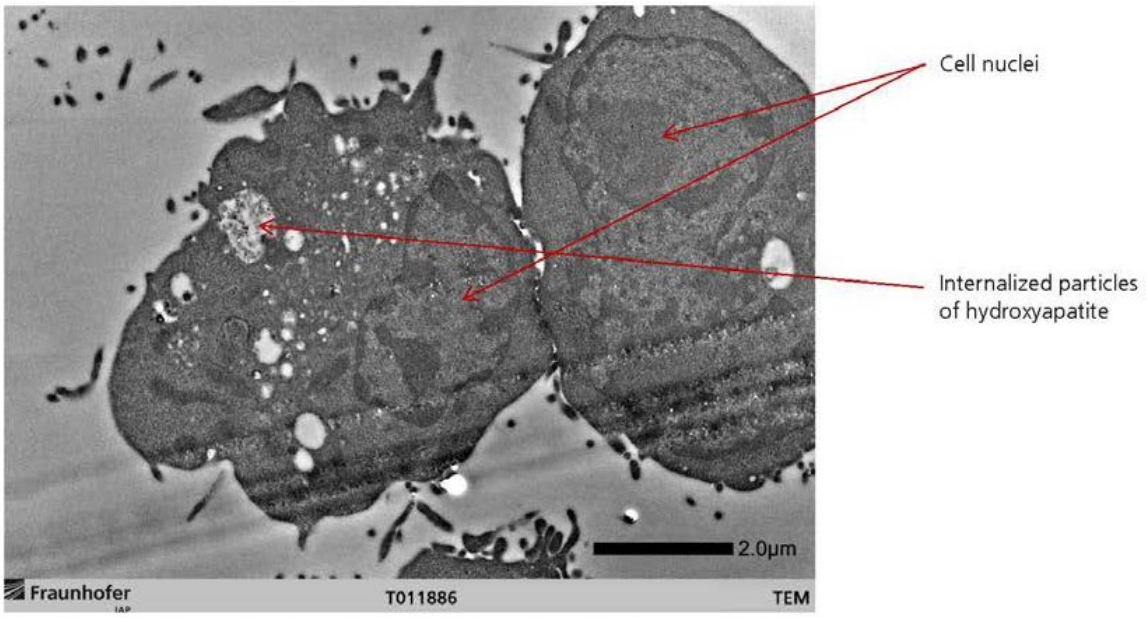

Fig.4: Sample 1, V79-cell (cell 2) with internalized particles of hydroxyapatite (5,000x)

Figure Annex.F.4: Sample 1, V79-cell (cell 2) with internalized particles of hydroxyapatite (5,000x)

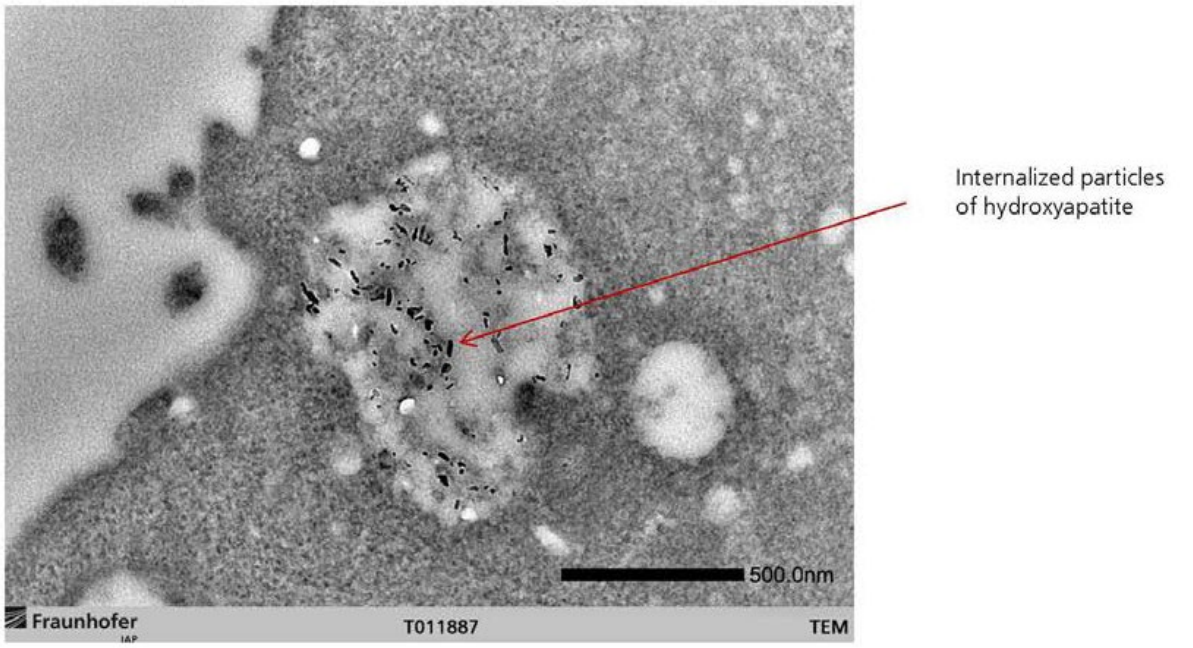

Fig.5: Sample 1, V79-cell (cell 2) internalized particles of hydroxyapatite (25,000x)

Figure Annex.F.5: Sample 1, V79-cell (cell 2) internalized particles of hydroxyapatite (25,000x)

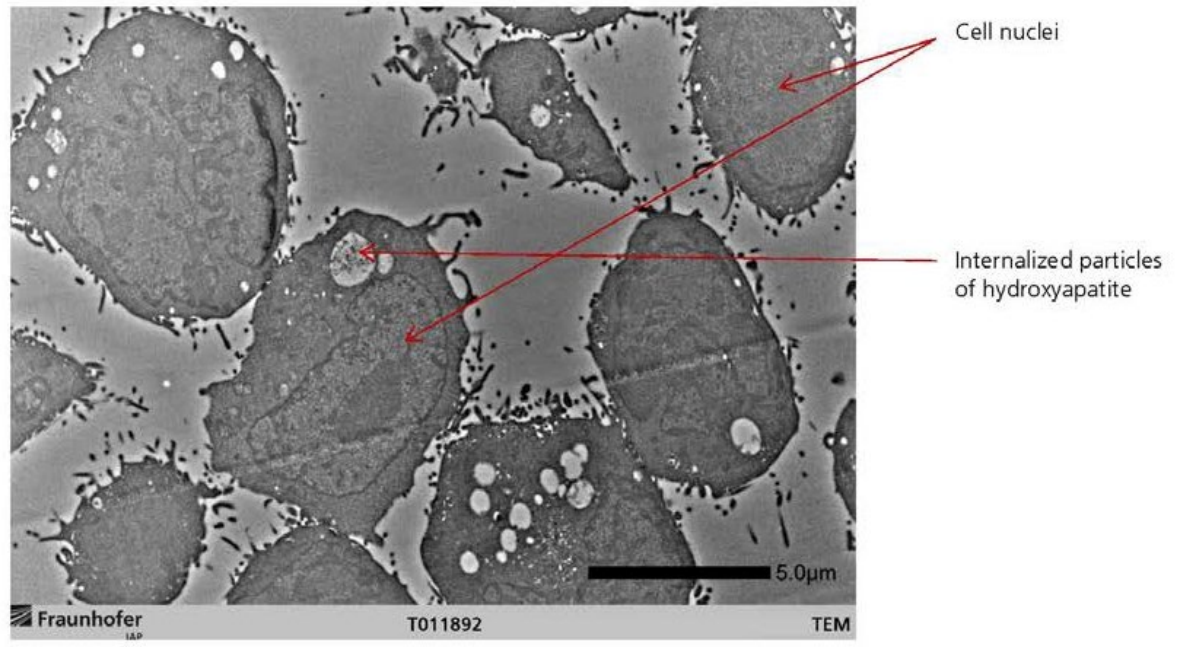

Fig.6: Sample 1, V79-cell (cell 3) with internalized particles of hydroxyapatite (2,500X)

Figure Annex.F.6: Sample 1, V79-cell (cell 3) internalized particles of hydroxyapatite (2,500x)

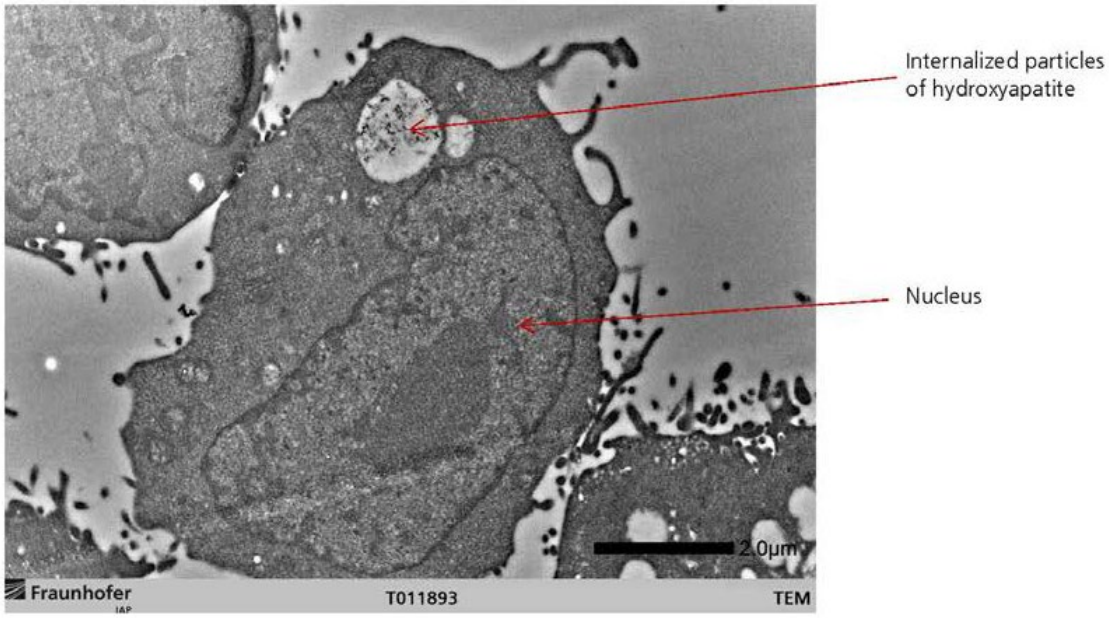

Fig.7: Sample 1, V79-cell (cell 3) with internalized particles of hydroxyapatite (5,000x)

Figure Annex.F.7: Sample 1, V79-cell (cell 3) internalized particles of hydroxyapatite (5,000x)

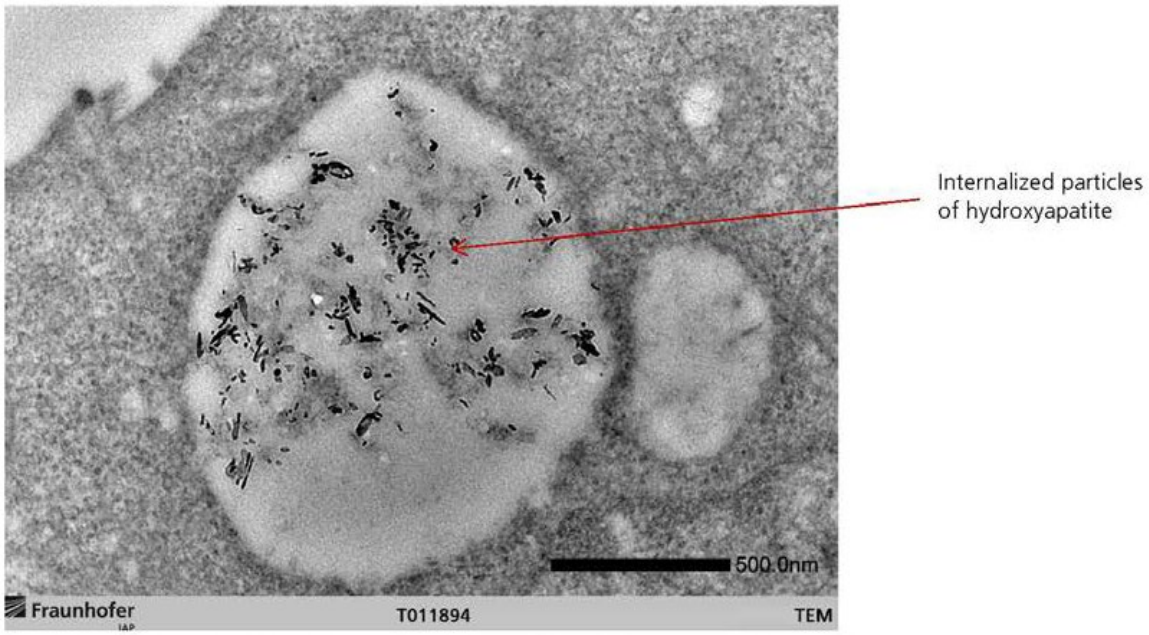

Fig.8: Sample 2, V79-cell (cell 3) with internalized particles of hydroxyapatite (25,000x)

Figure Annex.F.8: Sample 2, V79-cell (cell 3) internalized particles of hydroxyapatite (25,000x)

Concentrations 100 ug/mL: 29.5 % thixotropic aqueous dispersion of hydroxyapatite (sample 2)

In the case of sample 2, the hydroxyapatite particles were more difficult to find despite the higher concentration of the solution. The cells are closer together and the spaces between the cells are smaller. Nevertheless, cells with internalized hydroxyapatite particles can be found, as in the sample 1.

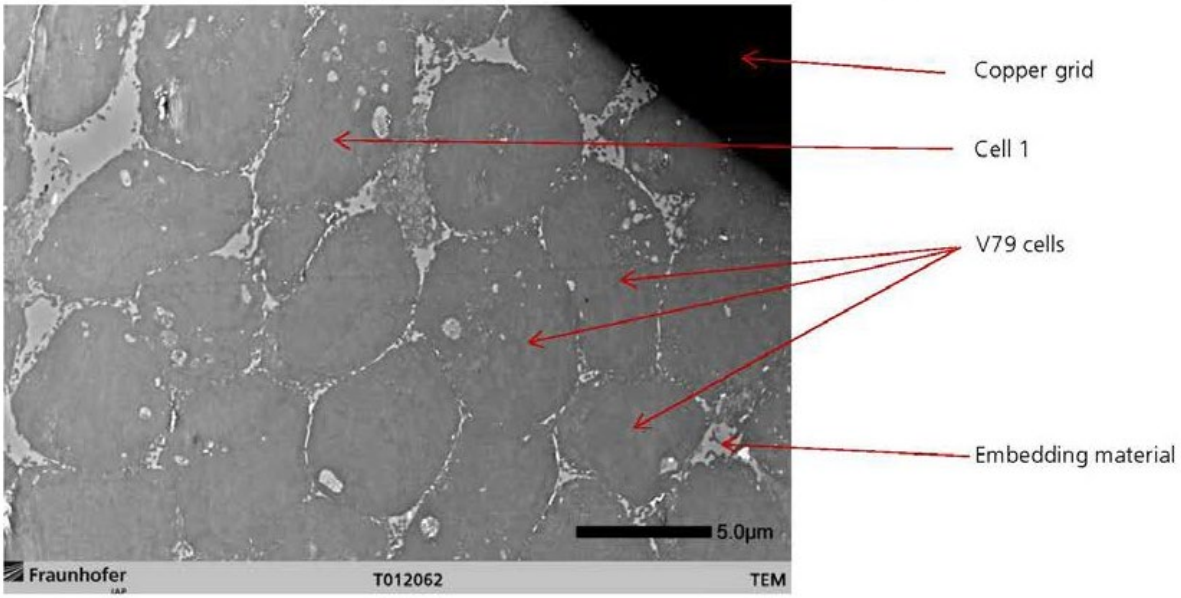

Fig.9: Sample 2, ultrathin cut of V79-cells, overview (2,000x)

Figure Annex.F.9: Sample 2, ultrathin cut of V79-cells, overview (2,000x)

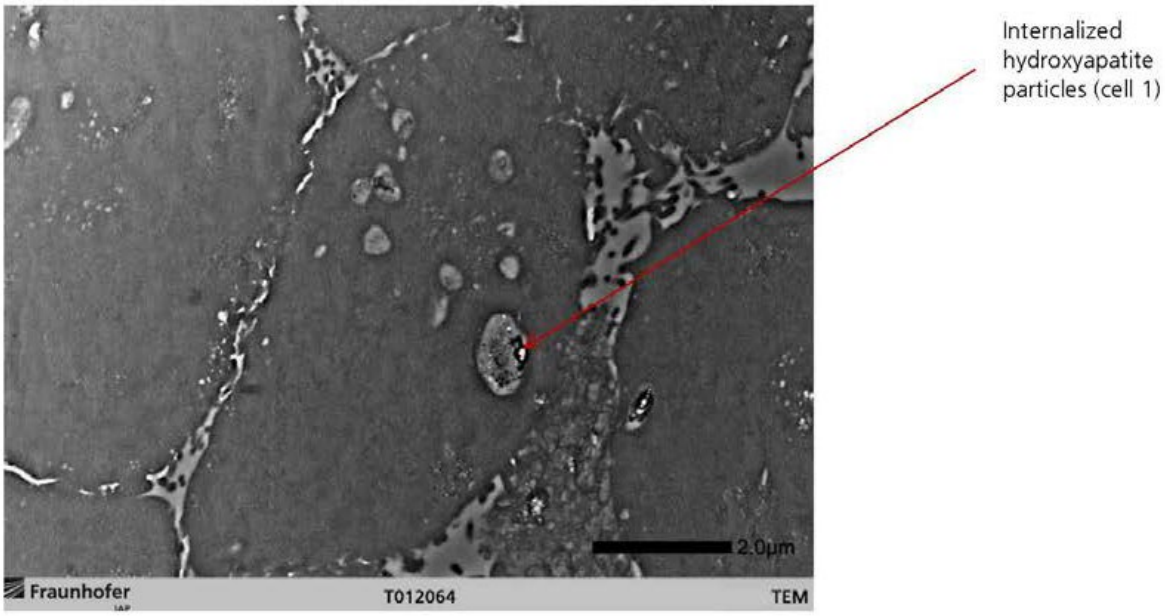

Fig.10: Sample 2, V79-cell (cell 1) with internalized hydroxyapatite particles (5,000x)

Figure Annex.F.10: Sample 2, V79-cell (cell 1) with internalized particles of hydroxyapatite (5,000x)

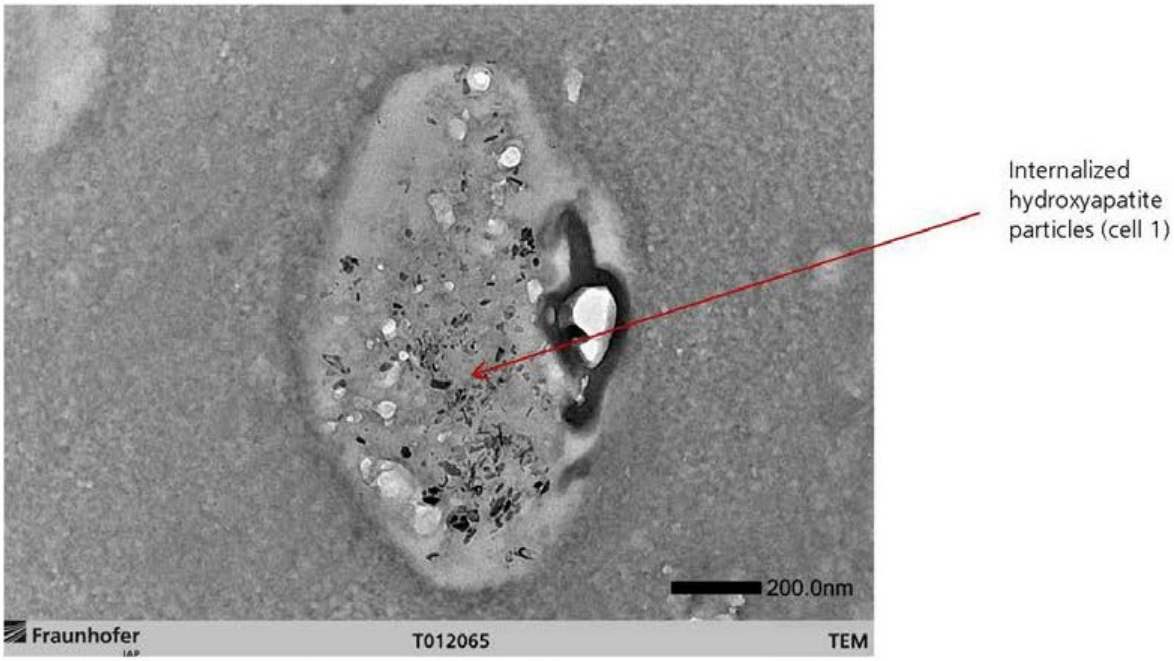

Fig.11: Sample 2, V79-cell (cell 1) with internalized hydroxyapatite particles (30,000x)

Figure Annex.F.11: Sample 2, V79-cell (cell 1) internalized particles of hydroxyapatite (30,000x)

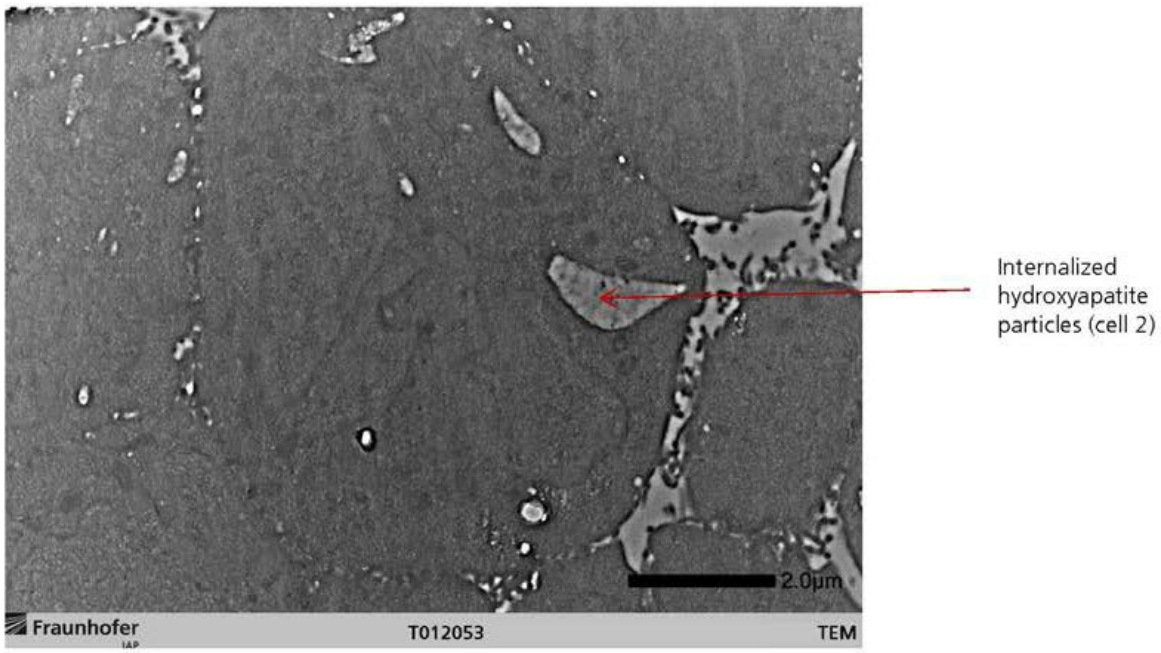

Fig.12: Sample 2, V79-cell (cell 2) with internalized hydroxyapatite particles (5,000x)

Figure Annex.F.12: Sample 2, V79-cell (cell 2) internalized particles of hydroxyapatite (5,000x)

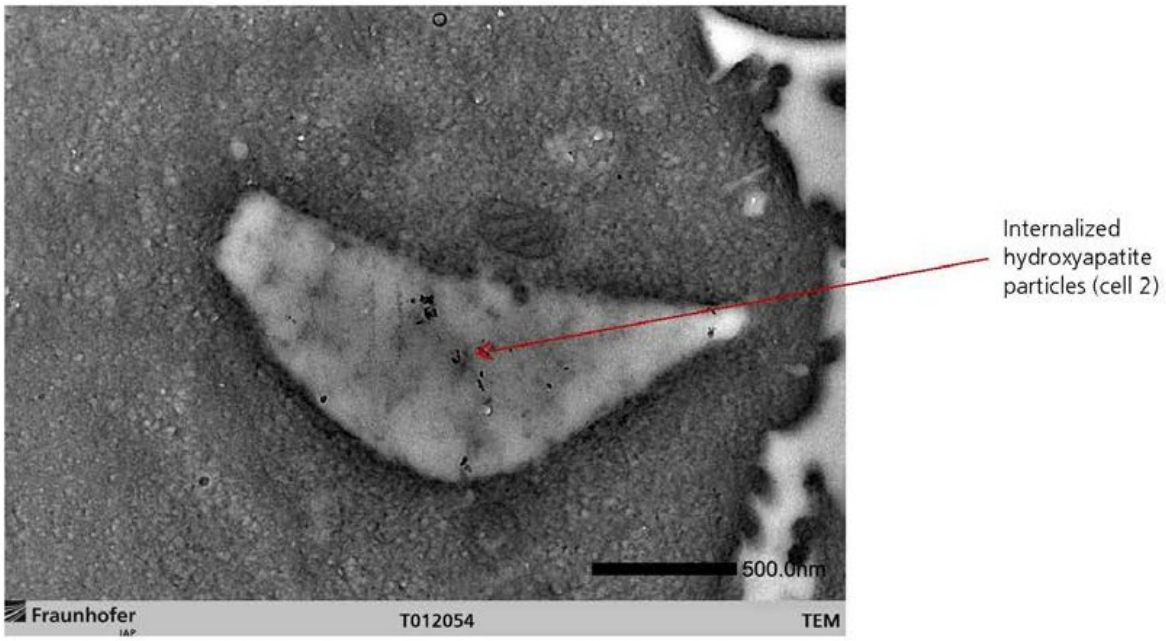

Fig.13: Sample 2, V79-cell (cell 2) with internalized hydroxyapatite particles (20,000x)

Figure Annex.F.13: Sample 2, V79-cell (cell 2) internalized particles of hydroxyapatite (20,000x)

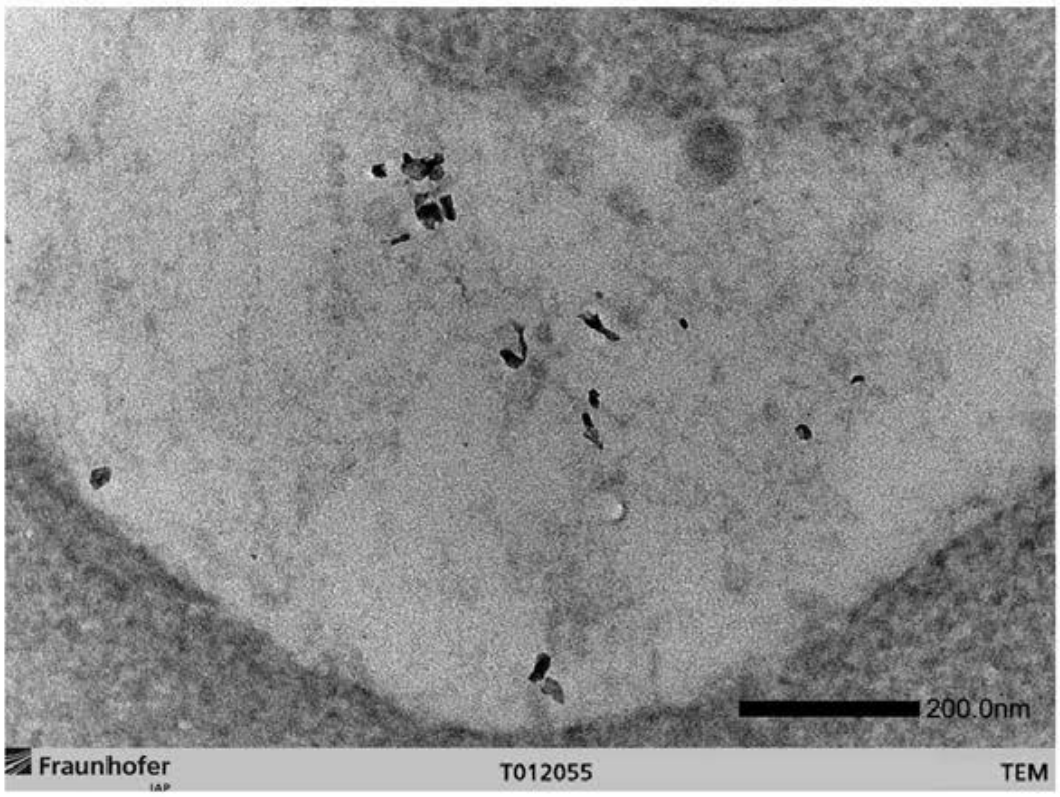

Fig.14: Sample 2, V79-cell (cell 2) with internalized hydroxyapatite particles (50,000x)

Figure Annex.F.14: Sample 2, V79-cell (cell 2) internalized particles of hydroxyapatite (50,000x)

Summary

Cross-sections of V79 cells were analysed by chemical staining with osmium tetroxide (contrast enhancement) and ultramicroscopy with a transmission electron microscope. Two samples with different concentrations of a 29.5% thixotropic aqueous dispersion of hydroxyapatite particles were analysed to detect the internalization of particles in V79 cells. At both concentrations of 6.4 ug/mL and 100 ug/mL, internalized particles were detected within the V79 cells. The majority of hydroxyapatite particles were found internalized in the cells. The particles are present separately or in smaller clusters in the cells. Only a limited number of hydroxyapatite were found outside the cells. In general, the hydroxyapatite particles were not detected in the cell nuclei.

In summary, cellular uptake of hydroxyapatite particles were detected for both concentrations of 6.4 ug/mL and 100 ug/mL and was observed exclusively in cytoplasmic vesicles but not in the nuclei.

SCCS comments

The presence of internalised HAP (nano) particles has been based only on TEM bright field images. No chemical information such as EDX / TEM observations or selected area diffraction patterns (nor dark field TEM Images) have been provided.

13. Annex G: Nano Characterisation of the test solution with dynamic light scattering (DLS)

From: Report 4114412 (ICCR, 2024; Fraunhofer IAP, 2024; ZentriForce, 2024) (provided in September 2024), Report PhPC-2022-3: Gene Mutation Assay in Chinese Hamster V79 Cells *in vitro* (V79/HPRT), –and attached to Report 4114412 Short Report Nano characterization of the test solution with dynamic light scattering (DLS) (non-GLP) - Final Technical Report – DLS Accelerated Stability Study.

The aim of this study was the analytical testing of nanoparticles via dynamic light scattering (DLS). For this purpose, an accelerated stability study at 37°C was conducted for approximatively 24 hours on nanoparticle samples.

The list of samples is given in the Table below:

Table Annex G.1: List of samples tested

Table 1: Samples for RICC005

Sample Name	Description	Storage conditions at ZentriForce Pharma
4114412 - 1.1	Solvent Control	Sample was measured upon arrival
4114412 - 6.1	Nanoparticle solution: 24 h treatment, Conc. 6.4 µg/ml (Konz. 5)	Sample was measured upon arrival
4114412 - 7.1	Nanoparticle solution: 24 h treatment, Conc. 16 µg/ml (Konz.6)	Sample was measured upon arrival
4114412 - 9.1	Nanoparticle solution: 24 h treatment, Conc. 100 µg/ml (Konz.8)	Sample was measured upon arrival

Sample preparation for DLS measurements
The samples were measured without pre-treatment.

DLS measurements
All light scattering services were executed on a DynaPro Plate Reader III (Wyatt Technology). Each sample was measured in triplicate (n=3). The adequate performance of the instrument regarding its intended application was verified via a system suitability (SST) prior to sample measurement. The software Dynamics (V. 7.10.1.21, Wyatt Technology) was used for sample measurements and data evaluation. Measurements parameters for the SST are depicted in the Table below (Table Annex G.2).

Table Annex G.2: DLS SST measurement parameters (from Applicant)

DLS acquisition time (s)	DLS acquisitions per measurement	Laser power (%)	Attenuation level (%)	Measurements per well within a scan	Number of scans	Temperature (°C)	Plate sealant
5	5	100	0	1	1	20	none

Laser Power and attenuation for sample measurement were set to auto-attenuation to adjust to potential formation of larger particles during the accelerated stability experiment. The well-plate was centrifugated at 3000 rpm for 2 min. after sample loading, following a standard procedure to remove air bubbles for the wells. Sample-specific measurement parameter are listed in the Table below (Table Annex G.3).

Table Annex G.3: DLS sample measurement parameters

DLS acquisition time (s)	DLS acquisitions per measurement	Laser power (%)	Attenuation level (%)	Measurements per well within a scan	Number of scans	Temperature (°C)	Plate sealant
5	3	auto	auto	1	1000	37	sealing tape

Normalized intensities are calculated by the Dynamics software and reported for comparability between samples. For all reported parameters, the standard deviation was calculated with the standard deviation formula for samples.

Results
Four samples were measured in triplicate via DLS at 37°C for ca. 24 hours.
Results for the first and last data point of the experiment for each sample are listed in the Tables below (from Table Annex G.4 to Table Annex G.9).

Table Annex G.4: Averages and standard deviation of z-average and intensity-based D10, D50 and D90 radii, T_0

Sample name	z-average diameter (nm)	z-average radius (nm)	D10 (nm)	D50 (nm)	D90 (nm)
4114412 - 1.1	16.3 ± 0.3	8.1 ± 0.2	3.2 ± 0.1	11.7 ± 0.6	59.7 ± 15.0
4114412 - 6.1	28.4 ± 7.5	14.2 ± 3.7	3.3 ± 0.2	21.2 ± 10.2	160.9 ± 51.0
4114412 - 7.1	48.9 ± 27.1	24.4 ± 13.5	3.6 ± 0.6	48.8 ± 55.4	139.8 ± 55.5
4114412 - 9.1	238.0 ± 27.2	119.0 ± 13.6	86.1 ± 24.7	127.6 ± 13.0	287.9 ± 149.3

Table Annex G.5: Average and standard deviations of mass-based D10, D50 and D90 radii, T_0.

Sample name	D10 (nm)	D50 (nm)	D90 (nm)
4114412 - 1.1	2.1 ± 0.3	2.8 ± 0.2	4.8 ± 0.1
4114412 - 6.1	2.3 ± 0.2	3.0 ± 0.3	4.6 ± 0.2
4114412 - 7.1	2.4 ± 0.3	3.0 ± 0.2	4.5 ± 0.5
4114412 - 9.1	3.9 ± 1.2	70.0 ± 58.3	177.8 ± 31.8

Table Annex G.6: Average and standard deviations of normalized intensities, T_0

Sample name	Normalized Intensity (kCnt/s)
4114412 - 1.1	30156 ± 5756
4114412 - 6.1	37348 ± 4288
4114412 - 7.1	52006 ± 13650
4114412 - 9.1	278309 ± 38565

Table Annex G.7: Averages and standard deviations of z-average and intensity-based D10, D50 and D90 radii, T_{end}

Sample name	z-average diameter (nm)	z-average radius (nm)	D10 (nm)	D50 (nm)	D90 (nm)
4114412 - 1.1	15.6 ± 0.2	7.8 ± 0.1	3.1 ± 0.1	10.6 ± 0.4	58.5 ± 10.2
4114412 - 6.1	32.6 ± 0.4	16.3 ± 0.2	3.3 ± 0.1	20.2 ± 1.1	172.0 ± 19.9
4114412 - 7.1	58.3 ± 17.7	29.2 ± 8.8	3.7 ± 0.4	78.9 ± 19.5	239.0 ± 147.3
4114412 - 9.1	203.5 ± 19.0	101.8 ± 9.5	79.5 ± 14.6	117.0 ± 15.6	164.6 ± 19.3

Table Annex G.8: Averages and standard deviations of mass-based D10, D50 and D90 radii, T_{end}.

Sample name	D10 (nm)	D50 (nm)	D90 (nm)
4114412 - 1.1	2.1 ± 0.1	2.7 ± 0.1	4.7 ± 0.1
4114412 - 6.1	2.3 ± 0.3	2.9 ± 0.2	4.5 ± 0.3
4114412 - 7.1	2.3 ± 0.1	2.9 ± 0.1	4.6 ± 0.5
4114412 - 9.1	3.8 ± 0.6	37.2 ± 57.1	126.8 ± 20.9

Table Annex G.9: Averages and standard deviation of normalized intensities, T_{end}

Sample name	Normalized Intensity (kCnt/s)
4114412 - 1.1	27853 ± 1073
4114412 - 6.1	39474 ± 2470
4114412 - 7.1	58629 ± 14699
4114412 - 9.1	212366 ± 41353

The change in the z-average diameter over time of each sample is shown in the following Figure Annex G.1 (a, b, c, d).

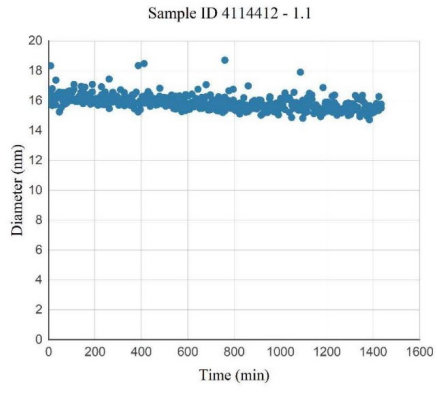

Figure 1: Z-average diameters of all replicates of sample 4114412 - 1.1

(a)

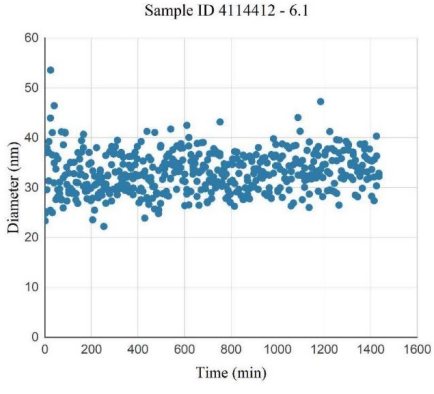

Figure 2: Z-average diameters of all replicates of sample 4114412 - 6.1

(b)

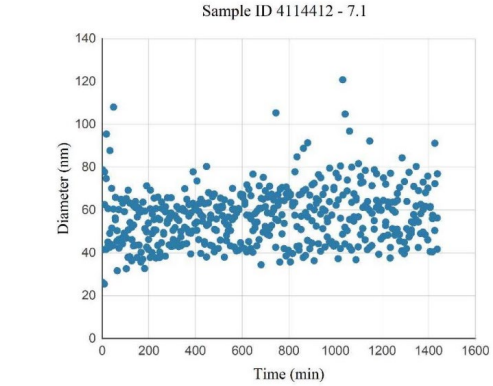

Figure 3: Z-average diameters of all replicates of sample 4114412 - 7.1

(c)

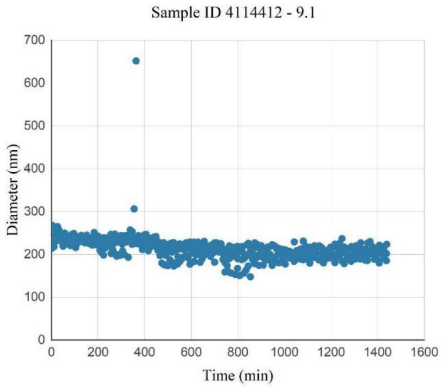

Figure 4: Z-average diameters of all replicates of sample 4114412 - 9.1

(d)

Figure Annex.G.1: z-average diameters of all replicates of the four samples (a): ID 4114412-1.1, (b): ID 4114412-6.1, (c) : 4114412-7.1, (d) : 4114412-9.1.

Conclusion of the DLS accelerated stability experiment (from Applicant)
The z-average diameter of the solvent control sample was 16.3 nm at T_0 and 15.6 nm at T_{end}. The z-average diameters ranged from 28.4 nm to 238 nm at T_0, and from 32.6 to 203 nm at T_{end}.
For neither of the nanoparticle samples, a systematic change in the particle size could be in the tested time frame.